Identification of immunological properties of natural products for the treatment of resistant tumors and bacterial pathogens

Inaugural dissertation

for the attainment of the title of doctor
in the Faculty of Mathematics and Natural Sciences
at the Heinrich Heine University Düsseldorf

presented by

Lisa Richter
from Duisburg

Düsseldorf, November 2019

from the Institute of Medical Microbiology and Hospital Hygiene
at the Heinrich Heine University Düsseldorf

Published by permission of the
Faculty of Mathematics and Natural Sciences at
Heinrich Heine University Düsseldorf

Supervisor: Prof. Dr. Stefanie Scheu

Co-supervisor: Prof. Dr. Rainer Kalscheuer

Date of oral examination: December 20th, 2019

Parts of this thesis have been published in:

Lisa Richter, Sonja Kropp, Peter Proksch, Stefanie Scheu, A mouse model-based screening platform for the identification of immune activating compounds such as natural products for novel cancer immunotherapies, Bioorganic and Medicinal Chemistry, 2019

Lisa Richter has performed all experiments, done the literature research for development and establishment of the screening guidelines, created the concept of the manuscript and written the manuscript (contribution: 75%). Sonja Kropp has assisted with the experiments (contribution: 5%), Peter Proksch has provided all tested natural products (contribution: 5%) and Stefanie Scheu has helped in conception of the screening guidelines and the manuscript (contribution: 15%).

Summary

Both cancer and diseases caused by bacterial infections are among the most common causes of death worldwide. Due to increasing population numbers and a higher life expectancy, incidence rates are expected to grow. Treatment gets even more challenging due to the existence and continuous development of resistances against established therapies. Alternative approaches are provided by immunotherapy which aims at the direct targeting of immune functions. Promising targets for immunotherapy are antigen-presenting cells which are key for the induction of effective adaptive immune responses.

An auspicious source of novel compounds suitable for drug development is represented by natural products. Natural products comprise a great variety of highly bioactive molecules produced by various organisms as adaption to biotic and abiotic stress factors and have already inspired drug development. Furthermore, histone deacetylase inhibitors are derivatives of natural products and exhibit advantageous features especially for anti-cancer treatment.

Due to the lack of appropriate screening guidelines for the definition of immune activating properties of natural products and their suitability for immunotherapeutic application, new guidelines have been established under the comprehensive application of different mouse models and are described in this thesis. Following this, natural products should be non-toxic to immune target cells, exhibit beneficial direct activities against cancer cells or pathogens and promote immune activation. 240 natural products derived from endophytic fungi and marine sponges have been analyzed accordingly. Three compounds have been found to be promising for further drug development accompanied by potential biochemical optimization. Additionally, two histone deacetylase inhibitors with preferences for histone deacetylase 6 or histone deacetylases 6 and 1 have been identified to enhance type I interferon production by plasmacytoid dendritic cells at simultaneous stimulation with the double-stranded RNA analog poly I:C. Promising, optimized natural products and histone deacetylase inhibitors might be administered in *in vivo* tumor and infection mouse models and analyzed in clinical trials.

In summary, the experiments and guidelines presented in this thesis aim at the identification of compounds that simultaneously (re-) activate immune cells and target tumors and bacteria thus helping to overcome resistance mechanisms.

Zusammenfassung

Krebs und Krankheiten ausgelöst durch bakterielle Infektionen zählen zu den weltweit häufigsten Todesursachen. Aufgrund wachsender Bevölkerungszahlen und höherer Lebenserwartungen wird gleichermaßen ein Anstieg an Krankheitsfällen erwartet. Durch die Existenz und kontinuierliche Entwicklung von Resistenzen gegenüber etablierten Therapien werden Behandlungen weiter erschwert. Die Immuntherapie bietet alternative Behandlungsmöglichkeiten, die direkt auf Immunfunktionen abzielen. Vielversprechende Ziele sind antigenpräsentierende Zellen, die Schlüsselfunktionen für die Initiierung adaptiver Immunantworten ausüben.

Eine aussichtsreiche Quelle neuer Kandidaten, die sich für die Medikamentenentwicklung eignen, sind Naturstoffe. Naturstoffe umfassen eine Vielzahl hoch bioaktiver Moleküle, die von unterschiedlichen Organismen als Anpassung an biotische und abiotische Stressfaktoren produziert werden und bereits vielfach die Medikamentenentwicklung inspirieren konnten. Zusätzlich besitzen Histondeacetylase-Inhibitoren, die ebenfalls von Naturstoffen abgeleitete Moleküle sind, vorteilhafte Eigenschaften gerade für die Behandlung von Krebs.

Aufgrund fehlender geeigneter *Screening*-Richtlinien für die Identifizierung von immunaktivierenden Eigenschaften von Naturstoffen und ihrer Eignung für die Anwendung in der Immuntherapie wurden neue Richtlinien unter intensivem Einsatz verschiedener Mausmodelle etabliert und sind in dieser Arbeit beschrieben. Demnach sollen Naturstoffe nicht toxisch für Zielimmunzellen sein, vorteilhafte direkte Effekte gegen Krebszellen und Pathogene ausüben sowie immunaktivierend wirken. 240 Naturstoffe aus endophytischen Pilzen und marinen Schwämmen wurden entsprechend dieser Richtlinien untersucht und drei Stoffe als vielversprechend für die weitere Medikamentenentwicklung nach potenzieller biochemischer Optimierung definiert. Zusätzlich wurden zwei Histondeacetylase-Inhibitoren mit Präferenz für Histondeacetylase 6 oder Histondeacetylase 6 und 1 gefunden, die die Typ I Interferon Produktion von plasmazytoiden dendritischen Zellen bei gleichzeitiger Stimulation mit dem dsRNA-Analog Poly I:C erhöhen. Vielversprechende, optimierte Naturstoffe und Histondeacetylase-Inhibitoren können nun in *in vivo* Tumor- und Infektionsmausmodellen und klinischen Studien untersucht werden.

Zusammengefasst zielen die in dieser Arbeit präsentierten Experimente und Richtlinien darauf ab, Stoffe zu identifizieren, die Immunzellen (re-) aktivieren, gleichzeitig gegen Tumoren und Bakterien wirken und somit helfen, Resistenzen zu überwinden.

Table of contents

1. Introduction

The growing need to find new drugs for the treatment of cancer and bacterial infections paves the way for innovative drug discovery approaches as presented by immunotherapy. In the following sections, an introduction into current immunotherapeutic approaches and promising target cell groups is given. Dendritic cells (DCs) and macrophages as well as their capacities to induce effective adaptive immune responses are a central topic of this thesis. Furthermore, sources for novel drugs including natural products and histone deacetylase inhibitors (HDACi) are illustrated and described in the context of their application in immunotherapy.

1.1 The need to find new drugs for the therapy of cancer and bacterial infections

With an increasing world population and enhanced life expectancy more disease-associated deaths are expected to occur (Kontis *et al.* 2017). The World Health Organization (WHO) states that cancer and diseases caused by bacterial infections are among the top ten causes of death in industrialized as well as in developing countries. In 2016, cancer itself caused 22% of all deaths worldwide while in Germany it is estimated that 43-51% of the people will develop cancer during life with 20-25% expected to die from this disease (Quante *et al.* 2016; World Health Organization 2018). Globally, cancer incidence rates are expected to increase from 15.2 million cases in 2015 to up to 24 million cases in 2035 (American Association for Cancer Research 2018). The most common cancer types comprise respiratory cancers as well as breast cancer, prostate cancer and colorectal cancer. Bacterial infections, on the other side, show high incidence rates for infections of the lower respiratory tract as well as for tuberculosis (World Health Organization 2018). Both cancer and bacterial infections become even more challenging to cure due to the development of resistances against prevailing treatment approaches (Mansoori *et al.* 2017). Today, resistances for all antibiotics commonly used in anti-bacterial therapy are described (Blair *et al.* 2015). While bacterial infections are generally treated with antibiotics, traditional cancer therapy deploys surgery, radiotherapy and chemotherapy. However, patients undergoing the latter two options often suffer from severe side effects like fatigue, nausea and changes in blood cell counts (Iwamoto 2013). Resistance mechanisms of cancer cells and bacteria show parallels thus prompting respective drug development (Naran *et al.* 2018). Malignant tissues as well as bacterial communities represent cellular clusters that modulate the

host's metabolic and defense functions to facilitate their resistance and hence survival (Lambert *et al.* 2011). Such resistance mechanisms can be either intrinsic or acquired. Intrinsic modes of resistance involve, for example, decreased drug access to the respective target by reduced cell permeability or enhanced efflux of the drug. Furthermore, gram-negative bacteria intrinsically display lower cell permeability (Blair *et al.* 2015). In contrast, acquired resistance mechanisms involve e.g. an enzymatic inactivation of the drug or modification of the target by mutation or post-translational alteration (Blair *et al.* 2015; Sharma *et al.* 2017). Popular escape mechanisms of cancer cells are the expression of immune checkpoint molecules but also a reduced expression of tumor antigens which both prevent appropriate immune responses (Sharma *et al.* 2017). Although resistance mechanisms of cancer cells and bacteria might involve different molecular targets, the fundamental mechanistic principles are similar.
Consequently, new treatment options are urgently needed to counteract the rise in disease-associated deaths and the occurrence of resistances. Similar modes of resistance of cancer cells and bacteria support the idea of developing drugs that are effective against both. Immunotherapy which aims at the reactivation of immune responses that have been silenced by resistance mechanisms is becoming an increasingly important focus of research and alternative for traditional treatment options. Drugs are needed that simultaneously activate the immune system and target cancer cells and bacteria (Naran *et al.* 2018; Anguille *et al.* 2015; Papaioannou *et al.* 2016). Promising sources for new drugs are provided by natural products and HDACi. Natural products provide a broad variety of highly bioactive molecules with various structural compositions and have already inspired many drug development approaches. Moreover, pan HDACi targeting all types of HDACs are frequently used for cancer treatment but specific HDACi might offer more advantageous solutions. Current immunotherapeutic approaches and the role of natural products and HDACi are illustrated in the following sections.

1.2 Immunotherapy

Immunotherapy as an alternative treatment approach has attracted attention not just since the awarding of the Nobel Prize 2018 in Physiology or Medicine to James Allison and Tasuku Honjo. Both researchers detected mechanisms of immune checkpoints which can be co-opted by cancer cells to evade immune responses. Immunotherapy exploits immune functions to reactivate the immune system and effectively mount anti-cancer and anti-bacterial immune responses. In contrast to traditional therapies,

immunotherapy enables more targeted approaches. Its success depends on the type of agents used and the patient's immune status. Immunotherapy is called "active" in the case of e.g. the direct stimulation of cell effector functions via application of cytokines. "Passive" immunotherapy aims to balance missing immune responses by e.g. administration of *ex vivo* activated cells (Papaioannou *et al.* 2016). Here, similar approaches for the treatment of cancers and bacterial infections exist and comprise amongst others the application of antibodies targeting diseased cells, vaccination approaches and the administration of cytokines for enhancement of immune functions. All those approaches are primarily used for the therapy of cancer but are increasingly investigated for the treatment of diseases caused by bacterial infections (Naran *et al.* 2018). Immune checkpoint inhibition as one treatment opportunity represents an active immunotherapeutic approach. Prominent examples that were also a focus of research of the two Nobel laureates are the molecules CTLA-4 and PD-1. In healthy individuals, immune checkpoint molecules keep the immune system in balance and prevent overreactions as found in autoimmunity (Wei *et al.* 2018). Cancer cells can express immune checkpoint molecules which causes a suppressed anti-cancer immune reaction. Administration of immune checkpoint inhibitors such as anti-CTLA-4 and anti-PD-1 counteracts these resistance mechanisms and promotes an effective immune response (Wei *et al.* 2018). Despite their promising long-term effects, immune checkpoint inhibition therapies are often accompanied by severe but treatable side effects, called immune-related adverse effects. These mainly affect skin, liver and the gastrointestinal and endocrine system. Immunosuppressants are usually administered to treat these side effects (Postow 2015). Immune checkpoint inhibitors are not only applied in cancer but are also tested in clinical trials for infectious diseases mainly involving viruses (Naran *et al.* 2018).

So far, immunotherapy has limited success as it shows positive effects only in a few patients while strongly depending on the type of cancer and the responsiveness of the patient's immune system. To enclose more patients in the success of immunotherapy, combination therapies using e.g. immune checkpoint inhibitors and immune cell vaccination approaches are evaluated in clinical trials (Sharma *et al.* 2017). Studies involving combinations of immunotherapeutic drugs and epigenetic regulators such as HDACi have already shown to inhibit tumor progression and potentially reduce side effects (Banik *et al.* 2019). Such combination therapies are promising approaches for building immunogenic environments and combating resistances (Naran *et al.* 2018; Anguille *et al.* 2015; Papaioannou *et al.* 2016). Nevertheless, immune checkpoint inhibition, vaccination and epigenetic regulation are just a few approaches among a wide field of possibilities used in immunotherapy.

DCs but also macrophages are already important targets for immunotherapy as they are key for the transition of innate to adaptive immune responses. Hence, the characteristics of these cell types and their application in immunotherapeutic approaches are described in the following sections.

1.3 Dendritic cells and macrophages

The immune system can be divided into the innate and the adaptive immune system each comprising different subsets of cells which play specific roles in the response to dangers. Innate immune responses represent the immediate, antigen-unspecific reaction towards a dangerous situation. Innate immune cells are capable of inducing adaptive immune responses and act relatively fast and unspecific in regard to a cancer cell or pathogen. In contrast, adaptive immune reactions occur more slowly but are highly specific (Iwasaki and Medzhitov 2010).
Two hematopoietic cell types belonging to the innate immune system are represented by DCs and macrophages. Both are antigen-presenting cells (APCs) but especially DCs are essential for activation of naïve T cells and thus induction of an effective adaptive immune response (see section 1.3.4 T cell activation by dendritic cells). In 2011, Ralph Steinman received the Nobel Prize in Physiology or Medicine for his discovery of DCs in 1973 and the pivotal contribution to understand functionalities of the innate immune system. DCs can further be divided into classical or conventional DCs (cDCs) and plasmacytoid DCs (pDCs). Granulocyte-macrophage colony-stimulating factor (GM-CSF) and FMS-like tyrosine kinase ligand (Flt3L) bone marrow cell cultures are usually applied to obtain cDCs and pDCs, respectively, while macrophage colony-stimulating factor (M-CSF) cultures are used to enrich macrophages from bone marrow (Helft *et al.* 2015; Scheu *et al.* 2008).
In the following sections, DCs and macrophages will be described in more detail and their role for the activation of T cells and thus of adaptive immune responses will be illustrated. Additionally, application of these cell types in immunotherapeutic approaches will be depicted.

1.3.1 Conventional dendritic cells

cDCs comprise roughly all DCs except for pDCs and are known for their pronounced antigen-presenting capacity. With origin in the bone marrow, cDCs can be found in most lymphoid and non-lymphoid tissues where they detect invading pathogens, mutated cells or damaged tissues. Here, cDCs count for 1-5% of all tissue cells. As APCs, cDCs are

essential key regulators of effective innate and adaptive immune responses towards dangers as well as of the induction of tolerance towards self-antigens (Merad *et al.* 2013) (see section 1.3.4 T cell activation by dendritic cells). Various cDC subtypes are found which comprise DCs in non-lymphoid tissues, Langerhans cells in epidermal compartments, tissue-migratory DCs and DCs that reside in lymphoid organs such as lymph nodes (Merad *et al.* 2013). Classical surface expression markers of cDCs used for discrimination from other cell types are the α integrin CD11c and major histocompatibility complex class II (MHCII) molecules as well as Flt3/CD135 (Merad *et al.* 2013; Helft *et al.* 2015).

1.3.2 Plasmacytoid dendritic cells

pDCs are known as professional type I interferon (IFN) producers upon viral infection. For their development, pDCs depend on recognition of Flt3L by its receptor Flt3/CD135. pDCs can be found in lymphoid organs where they account for 0.1-0.5% of nucleated cells. They highly express the toll-like receptors (TLRs) 7 and 9 which are responsible for detection of single-stranded RNA and CpG-rich DNA, respectively. Following activation, a signaling cascade is induced that involves myeloid differentiation primary response protein 88 (MyD88), IFN-regulatory factor (IRF) 7 and nuclear factor κ-light-chain-enhancer of activated B cells (NFκB) and ultimately leads to the extensive production of type I IFNs and other cytokines. Remarkably, mouse pDCs do not express TLR3 for recognition of double-stranded RNA (dsRNA) (Jelinek *et al.* 2011).

Depending on their localization, pDCs can pursue different tasks. In the spleen, for example, only a specific subset of pDCs is responsible for type I IFN production upon stimulation (Bauer *et al.* 2016). pDCs are not only essential for type I IFN production but also play important roles as APCs for the activation of T cells and the induction of adaptive immune responses (Reizis 2019; Wculek *et al.* 2019). They exhibit rather low antigen-presenting capacities which nevertheless are increased after activation (Barrat and Su 2019). In comparison to cDCs, pDCs show only low expression of the surface markers CD11c and MHCII (Reizis 2019; Wculek *et al.* 2019). Instead, they can be distinguished by the expression of the surface markers B220, CD317, Siglec-H, CD45RA and Ly6C (Musumeci *et al.* 2019).

pDCs are considered to play essential roles in the development and persistence of viral infections and autoimmunity (Figure 1). In chronic infections, pDCs show a consistently high activation status that is often associated with disease persistence. This has especially been shown in infections with the human immunodeficiency virus (HIV)-1. Furthermore, autoimmunity is frequently accompanied by high levels of type I IFNs and

IFN-stimulated genes (ISGs) (Barrat and Su 2019). More information about the functions of type I IFNs can be found in section 1.4.4 Type I interferons.

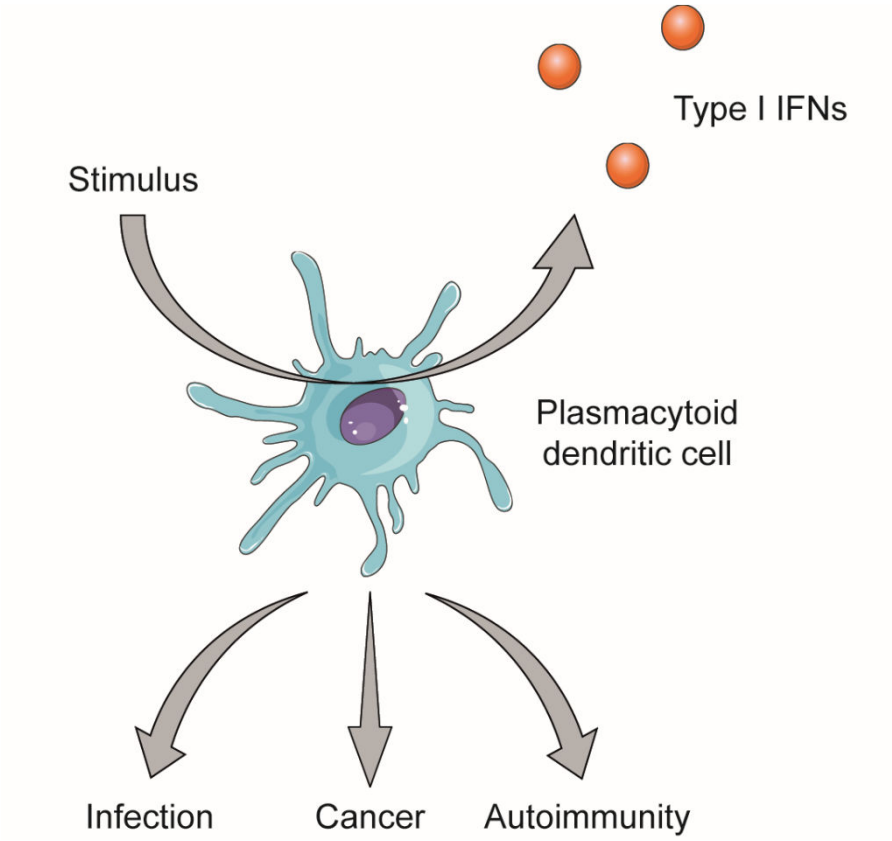

Figure 1: pDCs are professional type I IFN producers and play crucial roles in infection, cancer and autoimmunity.

In cancer, pDCs often exhibit attenuated or abrogated functions. They have been shown to weakly produce type I IFNs in breast and ovarian cancer but to have a higher capacity to induce differentiation of regulatory T cells, thus promoting an immunosuppressive state (Labidi-Galy *et al.* 2012; Mitchell *et al.* 2018; Reizis 2019). Consequently, pDCs are discussed as potential targets in cancer immunotherapy and have already been tested in *in vivo* approaches involving direct stimulation of pDC functions (Mitchell *et al.* 2018; Reizis 2019). Nevertheless, the presence of balanced levels of type I IFNs is necessary for successful therapy. It is a matter of discussion whether the effects of pDCs in cancer as well as in infections and autoimmunity depend on their exceptional capacity to produce type I IFNs or additionally on any other pDC function (Barrat and Su 2019).

1.3.3 Macrophages

Macrophages are widely distributed throughout the body and can be found in all lymphoid and non-lymphoid tissues. They are phagocytic cells which ingest surrounding particles and help in the clearance of senescent cells and pathogens thus promoting a homeostatic environment. Additionally, macrophages possess antigen-presenting capacities although to a lesser extent than DCs (Gordon and Pluddemann 2017).
Macrophages play relevant roles in the context of cancer. Tumor-associated macrophages are the main cell group represented in the tumor microenvironment of malignant tissues and known to promote tumor growth. Mechanistically, tumor-associated macrophages promote angiogenesis, suppress anti-tumor immune responses and support metastasis (Yang, McKay*, et al.* 2018). Consequently, besides DCs, these cells represent a possible target for immunotherapy. Respective approaches aim at changing macrophage activities from homeostatic toward anti-tumor and seem especially effective in combination with chemotherapy or other immunotherapeutic approaches (Mantovani *et al.* 2017).

1.3.4 T cell activation by dendritic cells

Immature DCs constantly survey tissues for tissue damage and antigens from e.g. cancer cells or bacteria (Figure 2). Upon sensing via pattern recognition receptors (PRRs), antigens are internalized, processed and broken down to peptides in endosomes. Subsequently, DCs mature and migrate to lymph nodes for the activation of adaptive immune cells such as T cells (Banchereau *et al.* 2000). T cells arise in the thymus and reside in a naïve state in various tissues including lymph nodes (Hemann and Legge 2014). DCs present antigen peptides via MHC complexes which are constitutively expressed on their surface. These antigen-MHC complexes can be recognized by T cells via T cell receptors (TCRs) specific for that antigen (Banchereau *et al.* 2000).
The whole process of T cell activation by DCs requires three signals: Firstly, an interaction of an MHC-antigen complex with its counterpart TCR is needed. Secondly, additional TCRs have to bind to costimulatory molecules on the surface of the DC e.g. CD86. Lastly, a complex cytokine environment is necessary that comprises cytokines such as interleukin (IL)-12 and IFNγ secreted by DCs and other surrounding activated cells (Liechtenstein *et al.* 2012).

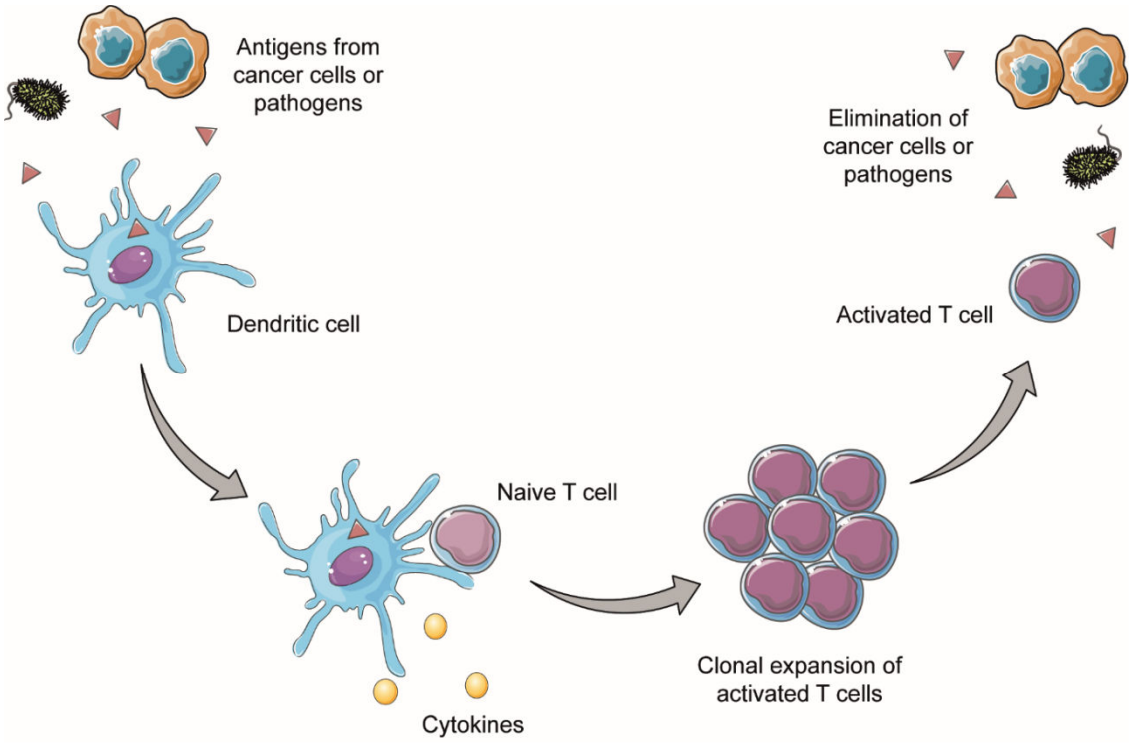

Figure 2: T cell activation by DCs. DCs constantly survey tissues for the presence of cancer cells or pathogens such as bacteria. Upon detection and internalization of cancer cells, pathogens or compounds thereof, DCs migrate to lymph nodes where they activate antigen-specific T cells via presentation of antigen-loaded MHC molecules on the surface of the DC in the presence of costimulatory cytokines. This induces clonal expansion of the now activated T cells which ultimately aid in the clearance of the cancer cell or pathogen by e.g. secretion of IFNγ for the activation of phagocytic cells. This figure has been modified from Richter et al. (2019).

In general, two types of MHC molecules exist: MHCI and MHCII. MHCI continuously presents endogenous antigens that are produced by the cell itself to $CD8^+$ T cells. These antigens are recognized by T cells as self-antigens and thus do not induce T cell activation. However, if a cell expresses mutated genes like in the context of cancer or microbial antigens from pathogens, these are recognized as non-self antigens and trigger T cell activation. Nevertheless, tumor cells and pathogens are able to escape these mechanisms by, for example, attenuated expression of essential MHCI pathway molecules or expression of inhibitory molecules (Rock *et al.* 2016). MHCII on the other side is capable of presenting larger molecules such as exogenous antigens and cellular proteins that were degraded in the endosome to $CD4^+$ T cells. These rules can be bent in the case of cross-presentation which can take place in DCs and other phagocytic cells. In cross-presentation, exogenous antigens derived from tumor cells or pathogens are presented via MHCI to $CD8^+$ T cells (Rock *et al.* 2016; Cruz *et al.* 2017).

Activation of antigen-specific $CD4^+$ or $CD8^+$ T cells induces their rapid proliferation and clonal expansion accompanied by modulated transcriptional and metabolic activity. Depending on the stimuli during T cell activation, T cells differentiate into distinct effector T cells (Wherry and Kurachi 2015). For example, $CD4^+$ T cells recognize antigens presented via MHCII molecules and differentiate into T helper 1 cells in the presence of IL-12 and IFNγ while T helper 2 cells depend on IL-2 and IL-4 (Zhu *et al.* 2010; Luckheeram *et al.* 2012). Effector T cells subsequently migrate to the affected tissues to aid in the clearance of the cancer cells or bacteria. For this, they fulfill various effector functions by e.g. secretion of cytokines such as IFNγ, lymphotoxin α and IL-2 which in turn activate additional immune cells. IFNγ, for example, besides being necessary for T helper 1 cell differentiation is needed for the activation of macrophages, while IL-2 promotes the proliferation of cytotoxic $CD8^+$ T cells (Luckheeram *et al.* 2012; Banchereau *et al.* 2000). After clearance of the cancer cell or pathogen and loss of continuous antigen stimulation, most effector T cells die. A subset, however, develops into memory T cells allowing a faster response to reoccurrence of specific cancers or pathogens (Wherry and Kurachi 2015; Hemann and Legge 2014).

In the context of cancer and infections, exhausted T cells play a substantial role. Exhausted T cells represent a state of dysfunctional cells which are induced by constant antigen exposure significant for both cancer and infection. These T cells lose effector functions, express inhibitory receptors and show a modified function and expression of transcription factors thus leading to a state of imbalance associated with insufficient combat of dangers (Wherry and Kurachi 2015). In immunotherapy, various approaches are currently discussed that aim at the reactivation of T cells by, for example, administration of specific cytokines. Another promising field of research are chimeric antigen receptor (CAR) T cells which are modified T cells possessing recombinant TCRs that work independently of MHC molecules (Naran *et al.* 2018).

In summary, T cell activation by DCs is an essential part of the induction of an effective immune response and pioneering approaches exploiting this field of research seem promising for the treatment of cancers or bacterial pathogens.

1.3.5 Antigen-presenting cells in immunotherapy

Due to their vital role as key regulators of innate and adaptive immune responses, APCs and especially DCs are a highly discussed target of immunotherapeutic approaches. Simultaneously, many standard therapies already depend on the functions of DCs. In several chemotherapeutic and radiotherapeutic approaches, for example, cell death associated molecules such as opsonins or damage-associated molecular patterns

(DAMPs) are released and recognized by APCs which consequently present these antigens to specific T cells to mount effective anti-tumor immune responses (Wculek *et al.* 2019). Moreover, DCs are directly targeted in diverse immunotherapeutic approaches. Application of DC-based immunotherapeutics is usually considered safe with few side effects but also with limited response rates in patients (van Gulijk *et al.* 2018). DCs are, for instance, applied in vaccination approaches in which they are loaded with tumor antigens and are injected into patients to promote tumor-specific immune responses (Anguille *et al.* 2015). In detail, precursor cells are isolated from patients, cultivated *in vitro* with GM-CSF to obtain immature DCs before exposure to pro-inflammatory cytokines comprising e.g. tumor necrosis factor (TNF) and IL-6 and loading with tumor antigens (Tacken *et al.* 2007). After administration to patients, antigen-specific activation of T cells and other innate immune cells such as natural killer (NK) cells is triggered. Moreover, such vaccination approaches are also used to establish an immunological memory (Anguille *et al.* 2015). Instead of vaccination approaches with *ex vivo* loaded DCs, tumor antigens can also be directly administered to patients. Other approaches aim at the direct *in vivo* activation of DCs by application of cytokines or other activating agents such as GM-CSF, Flt3L or different TLR agonists like CpG or poly I:C (Wculek *et al.* 2019).

In general, one big challenge is to overcome the immune suppressive tumor microenvironment (Wculek *et al.* 2019). Thus, approaches involving DCs are promising but might be successful in more patients when applied in combination therapies that increase the activity of anti-tumor immune effector cells and simultaneously counteract tumor resistance mechanisms (Anguille *et al.* 2015; van Gulijk *et al.* 2018). In the following sections, cytokines relevant for this thesis and their application in immunotherapy are illustrated.

1.4 Toll-like receptors and cytokines

TLRs are important receptors for the recognition of molecular structures derived from pathogens and induce signaling cascades resulting in the expression of cytokines and other genes. In the following, the most relevant TLRs and cytokines for this thesis are presented and their functions are explained in the context of immune reactions and therapy.

1.4.1 Toll-like receptors

Invading microbes and damaged cells are recognized by DCs, macrophages and other innate immune cells via PRRs. PRRs are highly conserved, germline-encoded receptors for the detection of pathogen-associated molecular patterns (PAMPs) as well as DAMPs. Several classes of PRRs in mammals have been found so far and include TLRs, retinoic acid-inducible gene-I (RIG-I)-like receptors such as MDA5, Nod-like receptors, AIM2-like receptors, C-type lection receptors and additional intracellular DNA receptors. In mice, twelve TLRs exist and either localize to the cell surface for detection of microbial components such as lipopolysaccharide (LPS) or intracellularly for the recognition of nucleic acids. All TLRs are produced in the endoplasmatic reticulum, transported to the Golgi complex and further to their target location (Kawasaki and Kawai 2014).
Stimulation of the TLRs 3, 4 and 9 is a central part of the screening approach presented in this thesis (Figure 3). TLR3 is localized in the endosome and detects viral dsRNA such as the synthetic dsRNA analog poly I:C (Kawasaki and Kawai 2014; Matsumoto and Seya 2008). While TLR3 is expressed in cDCs and macrophages, pDCs mainly detect poly I:C via MDA5 which is ubiquitously expressed at low levels (Takeuchi and Akira 2008; Dias Junior *et al.* 2019). TLR4 is known to be localized on the cell surface and to recognize LPS (Kawasaki and Kawai 2014; Chow *et al.* 1999). LPS is found in the outer cell membrane of gram-negative bacteria (Chow *et al.* 1999). TLR9 also localizes to the endosome and detects bacterial and viral DNA that is rich in CpG motifs (Hemmi *et al.* 2000).

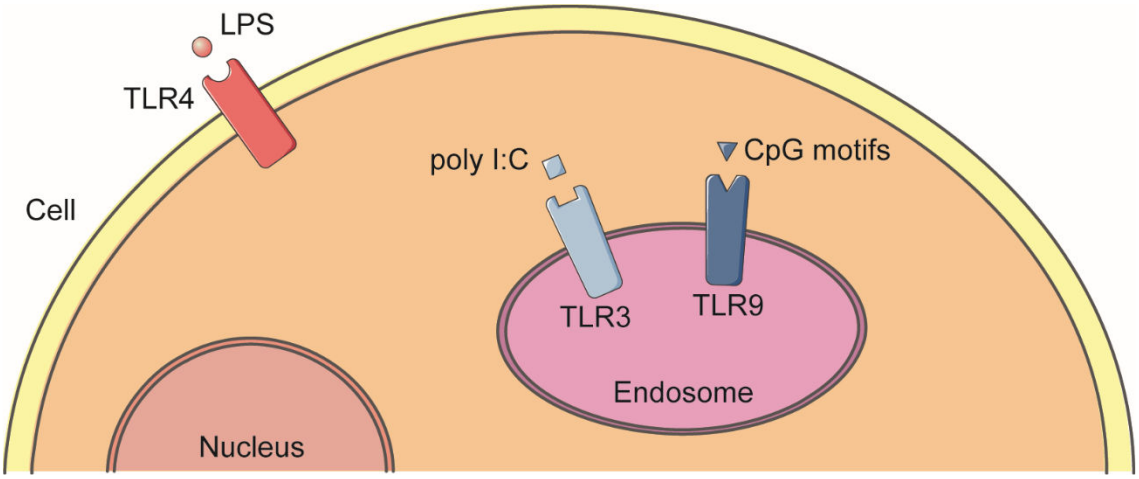

Figure 3: Localization of the TLRs 3, 4 and 9. TLR3 and 9 are intracellular receptors and localized to the endosome where they recognize dsRNA analogs like poly I:C or CpG-rich DNA motifs, respectively. TLR4 is found at the cell membrane where it detects LPS from the outer cell membrane of gram-negative bacteria.

Upon TLR engagement, a signaling cascade is induced that ultimately triggers the expression of various cytokines and other inflammatory molecules such as IL-12 and IFNβ (Figure 4). TLR signaling can roughly be separated into the MyD88-dependent pathway and the Toll/IL-1R domain-containing adapter-inducing IFNβ (TRIF)-dependent pathway which induce the expression of inflammatory genes or type I IFN expression, respectively (Kawasaki and Kawai 2014). Secretion of these cytokines further induces or inhibits immune responses and will be illustrated in the following sections.

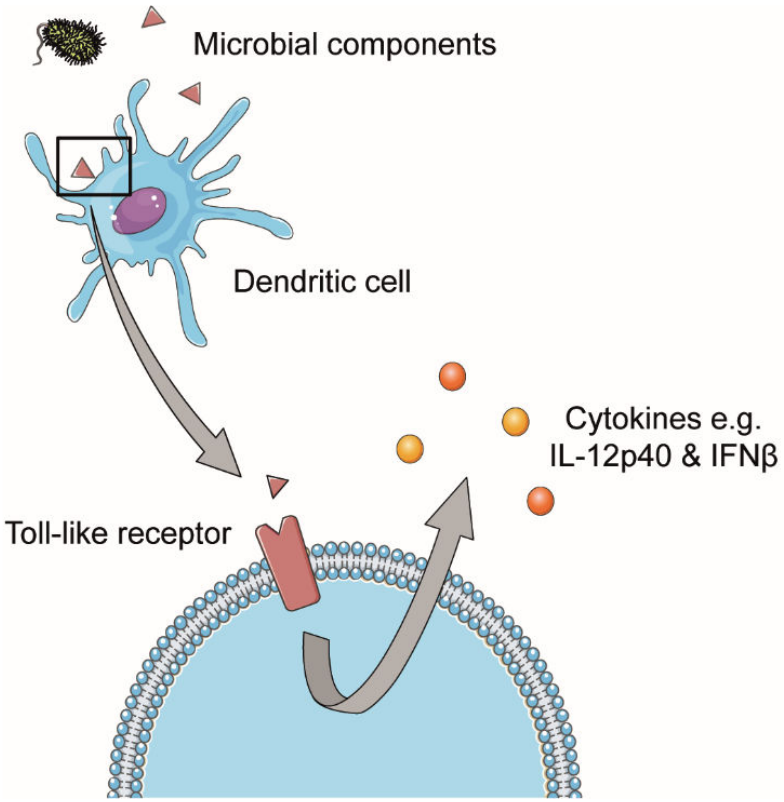

Figure 4: Cytokine production following TLR stimulation. DCs and macrophages detect microbial components via TLRs on their surface or in intracellular compartments. This induces the production of cytokines like IL-12p40 and IFNβ which activate further effector cells for clearance of the pathogen.

1.4.2 IL-12p40

IL-12 is a cytokine secreted by DCs and macrophages upon TLR stimulation (Zundler and Neurath 2015). IL-12 is a member of the class I hematopoietin family which signals via janus kinase (JAK)-signal transducer and activator of transcription proteins (STAT) pathways (Tait Wojno *et al.* 2019). It is a heterodimeric cytokine composed of the two subunits p40 and p35. While p40 is only produced upon TLR stimulation, p35 is constitutively expressed at low levels (Zundler and Neurath 2015). IL-12 is recognized

by activated T and NK cells via the heterodimeric IL-12 receptor which consists of IL-12Rβ1 and IL-12Rβ2 (Tait Wojno *et al.* 2019). Receptor binding triggers a signaling cascade via STAT4 and ultimately leads to IFNγ production. Consequently, IL-12 induces various downstream effects including T and NK cell proliferation, T helper 1 cell development and other IFNγ-dependent activities thus promoting both innate and adaptive immune responses (Abdi and Singh 2015; Zundler and Neurath 2015). The subunit IL-12p40 is several hundred-fold higher expressed than IL-12 itself and can additionally function as a monomer or homodimer (D'Andrea *et al.* 1992; Tait Wojno *et al.* 2019).

Besides being part of IL-12, IL-12p40 together with p19 serves as a component of the pro-inflammatory cytokine IL-23. IL-12 and IL-23 show opposing effects with implication of IL-23 in autoimmune diseases. Additionally, IL-23 is critical for IL-17-producing T helper 17 cell differentiation (Croxford *et al.* 2014; Oppmann *et al.* 2000).

All IL-12 and IL-23 subunits, namely p19, p35 and p40, are produced by activated DCs and macrophages with p40 to the greatest extent. Nonetheless, the tightly regulated expression of p35 and p19 decides about the formation of either IL-12 or IL-23, respectively (Croxford *et al.* 2014; Oppmann *et al.* 2000). Consequently, expression of IL-12p40 is being acknowledged as a reliable readout for immune activation (Garris *et al.* 2018).

It has been shown that an interaction of DCs and T cells with secretion of IL-12 and IFNγ is necessary for successful cancer therapy with the immune checkpoint inhibitor anti-PD-1 (Garris *et al.* 2018). Due to its considerable role in triggering adaptive immune responses, IL-12 is also in discussion as an immunotherapeutic drug. Over the past years, IL-12 has been administered in various clinical trials in combination with cancer vaccines, gene therapies or with additional immunotherapeutic drugs. Nevertheless, although being promising in *in vitro* approaches, it has shown only modest results in patients often accompanied by severe side effects like hepatotoxicity (Lasek *et al.* 2014). Recently, IL-12 has regained attention as immunotherapeutic drug when Garris *et al.* showed that the cytokine can stimulate tumor-infiltrating anti-tumor effector cells (Garris *et al.* 2018).

1.4.3 IL-2

While IL-12 is accepted as a marker for activation of DCs and macrophages, IL-2 is known as a cytokine produced by activated T cells. In the absence of antigen stimulation, it is mainly secreted by $CD4^+$ T cells but also to a lesser extent by $CD8^+$ T cells, NK cells and even DCs under specific conditions. Upon antigen presentation by APCs, IL-2

production is strongly increased especially in $CD4^+$ T cells (Boyman and Sprent 2012; Jiang *et al.* 2016). It signals via JAK1 and JAK3 and activates signaling cascades of STAT5, phosphoinositide 3-kinase (PI3K) and mitogen-activated protein kinase (MAPK) pathways (Klatzmann and Abbas 2015). IL-2 subsequently promotes the differentiation of $CD4^+$ T cells into effector T cells and is relevant for $CD8^+$ T and NK cell toxicity as well as for maintenance of regulatory T cells (Boyman and Sprent 2012; Jiang *et al.* 2016). DCs were shown to be capable of IL-2 secretion after stimulation with various microbial products such as LPS and CpG although to a low extent (Granucci *et al.* 2003). In NK cells, IL-2 promotes cell proliferation and effector functions by enhancing cytokine production and cytotoxicity. Nevertheless, IL-2 does not modulate NK cell functions as strongly as IL-12 (Klatzmann and Abbas 2015).
IL-2 is an approved drug for the treatment of renal cell carcinoma and metastatic melanoma as it promotes anti-tumor immune responses. These responses are based on the mutual effects of IL-2 on both effector and regulatory T cells. Usually, high-dose administration of IL-2 is most effective but also induces severe side effects in patients. Because of this, IL-2 is in discussion for combinational administration with other immunotherapeutic drugs (Jiang *et al.* 2016). IL-2 additionally attenuates autoimmune reactions and inflammatory conditions at low-dose administration based on the expansion and activation of regulatory T cells. Absence of IL-2 consequently leads to the development auf autoimmune diseases. Based on these findings, IL-2 is tested in clinical trials for the treatment of autoimmune and inflammatory diseases (Klatzmann and Abbas 2015).

1.4.4 Type I interferons

Type I IFNs are a cytokine family consisting of eleven IFNα subtypes in mice and 13 IFNα subtypes in humans, IFNβ and several other type I IFNs. Their expression is rapidly induced after PRR stimulation after sensing of viral components or danger signals released by dying cells (Zitvogel *et al.* 2015). Like IL-2 and IL-12, type I IFNs signal via the JAK-STAT pathway after binding to the IFNα receptor (IFNAR). Type I IFNs sensing triggers the activation and formation of STAT1-STAT2 complexes that can migrate into the nucleus and modulate gene expression. This ultimately leads to the binding to IRF9 and the transcription of ISGs which modulate innate as well as adaptive immune responses and induce an anti-viral state (Ali *et al.* 2019; Zitvogel *et al.* 2015).
In general, almost all cells are able to produce type I IFNs but pDCs are regarded as professional type I IFN-producing cells following TLR7 and 9 engagement (see section 1.3.2 Plasmacytoid dendritic cells) (Swiecki and Colonna 2015; Ali *et al.* 2019). Type I

IFNs promote an anti-viral state via induction of cytotoxic activity of $CD8^+$ T and NK cells, differentiation of T helper 1 cells and stimulation of IFNγ secretion. In innate immune cells, temporary presence of type I IFNs promotes an anti-viral state by upregulation of MHCII and costimulatory molecule expression, DC maturation and antigen presentation. Thus, type I IFNs fundamentally regulate processes necessary not only for clearance of pathogens but also for the defense of cancer (Swiecki and Colonna 2011; Lee and Ashkar 2018) (Figure 5). Nonetheless, prolonged type I IFN production causes a rather suppressive phenotype and disease progression (Swiecki and Colonna 2011). It has been observed that epithelial cells but also DCs lacking IFNAR are more prone to develop cancer, thus highlighting the importance of an intact type I IFN signaling for the prevention of cancer (Zitvogel *et al.* 2015). In the context of autoimmunity, a high abundance of type I IFNs has been observed. In lupus, for example, IFNα levels were shown to be increased thereby promoting disease progression (Barrat and Su 2019). In immunotherapy, impaired cytokine levels might induce resistance to therapy. This dependence is based on the involvement of type I IFNs in processes like DC maturation, activity of cytotoxic T cells and survival of memory T cells. Type I IFNs can also exhibit direct effects on tumor cells by inhibition of proliferation and induction of cell death via apoptosis (Budhwani *et al.* 2018).

It has been shown that traditional therapies including chemotherapeutics and oncolytic viruses but also new immunotherapies depend on balanced type I IFN signaling (Zitvogel *et al.* 2015). Application of type I IFNs in clinical settings has induced inferior results with severe side effects and poor response rates. Under specific conditions including loss of type I IFN signaling as well as chronic overexpression, type I IFNs can also promote tumor growth and immune escape (Budhwani *et al.* 2018). Nevertheless, type I IFNs have also shown advantageous results for cancers like ulcerative melanoma and hepatitis B virus-induced carcinoma (Zitvogel *et al.* 2015). New immunotherapeutic approaches aim at the combinatorial administration of type I IFNs with other immunotherapeutic drugs. These involve agents that stimulate signaling pathways leading to type I IFN expression, the binding of type I IFNs to tumor-specific antibodies which provides a target-directed delivery of the cytokine and genetically modified immune cells that express type I IFNs as soon as they reach the tumor microenvironment (Zitvogel *et al.* 2015).

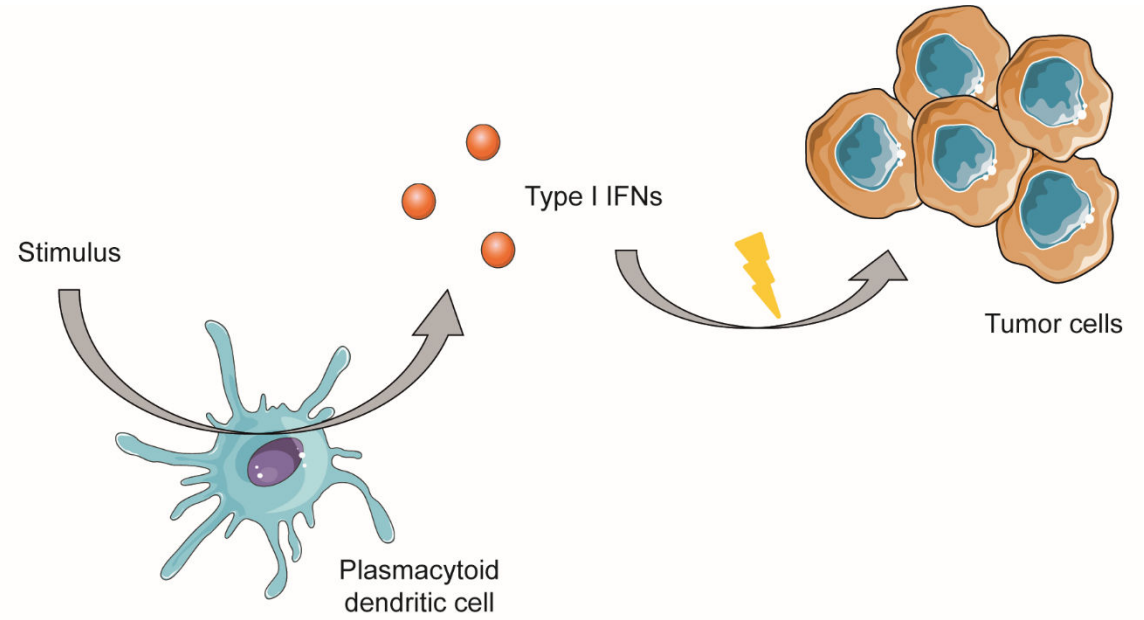

Figure 5: Type I IFNs are essential for successful anti-cancer responses. Upon recognition of stimuli such as the TLR9 ligand CpG, pDCs produce vast amounts of type I IFNs which ultimately are necessary for anti-cancer immune responses.

Taken together, the presence of type I IFNs is essential for successful therapy, thus highlighting the need for balanced immunotherapeutic approaches. Nevertheless, combination therapies might support immunotherapies involving type I IFNs. Natural products and HDACi provide potential sources for new drugs and are described in the following.

1.5 Natural products

Natural products provide a promising source for new anti-cancer and anti-bacterial drugs. They comprise many highly bioactive, chemically diverse secondary metabolites produced by organisms such as marine sponges or endophytic fungi as an adaption to biotic and abiotic stress factors (Haefner 2003; Yang, Wen*, et al.* 2018). Natural products have a long history in drug development especially for the treatment of cancer. Today, approximately half of all anti-cancer drugs are natural products or derived therefrom (Newman and Cragg 2016). Nevertheless, they are also extensively studied for the treatment of infections. Prominent examples of drugs are the antibiotics penicillin and gentamicin but also the development of aspirin has been inspired by natural products (Wright 2017; Butler 2004). In general, natural products have been tested in various clinical trials for disease groups like cancer, infections, diseases affecting the

cardiovascular system and metabolism as well as for the treatment of inflammation and neurologic diseases (Butler *et al.* 2014).

So far, natural products are not yet a focus of immunotherapeutic drug development, but compounds have been identified that show promising immunostimulatory features such as phomoxanthone A isolated from an endophytic fungus. Phomoxanthone A has been found to activate T and NK cells as well as macrophages with simultaneous killing of resistant cancer cells by induction of apoptosis (Rönsberg *et al.* 2013; Wang *et al.* 2019). Additionally, there are some studies that, for example, describe T cell activating effects and the induction of cytokine production by plant-derived natural products with subsequent anti-cancer effects (Baraya *et al.* 2017). Some other compounds like curcumin and flavonoids are in clinical trials for cancer therapy. The mode of action of curcumin, for example, relies on the suppression of regulatory T cell functions by decreased expression or secretion of inhibitory molecules and cytokines including reduced levels of IL-2 (Bahrami *et al.* 2019). In general, natural products are discussed to be suitable for combination treatment with known immunotherapeutic drugs for enhancement of immune modulating functions (Tewary *et al.* 2017).

1.6 Histone deacetylase inhibitors as epigenetic regulators

Epigenetics comprises heritable modifications of the DNA structure that do not alter the DNA sequence itself. Rather, addition and removal of chemical groups influences chromatin structure and DNA accessibility and thus gene transcription (Mohammad *et al.* 2019). HDACs are epigenetic regulators that remove acetyl groups from lysine residues of histone and non-histone proteins (Figure 6). HDACs work in balance with histone acetylases (HATs) hence modifying gene transcription. In an acetylated state, chromatin is transcriptionally active, while gene expression is repressed when chromatin is deacetylated (Li and Seto 2016; Banik *et al.* 2019). Non-histone targets that are modified by HDACs include proteins relevant for gene expression and transcription such as transcription factors, chaperone proteins and regulators of nuclear import (Banik *et al.* 2019).

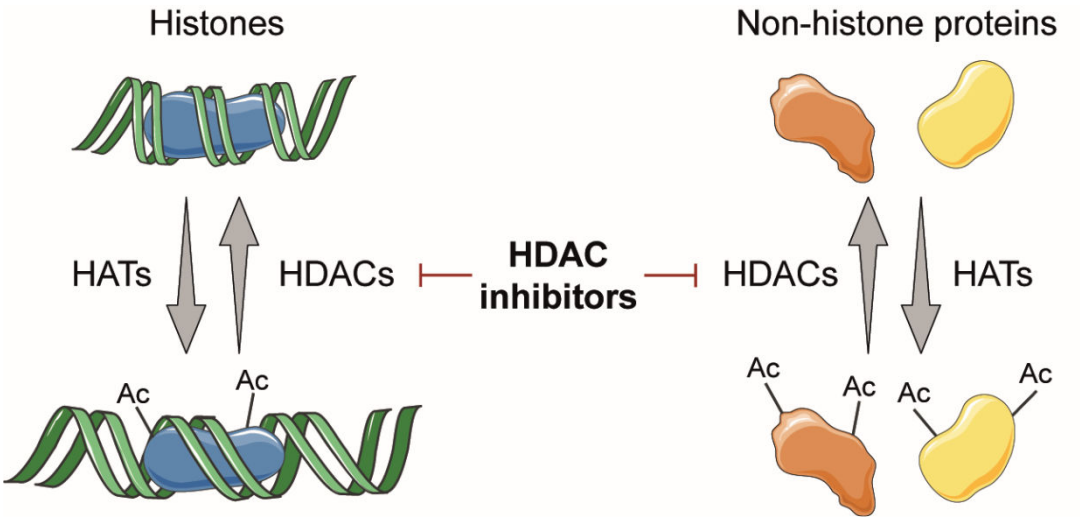

Figure 6: HDACs and HATs. HDACs deacetylate histones (blue) as well as non-histone proteins (yellow/orange), a process that is balanced with acetylation by HATs. HDACs can be inhibited by HDACi. Ac = acetyl group.

HDACs are classified based on their sequence similarity in yeast: HDAC1, 2, 3 and 8 belong to HDAC class I and are localized in the nucleus (Table 1). HDAC4, 5, 7 and 9 are members of class IIa and can be present in both nucleus and cytoplasm (Li and Seto 2016; Banik *et al.* 2019). Class IIb consists of HDAC6 and 10 which primarily can be found in the cytoplasm but also have been observed in the nucleus (Cheng *et al.* 2014). Class III is comprised of the sirtuins (SIRT) 1-7 which are nicotinamide adenine dinucleotide $(NAD)^+$-dependent and either localized in the nucleus, mitochondria or in the cytoplasm (Banik *et al.* 2019). The last class, class IV, has only one member, HDAC11. In contrast to class III HDACs, HDACs of class I, II and IV are zinc-dependent enzymes (Li and Seto 2016; Banik *et al.* 2019).

Table 1: Classes of HDACs and their members.

HDAC class		**Members**
Class I		HDAC1, 2, 3, 8
Class II	Class IIa	HDAC4, 5, 7, 9
	Class IIb	HDAC6, 10
Class III		SIRT1-7
Class IV		HDAC11

HDACs often show modified expression and function in cancer. HDAC1 has been shown to be upregulated in prostate, gastric and colon cancer, HDAC6 in mammary tumors but

also other HDACs display an imbalanced expression. This suggests a fundamental role of HDACs in the regulation of the expression of genes involved in tumor prevention and defense (Banik *et al.* 2019). Consequently, HDACi are a central research topic in cancer therapy. As HDACs are usually associated with repressed gene expression, treatment with HDACi can reverse this process (Shen *et al.* 2016). Pan HDACi like vorinostat are approved for treatment of relapsed and refractory T cell lymphoma. One big challenge of pan HDACi is their unspecificity which leads to a wide variety of effects on pathways related to survival and immune responses. This causes not only severe side effects in patients related to toxicity but also higher therapeutic success in hematological cancers compared to solid tumors (Knox *et al.* 2019). Additional HDACi were tested in combination with immune checkpoint inhibitors and showed promising results including reduced resistance and tumor regression. Other synergistic or additive effects might occur in combination with chemotherapeutic agents or radiation therapy (Banik *et al.* 2019). Here, it might be promising to first apply HDACi for induction of changes in gene expression of tumor cells prior to administration of other drugs that subsequently can target the sensitized tumor (Mohammad *et al.* 2019).

Some HDACi have also been found to possess immunomodulatory activities. For example, the pan HDACi panobinostat was shown to suppress DC functions by dampening expression of IL-6, IL-10, IL-12, IL-23 and TNF by activated DCs (Song *et al.* 2011). In contrast, other HDACi improved efficacy of immunotherapy and caused an increase in tumor antigen expression and a modified functioning of suppressive immune cells and signaling pathways (Banik *et al.* 2019). Especially HDAC6 is a promising target for epigenetic modulation in immunotherapy. It has several hundred targets including α tubulin, the chaperone HSP90 and cortactin as main targets thus inhibition disrupts cellular processes like aggresome formation. HSP90, for instance, functions as a chaperone for many oncoproteins as well as for the IKK complex which is part of the NFκB signaling cascade. Inhibition of deacetylation of HSP90 causes its hyperacetylation and loss of activity (Cosenza and Pozzi 2018; Schopf *et al.* 2017). HSP90 additionally complexes with STAT2, -3 and -5 which are important signal transmitters after cytokine stimulation (Schopf *et al.* 2017). In summary, HDAC6 regulates various cellular processes like cell migration, cell contact and immune responses (Valenzuela-Fernandez *et al.* 2008).

HDAC6 has directly been associated with several immune functions covering APC contact with T cells, inflammatory macrophage responses and functioning of regulatory T cells (Serrador *et al.* 2004; de Zoeten *et al.* 2011; Halili *et al.* 2010). As an encouraging feature, specific HDAC6i have shown to suppress tumor progression *in vivo* without inducing severe side effects (Woan *et al.* 2015). Moreover, complete genetic abrogation

of HDAC6 does not influence cellular functions and HDAC6 knockout mice develop normally (Zhang *et al.* 2008). This makes HDAC6 an encouraging target for epigenetic therapy that could complement immunotherapeutic approaches.

1.7 Lack of screening guidelines of natural products

Natural products provide an unelaborated pool of highly bioactive molecules making them promising sources for drug development (Newman and Cragg 2016). Nonetheless, natural products are not yet commonly used for immunotherapeutic drug development, thus appropriate screening guidelines for the definition of their suitability for immunotherapeutic application are missing.

In general, two screening approaches are used for the identification of promising compounds: Phenotype-based or target-based approaches (Zheng *et al.* 2013). Target-based drug discovery has become increasingly important over the last years although both approaches could present promising compounds. Target-based drug discovery starts with the decision for one specific target that is relevant or misregulated in a disease e.g. HDACs in cancer. Subsequently, assays are designed to screen libraries of natural products for compounds that target that molecule of interest. In following assays, the effectivity of an identified promising compound is verified and chemical optimization is performed. In contrast, in phenotypic screenings compounds are analyzed for desired activities such as activation of immune cells without initial knowledge of the molecular target. Consequently, such compounds can have different targets. Phenotypic screening approaches are less artificial than target-based approaches and often lead to the identification of lead compounds that inspire further drug development (Zheng *et al.* 2013).

In industry, natural products are usually tested in high throughput screenings (HTS) allowing the analysis of natural product libraries with ten thousands of compounds in short time (Zhang *et al.* 1999). One example of a phenotypic HTS platform is presented by Perez Del Palacio *et al*. for screening of microbial natural products for immunomodulatory characteristics (Perez Del Palacio *et al.* 2016). In this study, the aim was to identify compounds that can help in the treatment of inflammatory diseases. First, microbial extracts were analyzed for NO production by the macrophage cell line RAW264.7 before analysis of IL-8 secretion by the intestinal epithelial cell line Caco-2. This screening platform necessitates specific facilities and the availability of appropriate instruments for HTS (Perez Del Palacio *et al.* 2016).

Another target-based approach was established by Mo *et al*. aiming at the identification of compounds that target the inhibitor of apoptosis protein (IAP) (Mo *et al.* 2019). As this protein is important in cancer immunity, immune cell-cancer cell co-culture systems were applied and viability and antagonism of IAP evaluated. Nevertheless, this approach was initially restricted to the analysis of an apoptosis-related protein and the treatment of cancer (Mo *et al.* 2019).

In summary, there are screening approaches that aim at the identification of natural products targeting immune cells. However, these platforms usually are restricted to certain disease types or molecular targets, do not provide distinct guidelines and thus do not enable the analysis of immune activation in general. The work presented in this thesis aims at the identification of immune activating natural products and HDACi that target APCs and thus could inspire drug development for a wide range of diseases. The aim of this thesis is further described in the following.

1.8 Aim of this thesis

The increase in incidence rates and resistances causes an urgent need to find and develop new drugs especially for the most frequent disease groups of cancer and infections. Immunotherapy offers alternative, disease-specific treatment options instead of traditional therapies and provides opportunities for further development of drugs with less side effects and a higher effectiveness against resistant cells. APCs represent promising targets for immunotherapy while a balanced cytokine environment is necessary to maintain their functions. Nevertheless, these cells are often inactivated especially in the context of cancer and current drug development requires new approaches to reactivate these cells for the initiation of successful innate and adaptive immune responses. Natural products represent a great pool of highly bioactive yet unexplored compounds promising for drug discovery. However, the lack of appropriate screening guidelines for the identification of immune activating properties of natural products and their suitability for immunotherapeutic drug development hampers this process.

Consequently, one aim of this study was the definition and establishment of screening guidelines that help in the evaluation of auspicious natural products for immunotherapeutic approaches. To not be limited in specific targets, a phenotype-based screening approach was developed which allows the detection of natural products with a variety of possible targets. The usage of primary cells from mice facilitates screening

settings that are close to physiological conditions and simplifies the transition to *in vivo* experiments later on.

For validation of the newly created screening guidelines, 240 natural products obtained from endophytic fungi and marine sponges were screened accordingly. These provide a high diversity of structures, potential functions and modes of action and thus increase the likelihood of successful identification of promising structures that can serve as lead structures inspiring drug development.

Besides natural products in general, HDACi represent a group of molecules derived from natural products promising especially for anti-cancer development. This is based on the frequently aberrant expression and function of HDACs in the context of cancer. Pan HDACi are already used in clinics but often are associated with severe side effects. For successful natural defense and therapeutic treatment of cancer, the presence of type I IFNs is essential. Based on previous unpublished findings of our group that showed that a pan HDACi was capable of inducing type I IFN expression by pDCs when additionally stimulated with the synthetic dsRNA analog poly I:C, two HDACi with preferences for HDAC6 or HDAC6 and HDAC1 were analyzed for their potential to trigger type I IFN secretion by pDCs. HDAC6i have already been shown to reduce tumor growth *in vivo* without inducing side effects. Moreover, HDAC6i are generally regarded as encouraging immune stimulators probably based on their effects on non-histone targets. Thus, HDAC6i might provide more targeted anti-tumor responses with less severe side effects for patients.

Taken together, this study aims at the identification of new, promising compounds that aid in the development of drugs against cancer and infections and provide new tools to prevent and treat resistances.

2. Methods and material

In the following sections, all methods and material used in this thesis are illustrated. The methods section comprises the cultivation of bone marrow cells and HT1080 cells, assays for the analysis of cytotoxicity and cell numbers, comparative analyses for the determination of additional beneficial bioactivities of natural products, IL-12p40 assays with the application of flow cytometry and enzyme-linked immunosorbent assays (ELISA), T cell activation assays and the description of the HDACi experiments. Furthermore, all mouse lines used in the experiments are listed as well as the source of natural products and HDACi, cell lines, growth factors, the composition of media and buffers, devices and specific information regarding antibodies, beads, kits and further consumables. Finally, software used for analysis and presentation of results is given.

2.1 Mice

Experiments have been performed using wildtype C57BL/6N mice for cytotoxicity assays, IL-12p40/GFP reporter (get40) mice (Figure 7A) for IL-12p40 assays (Reinhardt *et al.* 2006), OVA-specific, MHC class II-restricted TCR-transgenic (OTII) mice for T cell activation experiments (Barnden *et al.* 1998) or IFNβ/YFP reporter (mob) mice (Figure 7B) for HDACi assays (Scheu *et al.* 2008). All mouse lines were genetically backcrossed to C57BL/6N background and were kept under specific pathogen-free conditions in the animal research facility of the University of Düsseldorf according to German animal welfare guidelines.

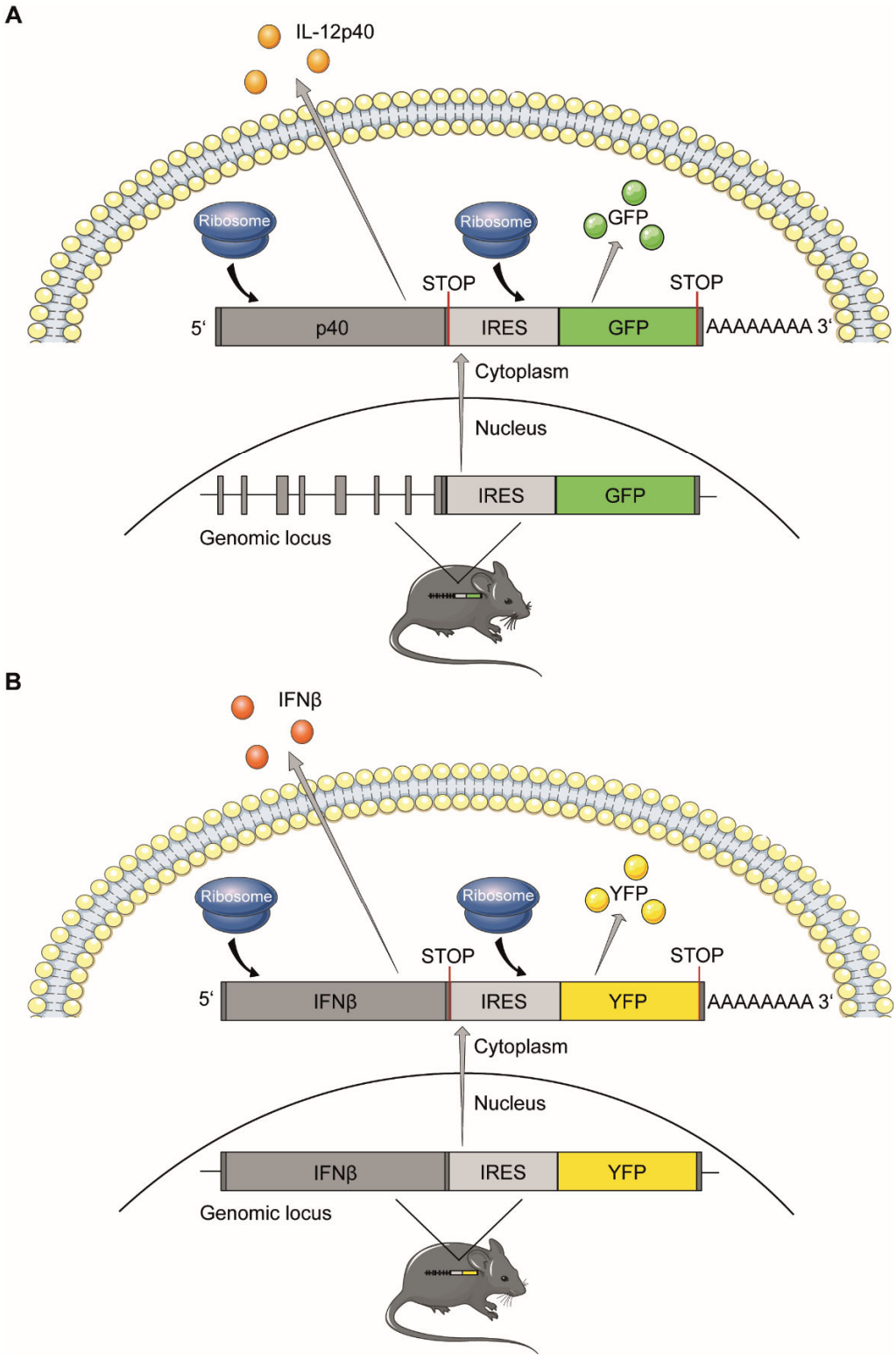

Figure 7: The get40 reporter mouse model (Reinhardt *et al.* 2006) (A) and the mob reporter mouse model (Scheu *et al.* 2008) (B). Get40 mice are knockin mice that express the *p40* gene linked with GFP via an internal ribosomal entry site (IRES). Mob mice are knockin mice that express the *ifnb* gene linked with YFP via an IRES. This allows detection of IL-12p40/GFP or IFNβ/YFP, respectively, by for example flow cytometry. This figure has been modified from Richter *et al.* (2019).

2.2 Bone marrow preparation and primary cell cultivation

For preparation of bone marrow for cell cultivation, mice were sacrificed via cervical dislocation. Femurs and tibias were isolated, disinfected for 3 min in 70% ethanol (EtOH) and the bone marrow was flushed out with FCS-containing medium. After a centrifugation step (1200 rpm, 4°C, 5 min), erythrocytes were removed by resuspension in 3 ml Morphisto erylysis buffer for 3 min. The reaction was stopped with at least the double amount of PBS or medium and cells were filtered through 100 µm cell strainers to remove remaining bone fragments. After centrifugation, cells were resuspended in medium and counted for cell cultivation (see section 2.4.1 Trypan blue cell exclusion).

2.2.1 GM-CSF cultures

GM-CSF cultures were performed as described previously (Scheu *et al.* 2008). Briefly, 2 x 10^6 bone marrow cells were resuspended in GM-CSF medium (see section 2.10.3 Media and buffers) and given to 94 x 16 mm (Greiner Bio-One) or 92 x 16 mm (Sarstedt) non-treated cell culture dishes. Culture plates have been changed to improve experimental conditions after reassurance of the robustness of the results. Subsequently, cells were incubated at 37°C and 10% CO_2. On day three, 10 ml fresh medium was added to the cultures. On day six, 10 ml supernatant were removed for centrifugation (1200 rpm, 4°C, 5 min). The cell pellet was resuspended in 10 ml fresh medium and added to the culture plates again. Stimulation experiments were performed on day nine according to experimental procedures.

2.2.2 Flt3L cultures

Flt3L cultures were applied as described previously (Scheu *et al.* 2008; Bauer *et al.* 2016; Ali *et al.* 2018). In short, 20 x 10^6 bone marrow cells were resuspended in Flt3L medium (see section 2.10.3 Media and buffers) and given to 94 x 16 mm non-treated cell culture dishes (Greiner Bio-One). Cells were incubated at 37°C and 10% CO_2. On day five, 5 ml supernatant were removed for centrifugation (1200 rpm, 4°C, 5 min). The cell pellet was resuspended in 5 ml fresh medium and added to the culture plates again. Stimulation experiments were started on day seven according to experimental procedures.

2.2.3 M-CSF cultures

M-CSF cultures were performed as described previously (Scheu *et al.* 2008). Briefly, 1.5 x 10^6 bone marrow cells were resuspended in M-CSF medium (see section 2.10.3

Media and buffers) and given to 94 x 16 mm non-treated cell culture dishes (Greiner Bio-One). Cells were incubated at 37°C and 10% CO_2. On day three, 10 ml fresh medium was added to the cultures. Stimulation experiments were performed on day six according to experimental procedures.

2.3 Cultivation of HT1080 cell lines

HT1080 cell lines (see section 2.10.2 Cell lines) which were used for compensation of flow cytometry analyses, were cultivated in 25 cm^2 culture flasks in HT1080 medium at 37°C and 10% CO_2 (see section 2.10.3 Media and buffers). Cells were split twice a week at 80-90% cell density or the day before the flow cytometry experiments. For this, culture flasks were washed with PBS before addition of 1 ml 0.05% trypsin-EDTA. After incubation at 37°C for 1-2 min, cells were resuspended in fresh HT1080 medium and transferred into new culture flasks or used for experiments.

2.4 Analysis of cytotoxicity

In the following sections, the two methods used for determination of live cell number or cell viability in general are described. Trypan blue cell exclusion was applied to calculate the number of live cells in a sample prior to seeding of cells. MTT assays were deployed for the analysis of toxic effects of compounds on the metabolic activity and thus viability of cells.

2.4.1 Trypan blue cell exclusion

For cell counting, cells were diluted 1:10 in 0.4% trypan blue and counted using a Neubauer cell chamber or a Nexcelom Cellometer Auto T4. For manual counting with a Neubauer cell chamber, cell numbers were calculated using the formula:

$$\text{cell number} = \frac{\text{counted cells x dilution factor x } 10.000}{\text{counted squares}} .$$

2.4.2 MTT assays

For the analysis of cytotoxicity, MTT assays have been performed. Initially, cell cultures were prepared as described previously in section 2.2 Bone marrow preparation and primary cell cultivation. After the respective incubation periods, cell culture dishes were kept at 4°C for 30 min before manual removal of the cells using cell scrapers. Cells were centrifuged (1200 rpm, 4°C, 5 min), resuspended in fresh medium and counted to be

seeded in non-treated 96 well plates. 8 x 10^4 GM-CSF-cultured cells, 4 x 10^5 Flt3L-cultured cells or 6 x 10^4 M-CSF-cultured cells were added to each well and stimulated with varying concentrations (0.1, 1 or 10 µM) of natural products. Cells treated with DMSO or staurosporine served as controls. After 24 h, 10% 5 mg/ml thiazolyl blue tetrazolium bromide (MTT) was added to each well for additional 3 h. Finally, the supernatant was removed and formazan crystals were dissolved in 5% formic acid in isopropanol. Optical densities (ODs) were measured at 570 nm using a microplate reader.

2.5 Comparative analyses for beneficial bioactivities

Comparative analyses for additional beneficial bioactivities were performed by cooperation partners within the research training group GRK2158 on compounds that were proven to be non-toxic for target immune cells in MTT assays. These screens comprised the determination of the toxicity for cancer cell lines (Jurkat, Ramos and p53-mutated pancreatic cancer cells) and for pathogens (*Toxoplasma gondii, Mycobacterium tuberculosis* and gram-negative bacteria such as *Escherichia coli*) as well as the evaluation of pro- or anti-autophagic effects. Natural products were determined as suitable for following analyses for immune activation if they showed promising activities in at least one screening conducted by cooperation partners and displayed direct anti-tumor or anti-pathogenic characteristics.

2.6 IL-12p40 assays

For the analysis of IL-12p40 production by natural product-treated cells, GM-CSF cultures were prepared from two separately treated get40 mice according to section 2.2.1 GM-CSF cultures. For stimulation on day nine, cell culture dishes were kept at 4°C for 30 min before manual removal of the cells using cell scrapers. Cells were centrifuged (1200 rpm, 4°C, 5 min), resuspended in fresh medium and counted to be seeded at 5 x 10^5 cells/well in 0.5 ml in non-treated 12 well plates. Cells were stimulated with varying concentrations (0.1, 1 or 10 µM) of natural products with or without additional 0.1 µM CpG 2216 or 1 ng/ml LPS to a final volume of 1 ml/well. Untreated cells or cells treated with CpG 2216 or LPS alone were used as controls. Before analysis of the impact of natural products, CpG 2216 and LPS were titrated on the cells. After overnight stimulation (16 h), supernatant was collected for ELISA experiments and the cell culture plates were incubated at 4°C for 30 min before manual removal of the cells using cell

scrapers and distribution into flow cytometry tubes. After centrifugation (1200 rpm, 4°C, 5 min), unspecific Fc-binding sites were blocked with a CD16/32 antibody (clone 93; 1:100) at 4°C for 10 min. Subsequently, cells were stained with an antibody mixture consisting of CD11c-APC Cy7 (clone N418; 1:100), CD86-PE Cy7 (clone GL-1; 1:200) and MHC class II-biotin (clone 2G9; 1:400) at 4°C for 30 min protected from light. Afterwards, samples were washed with flow cytometry buffer (1200 rpm, 4°C, 5 min) and incubated with streptavidin-PerCP Cy5.5 (1:300) at 4°C for additional 10 min protected from light. After a final centrifugation step, DAPI (1:2000) was added to the cells. For compensation, BD CompBeads and a mixture of HT1080 and HT1080 eGFP cells were used. Measurement was performed using a BD FACSCanto II by recording 50.000 events.
For definition of the amount of secreted cytokine from the collected supernatant, BD OptEIA Mouse IL-12 (p40) ELISAs were performed according to the manufacturer's protocol.

2.7 T cell activation assays

For the analysis of the T cell activation capacity of natural product-stimulated GM-CSF-cultured cells, T cell assays were performed. Initially, GM-CSF cultures were prepared from two separately treated wildtype mice according to section 2.2.1 GM-CSF cultures. For stimulation on day nine, cell culture dishes were kept at 4°C for 30 min before manual removal of the cells using cell scrapers. Cells were centrifuged (1200 rpm, 4°C, 5 min), resuspended in fresh medium and counted to be seeded in non-treated 96 well U-bottom plates. Before stimulation with natural products, GM-CSF cells were titrated to obtain optimal cell counts. Subsequently, 1 x 10^4 cells/well were seeded in 50 µl OTII medium (see section 2.10.3 Media and buffers). Cells were stimulated in duplicates with varying concentrations (0.1, 1 or 10 µM) of natural products with or without additional 0.1 µM CpG 2216 or 1 ng/ml LPS to a final volume of 100 µl/well. Untreated cells or cells treated with CpG 2216 or LPS alone were us-ed as controls. For samples with T cells only, the same stimulation conditions were set up without addition of GM-CSF-cultured cells. After 24 h stimulation, 2 x 10^3 $CD4^+$ cells from lymph nodes from OTII mice were added to the wells. For that, OTII mice were sacrificed via cervical dislocation and mesenterial, axial, brachial, inguinal, paraaortal and submandibular lymph nodes were isolated. For isolation of cells, lymph nodes were shredded with the help of cell strainers and pressure applied with syringe plugs. Cells were centrifuged (1200 rpm, 4°C, 5 min), counted and treated with a CD16/32 antibody (clone 93; 1:100) at 4°C for 10 min. For positive

selection of $CD4^+$ cells, cells were separated using magnetic cell separation (MACS, Miltenyi Biotec) according to the manufacturer's protocol. In short, cells were incubated with CD4-biotin (clone RM4-4; 1:50) at 4°C for 45 min. After washing, anti-biotin microbeads were added to the samples and incubated at 4°C for 15 min. Cells were separated by running the samples along LS columns in magnets. Afterwards, isolated $CD4^+$ cells were added to the GM-CSF-cultured cells as mentioned above and primed with 300 nM $OVA_{323-339}$ peptide. Supernatant was collected on day five of the co-cultivation. For definition of the amount of secreted cytokine, DuoSet mouse IL-2 ELISAs were performed according to the manufacturer's protocol.

2.8 HDACi assays

For the analysis of immune stimulation by HDACi, Flt3L cultures were prepared from mob mice according to section 2.2.2 Flt3L cultures. On day six, HDACi were directly added to the culture dishes in varying concentrations (KSK64: 0.1, 1, 10 or 100 nM; MPK264: 10, 100, 500, 1000 or 2000 nM) for 24 h. On day seven, cells were stimulated with poly I:C. For that, cell culture dishes were kept at 4°C for 30 min before manual removal of the cells using cell scrapers. Cells were centrifuged (1200 rpm, 4°C, 5 min), resuspended in fresh medium and counted to be seeded at 1 x 10^6 cell/well in 0.5 ml in non-treated 24 well plates. HDACi-treated cells were either left without an additional stimulus or stimulated with 100 µg/ml poly I:C in triplicates. Untreated cells and cells treated with poly I:C or 1 µM CpG 2216 were used as controls. After 24 h, cell culture plates were put at 4°C for 30 min before manual removal of the cells using cell scrapers and distribution into flow cytometry tubes. After centrifugation (1200 rpm, 4°C, 5 min), unspecific Fc-binding sites were blocked with a CD16/32 antibody (clone 93; 1:100) at 4°C for 10 min. Subsequently, cells were stained with an antibody mixture consisting of CD11c-PE Cy7 (clone N418; 1:200), CD11b-APC Cy7 (clone M1/70; 1:200), MHC class II-PE (clone N5/114.15.2; 1:200), CD86-PerCP Cy5.5 (clone GL-1; 1:200), B220/CD45R-APC (clone RA3-6B2; 1:100), TCRβ-BV421 (clone H57-597; 1:100) and CD19-BV421 (clone 6D5; 1:100) at 4°C for 30 min protected from light. After centrifugation (1200 rpm, 4°C, 5 min), DAPI (1:2000) was added to the cells. For compensation, BD CompBeads and a mixture of HT1080 and HT1080 eYFP cells were used. Measurement was performed using a BD FACSCanto II by recording 100.000 events.

2.9 Software

General data analysis was performed using Miscrosoft Excel and GraphPad Prism 5. Flow cytometry results were analyzed with FlowJo 10.5.3. All figures were created using Adobe Illustrator CS6. Graphics were designed with Servier Medical Art according to Creative Commons Attribution 3.0 Unported License (https://creativecommons.org/licenses/by/3.0/). Changes were made to the original cartoons.

2.10 Material

In the following sections, the origin of compounds, cells, devices and further material used in this thesis are listed.

2.10.1 Compounds

Natural products analyzed in this thesis were provided by the research group of Prof. Dr. Dr. h.c. Peter Proksch, Institute of Pharmaceutical Biology and Biotechnology, Heinrich Heine University Düsseldorf, Germany. The structures of the three most promising natural products obtained by the presented screening platform are illustrated in Figure 8. A detailed list with all natural products analyzed in this thesis can be found in the appendix in combination with the cytotoxicity data. Additional cytochalasin D was purchased from Sigma-Aldrich, catalogue number C8273.

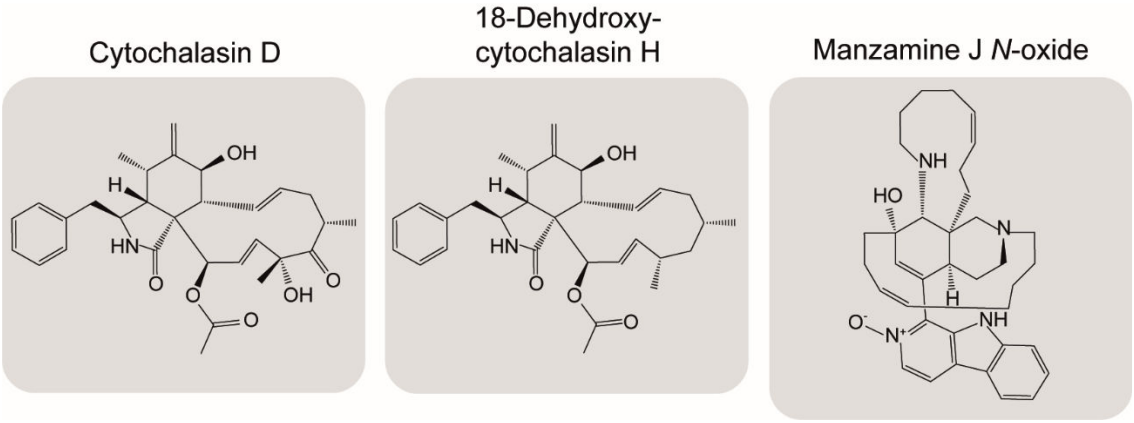

Figure 8: Structures of the three most promising natural products.

The two HDACi KSK64 and MPK264 were provided by Prof. Dr. Thomas Kurz and Marc Pflieger, Institute of Pharmaceutical and Medicinal Chemistry, Heinrich Heine University

Düsseldorf, Germany (Figure 9). According to this cooperation partner, KSK64 preferentially targets HDAC6 and HDAC1 while MPK264 preferentially targets HDAC6.

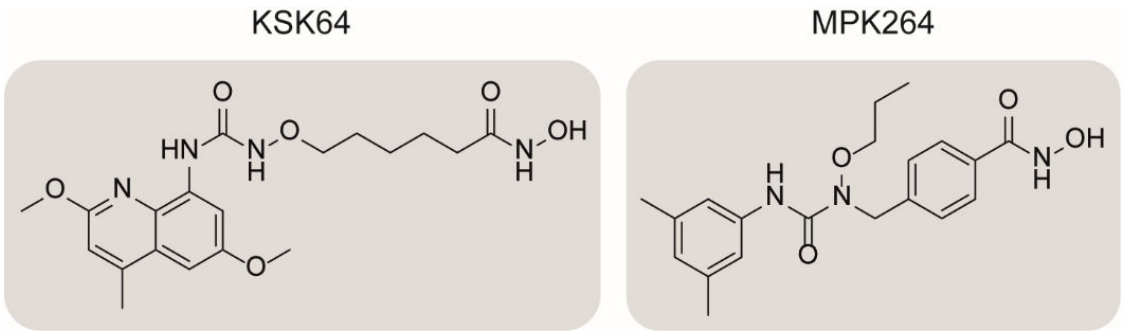

Figure 9: Structures of the two HDACi KSK64 and MPK264.

2.10.2 Cell lines

For compensation in flow cytometry, HT1080 cell lines have been used. The cell lines and their suppliers are listed in Table 2.

Table 2: Cell lines and their origin.

Cell line	**Origin**
HT1080	Leibniz Institute DMSZ, Braunschweig
HT1080 eGFP	Prof. Dr. Ingo Schmitz, Helmholtz Center for Infection Research, Braunschweig
HT1080 eYFP	Prof. Dr. Ingo Schmitz, Helmholtz Center for Infection Research, Braunschweig

2.10.3 Media and buffers

For cell cultivation and experimental setups, different media and buffers have been used and are listed in Table 3.

Table 3: Constituents of media and buffer.

Name	Constituents
GM-CSF medium	VLE DMEM medium 10% FCS 3-5% GM-CSF
Flt3L medium	VLE RPMI 1640 medium 10% FCS 5-7.5% Flt3L
M-CSF medium	VLE RPMI 1640 medium 10% FCS 15% M-CSF
OTII medium	RPMI medium 1640 10% FCS
HT1080 medium	VLE RPMI 1640 medium 10% FCS 1% penicillin/streptomycin
Flow cytometry buffer	PBS 2% FCS 2 mM EDTA

2.10.4 Growth factors

For cultivation of bone marrow cells, different growth factors have been used and are listed in Table 4. After production of growth factor-containing supernatant, the optimal concentrations for application in experiments have been determined and are indicated in the respective method sections.

Table 4: Origin of the growth factors.

Growth factor	Origin
GM-CSF	Supernatant of X63O cells
Flt3L	Supernatant of CHO cells
M-CSF	Supernatant of L929 cells

2.10.5 Consumables and kits

Consumables and kits that have been used throughout this thesis are listed in Table 5.

Table 5: Consumables and kits.

Name	Supplier	Catalog no.
2-mercaptoethanol (50 mM)	Thermo Fisher Scientific	31350-010
2-propanol	VWR Chemicals	20842-330
5 ml polystyrene round-bottom tube 12x75 mm style	Corning	352052
Assay Plate, 96 Well, Flat Bottom, Half Well	Corning	3690
BD OptEIA Mouse IL-12 (p40) ELISA Set	BD Biosciences	555165
Cell culture flask, 25 cm^2, angled	Corning	3056
Cell strainer 70 µm nylon	Corning	352350
Cell strainer 100 µm nylon	Corning	352360
CpG 2216	TIB Molbiol	
DAPI	Sigma-Aldrich	10236276001
Dimethyl sulphoxide (DMSO) Hybri-Max	Sigma-Aldrich	D2650
DPBS (1X), Dulbecco's phosphate buffered saline	Thermo Fisher Scientific	14190-094
DuoSet mouse IL-2 ELISA	R&D Systems	DY402
Erylysis buffer pH 7.2-7.4	Morphisto	12972-00500

Name	Supplier	Catalog no.
Ethanol absolute	VWR Chemicals	20821-330
Fetal bovine serum	PAN-Biotech	
Fetal bovine serum	Sigma-Aldrich	F7524
Formic acid	Merck	K13094964
LPS from *Salmonella minnesota* R595 (Re)	List Biological Laboratories, Inc.	304
LS columns	Miltenyi Biotec	130-042-401
Omnifix single-use syringe, 3 ml	Braun	4617022V
Ovalbumin (323-339)	Sigma-Aldrich	O1641
Penicillin/Streptomycin	Biochrom GmbH	A2212
Petri dish 92x16, non-treated	Sarstedt	821.473
Petri dish 94x16, non-treated	Greiner Bio-One	633181
Plate, 12 well, non-treated	Sigma-Aldrich	3737
Plate, 24 well, non-treated	Sigma-Aldrich	3738
Plate, 96 well, non-treated	Sigma-Aldrich	3370
Poly I:C	Amersham/GE Healthcare	274732
RPMI Medium 1640	Thermo Fisher Scientific	31870-025
Staurosporine	AdipoGen Life Sciences	AG-CN2-0022
Stripettes (1-50 ml)	Costar	
Thiazolyl blue tetrazolium	Sigma-Aldrich	M2128
Trypan Blue (0.4%)	Gibco	15250-061
Trypsin (0.05%)-EDTA	Gibco	25300-054
UltraPure 0.5 M EDTA, pH 8.0	Invitrogen	15575-038
VLE Dulbecco's MEM	Biochrom GmbH	FG 1445
VLE RPMI 1640 Medium	Biochrom GmbH	FG 1415

2.10.6 Antibodies and beads

Antibodies and beads that have been used for flow cytometry and MACS are listed in Table 6.

Table 6: Antibodies and beads.

Name	Clone	Supplier	Catalog no.
Anti-biotin MicroBeads		Miltenyi Biotec	130-090-485
Anti-mouse CD16/32 purified	93	Thermo Fisher Scientific	14-0161-85
APC anti-mouse CD45R/B220	RA3-6B2	BD Biosciences	553092
APC-Cy7 anti-mouse CD11b	M1/70	BD Biosciences	557657
APC-Cy7 anti-mouse CD11c	N418	Biolegend	117324
BD CompBeads anti-rat and anti-hamster		BD Biosciences	51-90-9000949
BD CompBeads negative control		BD Biosciences	51-90-9001291
Biotin anti-mouse CD4	RM4-4	BD Biosciences	557443
Biotin anti-mouse I-A/I-E	2G9	BD Biosciences	553622
Brilliant Violet 421 anti-mouse CD19	6D5	Biolegend	115549
Brilliant Violet 421 anti-mouse TCR β chain	H57-597	Biolegend	109229
PE anti-mouse I-A/I-E	N5/114.15.2	BD Biosciences	557000
PE-Cy7 anti-mouse CD11c	N418	Biolegend	117317

Name	Clone	Supplier	Catalog no.
PE-Cy7 anti-mouse CD86	GL-1	Biolegend	105014
PerCp-Cy5.5 anti-mouse CD86	GL-1	Biolegend	105027
PerCP-Cy5.5 streptavidin		BD Biosciences	551419

2.10.7 Devices

Devices that have been used for measurement of experimental results are listed in Table 7.

Table 7: Devices.

Name	Supplier
BD FACSCanto II	BD Bioscience
Cellometer Auto T4	Nexcelom Bioscience
Microscope Axiovert 100	Zeiss Germany
ST Sunrise remote microplate reader	Tecan
Neubauer-improved counting chamber	Marienfeld Superior

3. Results

The central aim of this thesis was the evaluation of immune stimulating properties of natural products and HDACi. As described in 1.8 Aim of this thesis, both natural products and HDACi represent promising sources for novel compounds inspiring drug development for the treatment of cancers and diseases caused by bacterial infections. In Figure 10, the workflow of the experiments conducted in this thesis is illustrated. By using different mouse models, natural products and HDACi were analyzed for their immune activating potential. After definition of screening guidelines, natural products were screened for cytotoxic effects on GM-CSF-, Flt3L- and M-CSF-cultured cells before determination of additional beneficial bioactivities against tumors or bacteria and immune activating characteristics via assessment of IL-12p40 production and T cell activation. Furthermore, the effects of HDAC6i and poly I:C stimulation on IFNβ production by pDCs obtained from Flt3L cultures were investigated. In the following sections, this newly established screening approach for the analysis of immune activating characteristics of natural products and their suitability for immunotherapeutic drug development as well as the potential of HDAC6i to induce type I IFN production is described in detail.

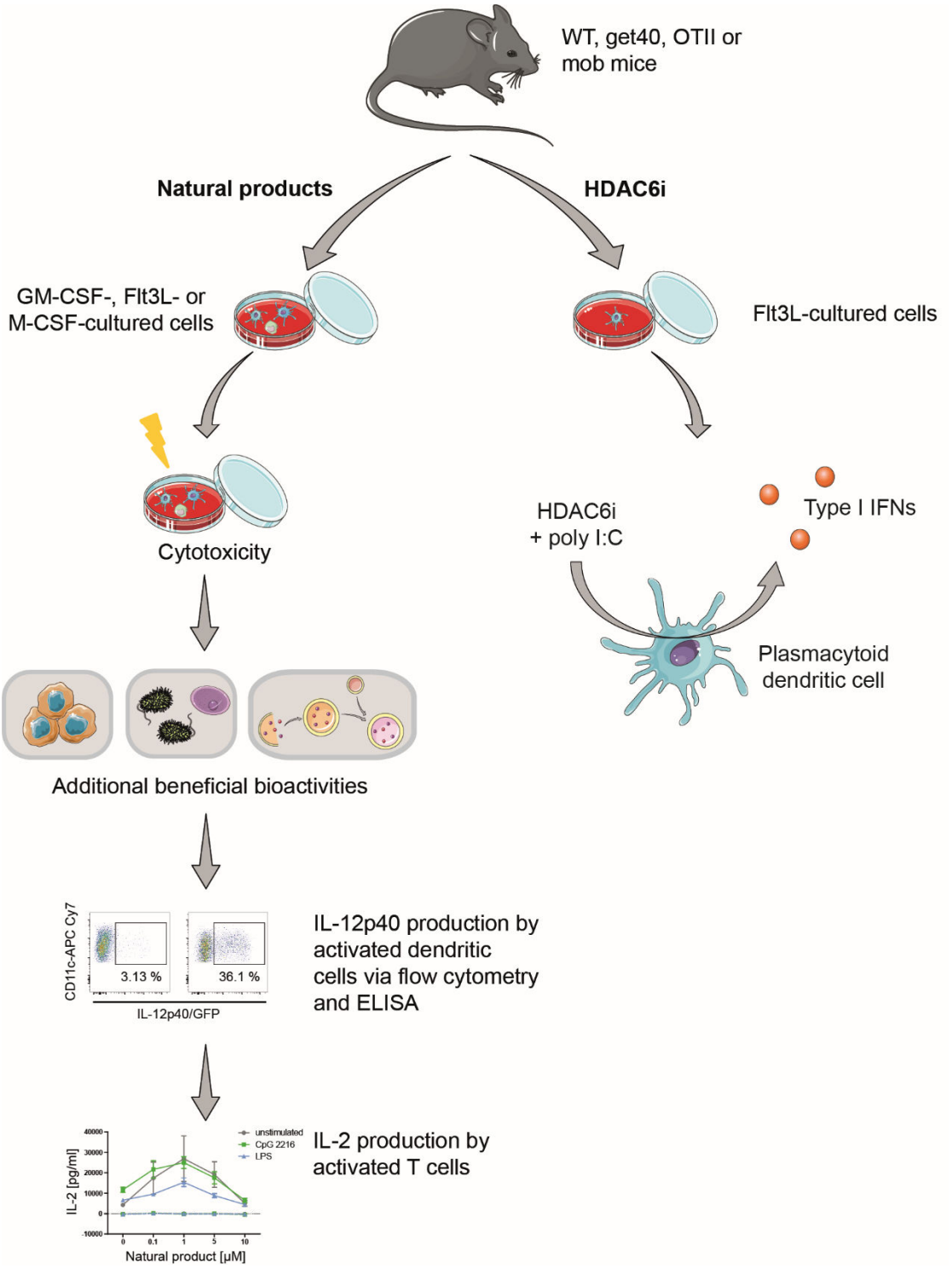

Figure 10: Workflow of the experiments conducted in this thesis. Different mouse models (WT, get40, OTII or mob mice) were used for the analysis of either the natural product library (left part) or HDAC6i (right part). Natural products were analyzed for cytotoxic effects, additional beneficial bioactivities, IL-12p40 production by activated DCs and the potential to activate T cells. Furthermore, two HDAC6i were tested for their capacity to induce type I IFN production by pDCs when additionally stimulated with poly I:C.

3.1 Guidelines for the definition of “appropriate” compounds

Due to the current lack of appropriate guidelines for screening big libraries of natural products or other compounds for immune activating potential and their suitability for immunotherapeutic drug development, new guidelines had to be defined and established initially. After intensive literature research, natural products are here defined to be promising for further anti-cancer and anti-infection drug development if they fulfill three criteria: They should not be toxic to immune target cells, exhibit additional beneficial bioactivities for anti-cancer or anti-infection treatment and induce an immune activating phenotype (Figure 11).

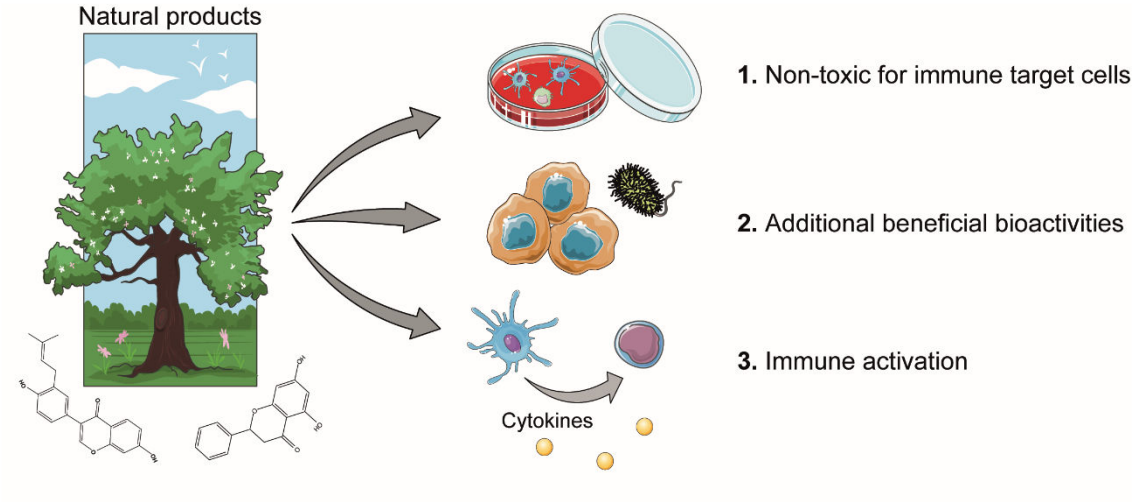

Figure 11: Guidelines for the definition of appropriate compounds. In this thesis, natural products are defined to be suitable for further immunotherapeutic drug development if they are non-toxic for immune target cells, here cDCs, pDCs and macrophages, if they display additional beneficial bioactivities and if they induce immune activation. This figure has been modified from Richter *et al.* (2019).

These screening guidelines should by itself be independent of the type of compounds tested. In this thesis, a natural product library was analyzed that contains compounds derived from endophytic fungi as well as marine sponges with a wide variety of structures and possible activities as well as known and unknown compounds. Screening of approved or known drugs might be useful for the identification of new targets and effects especially for diseases without effective therapies while unknown structures can inspire drug development by exerting new modes of action (Zheng *et al.* 2013).
Here, immune target cells are cDCs, pDCs and macrophages from GM-CSF-, Flt3L- and M-CSF-cultured bone marrow cell cultures, respectively. Nevertheless, any kind of cells could be used. The application of primary cells instead of cell lines offers the advantage

that these cells are closer to physiological conditions. They are non-transformed and non-immortalized, thus do not feature genetic changes. Additionally, although cultured with specific growth factors, bone marrow cultures comprise different cell types which reflects the complexity of the immune system. Natural products defined as promising for further drug development should accordingly not be toxic to cDCs, pDCs and macrophages. Furthermore, the identification of additional advantageous bioactivities exhibited by natural products in comparative analyses is important for the determination of any direct anti-cancer or anti-infection properties. In this thesis, this approach was conducted by the help of cooperation partners. Finally, the focus was set on compounds that activate immune cells and thus are candidates to counteract the suppressive phenotype of, for example, the tumor microenvironment.
In the following sections, experimental approaches that can be used to determine the fulfilment of these guidelines are given and the screening of the natural product library is presented.

3.2 Cytotoxicity assays

The first step in the definition of the suitability of compounds in general and natural products in particular is the analysis of cytotoxicity for target cells. Cell viability assays are extensively used experimental approaches applied in phenotypic screening approaches and can be deployed to determine e.g. metabolic turnover, mitochondrial activity or the activity of specific enzymes (Zheng *et al.* 2013). In this study, the impact of 240 natural products derived from endophytic fungi and marine sponges on GM-CSF-, Flt3L- and M-CSF-cultured bone marrow cells was examined by application of MTT assays. MTT assays are simple, widely accepted cytotoxicity assays providing highly reproducible results. They are based on the conversion of water-soluble, yellow MTT into violet crystal-like formazan by metabolic active cells. Dying cells lose this capacity, thus, measurement of formazan absorbance is a reliable benchmark for determination of cell viability. Consequently, absorbance is proportional to metabolically active cells. Alternatively to MTT assays, one step solutions such as MTS assays can be used (Riss *et al.* 2004).
For determination of optimal cell numbers in advance to the analysis of natural products, all three cell types were titrated to obtain an optimal OD of 0.75-1.25 (Figure 12). Based on this, GM-CSF-cultured cells were used at a density of 8 x 10^4 cells/well, Flt3L-cultured cells at 4 x 10^5 cells/well and M-CSF-cultured cells at 6 x 10^4 cells/well in the following assays.

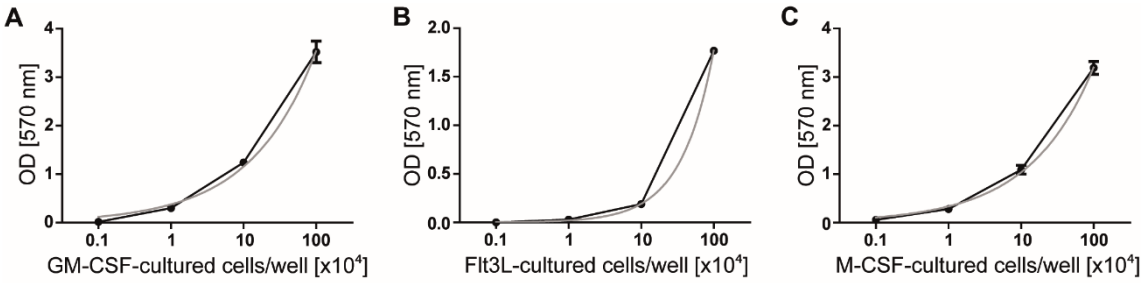

Figure 12: Optimal cell counts for MTT assays. GM-CSF-, Flt3L- and M-CSF-cultured cells were titrated prior to analysis of the cytotoxicity of natural products to determine the optimal cell count for an OD [570 nm] of 0.75-1.25 after treatment with DMSO alone. Error bars indicate standard deviations (SDs) of one biological replicate measured as technical duplicates. This figure has been modified from Richter *et al.* (2019).

The impact on viability of the natural products library was tested at 0.1, 1 and 10 µM after 24 h to provide a range of concentrations that allows the detection of promoting as well as inhibiting effects (Figure 13). As controls, cells were incubated with DMSO at the same concentration as the 10 µM samples for determination of toxic effects of the solvent itself or with the protein kinase inhibitor staurosporine, a potent inductor of apoptosis (data not shown). Data of the natural product-stimulated samples were normalized to the respective DMSO control to visualize percentage increase or decrease of viability. Thus, the DMSO control meets to 100% viability. Detailed results can be found in the appendix of this thesis.

Natural products were here defined to be promising for further evaluation if they induced viability rates of at least 80% for all concentrations and cell types tested (Figure 13, red line). Consequently, only natural products that did not negatively influence metabolic activity of GM-CSF-, Flt3L- and M-CSF-cultured cells were chosen to be promising and to be analyzed in following screenings. These compounds are highlighted in green (Figure 13). An increase in viability can indicate either elevated metabolic activity or cell proliferation. Appearing patterns in cytotoxicity as illustrated might be explained by similar structures of the natural products tested or additional, so far unknown structure-activity relationships.

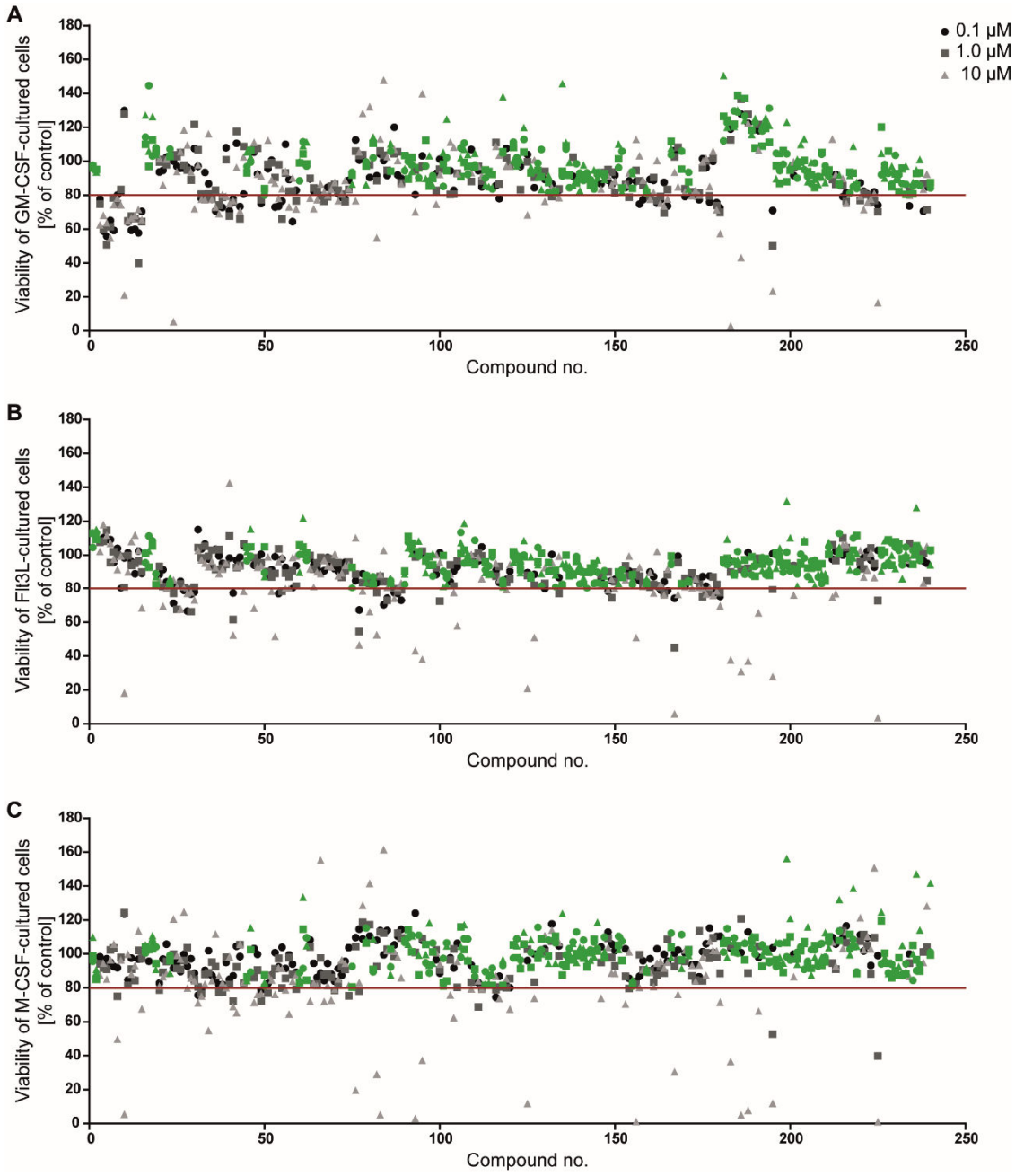

Figure 13: Cytotoxicity of natural products on the different cell types. 240 natural products were analyzed for their toxicity for immune target cells obtained by GM-CSF cultures (A), Flt3L cultures (B) and M-CSF cultures (C). Cells were incubated with three concentrations of natural products (0.1, 1 and 10 µM) for 24 h and the viability was determined via MTT assays (one biological replicate and one sample per condition). Results were normalized to the DMSO negative control (= 100% viability). Natural products were defined to be non-toxic if they show a viability of at least 80% (indicated by the red line) for all concentrations tested and all cell types. Natural products that fulfill that condition are marked in green. Compound no. = compound number. This figure has been modified from Richter *et al.* (2019).

Out of the tested 240 natural products 103 compounds were found to be non-toxic to immune target cells (Figure 14). Of the remaining 137 natural products 34 and 89 were non-toxic for one or two cell types, respectively, while 14 compounds were toxic for all cell types. Toxicity was mainly detected at 10 µM (Figure 13, light grey triangles). In the context of diseases that struggle with pathological increases in cDC, pDCs or macrophages, such toxic natural products might be interesting drugs. In contrast, 41 natural products were found to induce a viability of at least 120% for at least one concentration and cell type. Such compounds could be interesting for studies with focus on compounds that induce cell proliferation or increase metabolic activity. Proliferation of APCs would be promising for propagation and effective induction of adaptive immune responses.

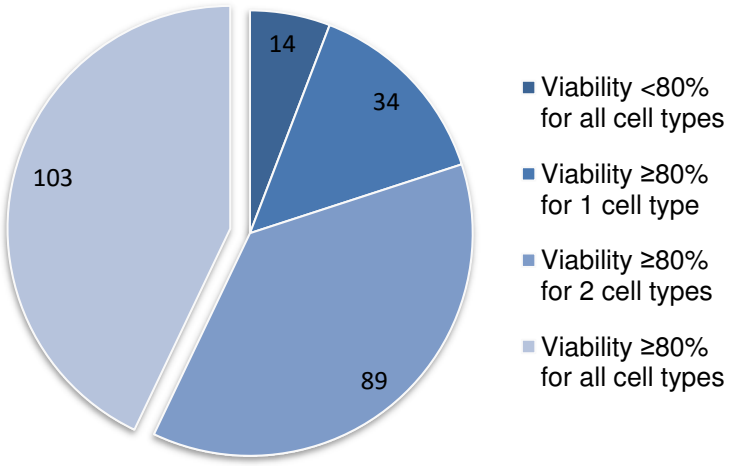

Figure 14: Distribution of the cytotoxicity of 240 natural products. 103 natural products induced a viability of at least 80% for all cell types. Among the remaining 137 compounds, 89 showed a viability of at least 80% for two cell types and 34 for one cell type while 14 natural products induced viability below 80% for all cell types. This figure has been modified from Richter *et al.* (2019).

Here, the non-toxic 103 natural products have been selected for analysis for beneficial bioactivities which is described in the following section.

3.3 Additional beneficial bioactivities

Natural products that show direct activity against tumors or bacteria are promising candidates for drug development. Tumor tissues as well as bacterial communities both represent cell clusters that exhibit similar resistance mechanisms as a result of cell

interactions under stress conditions (Lambert *et al.* 2011). Thus, analysis of modes of action of one disease type might provide insights into those of another. This implicates that immunotherapeutic approaches might help in a diversity of diseases.

Consequently, in this thesis, compounds that were shown to be non-toxic to immune target cells were additionally analyzed in screenings of cooperation partners within the DFG-funded Research Training Group 2158 “Natural products and natural product analogs against therapy-resistant tumors and microorganisms: new lead structures and modes of action”. These cooperation partners comprise the research groups of Prof. Dr. Rainer Kalscheuer from the Institute of Pharmaceutical Biology and Biotechnology, Prof. Dr. Klaus Pfeffer from the Institute of Medical Microbiology and Hospital Hygiene, Prof. Dr. Gerhard Fritz from the Institute of Toxicology and Prof. Dr. Sebastian Wesselborg as well as Prof. Dr. Björn Stork from the Institute of Molecular Medicine I, all belonging to the Heinrich Heine University Düsseldorf. They are experts on different topics and form a research consortium working on the same natural product library. Besides toxicity for immune target cells, natural products were analyzed for toxicity for lymphoma cells (Jurkat and Ramos cell lines) and for p53-mutated pancreatic carcinoma cells, for toxicity for pathogens including *Mycobacterium tuberculosis,* the gram-negative bacterium *Escherichia coli* as well as the intracellular parasite *Toxoplasma gondii* and for the modulation of autophagy (Figure 15). For the latter one, both pro- and anti-autophagic natural products might be interesting. Anti-autophagic compounds are more favored and already used in clinical trials while pro-autophagic compounds are mainly applied to increase immune responses against cancer (Rebecca and Amaravadi 2016; Zhong *et al.* 2016).

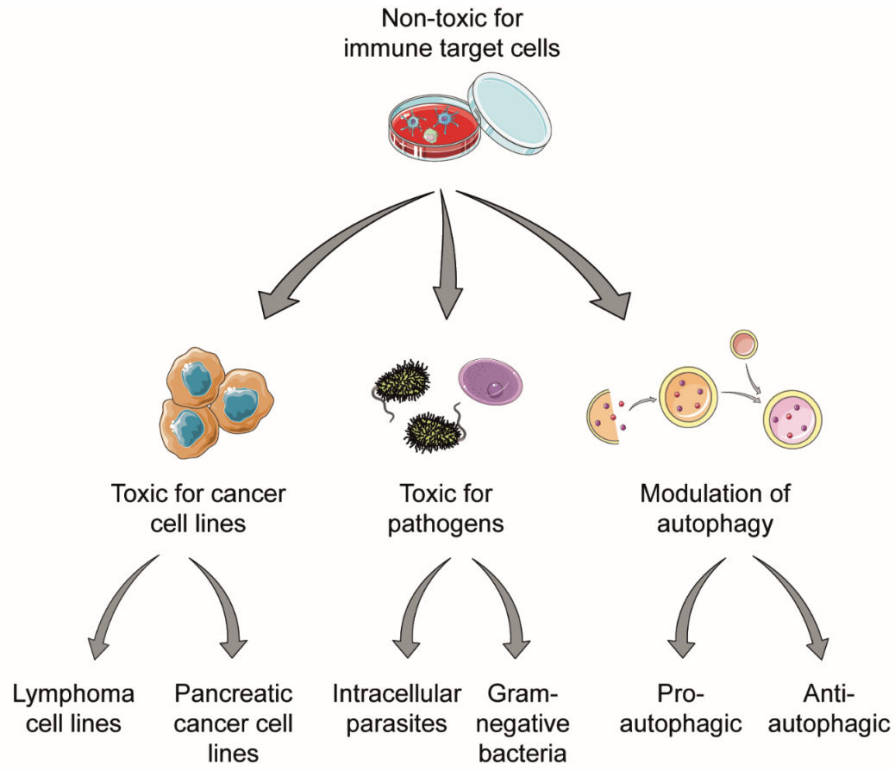

Figure 15: Potential additional beneficial characteristics of natural products. Natural products that are non-toxic for immune target cells were screened for additional preferable bioactivities by cooperation partners including toxicity for cancer cells (lymphoma cell lines, pancreatic cancer cell lines), toxicity for pathogens (intracellular parasites, bacteria) and the modulation of autophagy.

Taken together, besides being non-toxic to immune target cells, natural products could potentially exhibit six additional beneficial bioactivities. In the analyzed natural product library, one compound was found to possess four additional bioactivities: manzamine J *N*-oxide not only was non-toxic to immune target cells but simultaneously toxic for lymphoma cells and p53-mutated carcinoma cells, inhibited growth of *Mycobacterium tuberculosis* and modulated autophagy (Table 8). Its derivative, manzamine F, showed fewer activities and was toxic to lymphoma cells and modulated autophagy. Three other natural products were found to exhibit three additional bioactivities, namely 6-methoxycomaparvin-5-methyl ether, (-) arctigenin and dienone. Ten compounds including cytochalasin D showed two additional characteristics while 27 natural products including 18-dehydroxycytochalasin H exhibited one additional beneficial activity.

Table 8: Detailed results of the comparative analyses for additional beneficial bioactivities. 41 out of 103 natural products were examined by cooperation partners and exhibited additional beneficial anti-tumor or anti-pathogen bioactivities. "✓" indicates a positive, beneficial result while "×" represents a negative. *T. gondii* = *Toxoplasma gondii*; *M. tuberculosis* = *Mycobacterium tuberculosis*; *E. coli* = *Escherichia coli*.

	Toxicity for cancer cell lines		Toxicity for pathogens			Modulation of autophagy
Natural product	**Lymphoma cells**	**Pancreatic cancer cells**	***T. gondii***	***M. tuberculosis***	***E. coli***	
Manzamine J *N*-Oxid	✓	✓	×	✓	×	✓
6-Methoxycomaparvin-5-methyl ether	✓	✓	×	×	×	✓
(-) Arctigenin	✓	✓	×	×	×	✓
Dienone	✓	×	×	×	✓	✓
Cytochalasin D	✓	✓	×	×	×	×
Altersolanol C	✓	✓	×	×	×	×
Paspaline	✓	✓	×	×	×	×
Piperanine	✓	✓	×	×	×	×
Aristolochic acid	✓	✓	×	×	×	×
Aaptamine	✓	×	×	×	×	✓
Manzamine F	✓	×	×	×	×	✓
Br_2 hexylamide	×	✓	✓	×	×	×
Anomalin A	×	×	✓	×	×	✓
Sceptrin	×	×	×	✓	✓	×
3,5-Dibromo-2-hydroxy-4-methoxyphenylacetonitril	✓	×	×	×	×	×
Unguisin E	✓	×	×	×	×	×
Asterric acid	✓	×	×	×	×	×
Kämpferol-3-rutinoside	✓	×	×	×	×	×
12-Carboxyl-paspaline	✓	×	×	×	×	×
Amorphastilbol	✓	×	×	×	×	×
18-Dehydroxycytochalasin H	×	✓	×	×	×	×
Pinocembrin	×	✓	×	×	×	×

	Toxicity for cancer cell lines		Toxicity for pathogens			Modulation of autophagy
Natural product	**Lymphoma cells**	**Pancreatic cancer cells**	***T. gondii***	***M. tuberculosis***	***E. coli***	
N-methyl-4,5-dibromopyrrole-2-methylcarboxylate	×	✓	×	×	×	×
Tryptamide	×	✓	×	×	×	×
Dienone dimethoxyketal	×	✓	×	×	×	×
3-O-Methylgallic acid methyl ester	×	✓	×	×	×	×
Isosulochrin	×	✓	×	×	×	×
Dammarenolsäure	×	✓	×	×	×	×
(+) Isochromophilone VI	×	✓	×	×	×	×
Andrographolide	×	✓	×	×	×	×
Precocene I	×	✓	×	×	×	×
Precocene II	×	✓	×	×	×	×
p-Coumaric acid	×	✓	×	×	×	×
Neobavaisoflavone	×	×	✓	×	×	×
Piperine	×	×	✓	×	×	×
Bionectriamide A	×	×	✓	×	×	×
3-O-Methylgallic acid butyl ester	×	×	×	✓	×	×
Aerothionin	×	×	×	×	×	✓
Dasyclamide	×	×	×	×	×	✓
4,5-Dibromo-1H-pyrrol-2-carbon acid	×	×	×	×	×	✓
Xanthoangelol	×	×	×	×	×	✓

The remaining 62 natural products only were non-toxic to immune target cells without any additional bioactivities (Figure 16). These compounds were consequently excluded from follow up screenings.

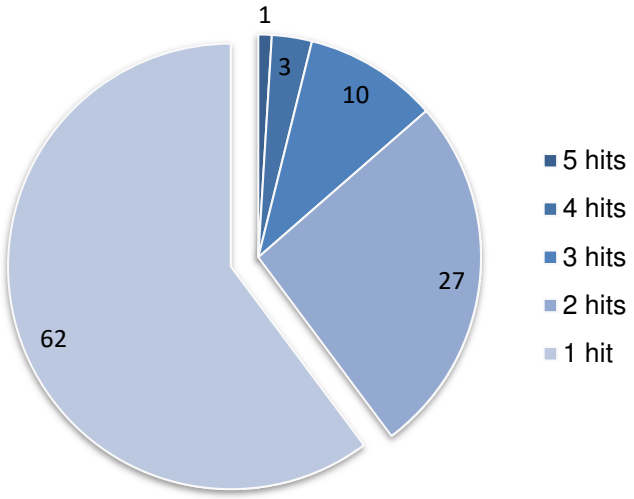

Figure 16: Distribution of additional beneficial bioactivities of natural products. Natural products that were non-toxic to immune target cells were analyzed for promising results ("hits") from screenings conducted by cooperation partners. "1 hit" corresponds to compounds that were non-toxic to immune target cells only and did not display any additional bioactivity. Thus, only natural products with at least two hits were chosen for further analyses.

In summary, 41 out of 103 natural products were non-toxic for immune target cells and displayed additional beneficial bioactivities in the screenings of the expert groups. Of those 41 compounds, 33 showed direct effectivity against cancer while 9 were active against pathogens including bacteria as well as parasites. These 41 natural products were selected to be analyzed in the following screenings for immune activation.

3.4 IL-12p40 assays

Natural products that have been shown to be non-toxic to immune target cells and to exhibit additional beneficial bioactivities were analyzed in IL-12p40 assays for immune activating capacities. Here, GM-CSF-cultured cells were used as these cells are especially potent in IL-12p40 production upon stimulation (Helft *et al.* 2015). IL-12p40 production was analyzed by flow cytometry as well as validated by ELISA. In flow cytometry, cells were gated on single, live cells and either directly analyzed for IL-12p40/GFP production and CD86 surface expression to determine immune activating effects of natural products on whole cell cultures or defined to be $CD11c^+$ $MHCII^+$ before evaluation of IL-12p40/GFP and CD86 levels (Figure 17).

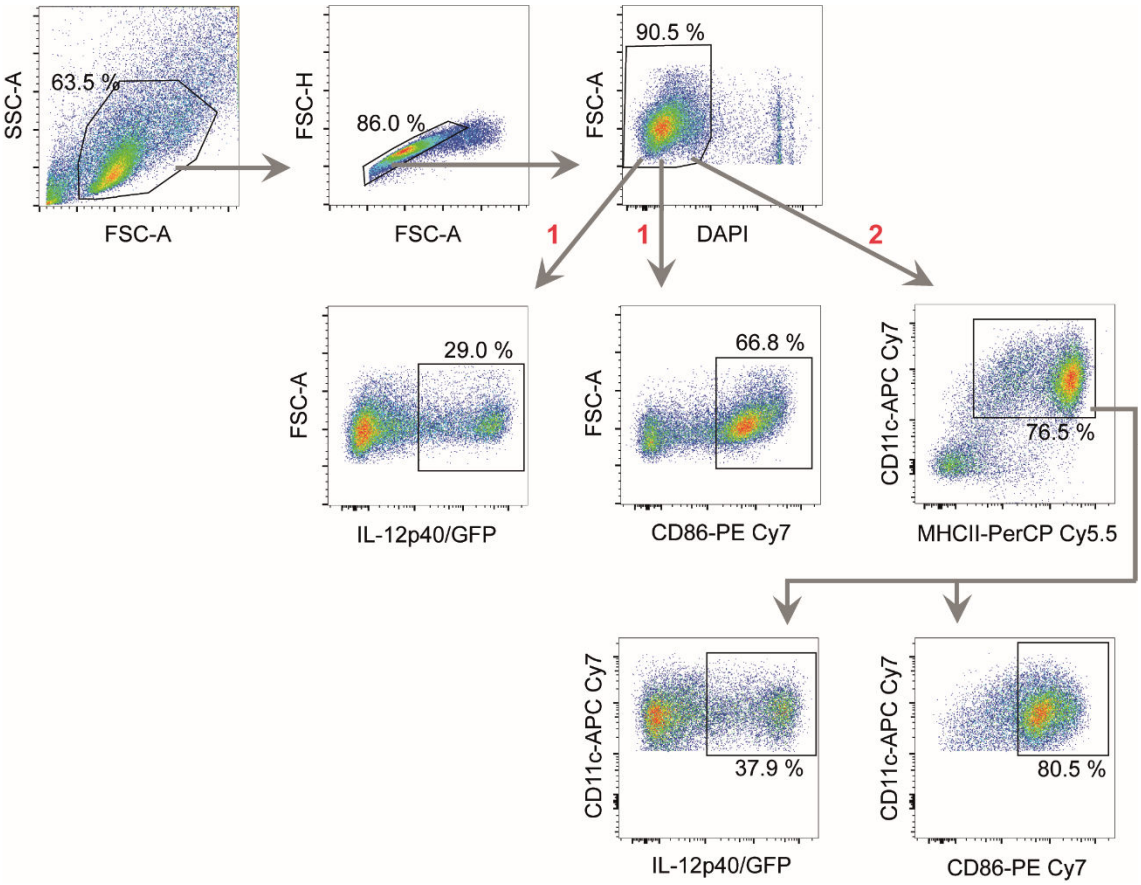

Figure 17: Gating strategy for GM-CSF-cultured cells. Samples were measured using a BD FACSCanto II and subsequently analyzed via FlowJo 10.5.3. Samples were initially gated for cells, single and live cells. IL-12p40/GFP and CD86 were analyzed directly from live cells (1) or live cells were further gated on CD11c$^+$ MHCII$^+$ cells for analysis of IL-12p40/GFP and CD86 expression by cDCs (2). Percentages indicate the frequencies of the parental populations.

For the analysis of natural products, GM-CSF cells were stimulated with varying concentrations (0.1, 1 or 10 µM) of the compounds in addition to a suboptimal concentration of the TLR stimuli CpG 2216 or LPS. CpG 2216 is a synthetic class A oligonucleotide that mimics bacterial DNA as unmethylated CpG motifs are enriched therein. CpG 2216 signals via TLR9 (Krieg 2002). LPS on the other hand is found in the outer membrane of gram-negative bacteria and is detected via TLR4 (Chow *et al.* 1999). Suboptimal concentrations of the two ligands have been used in this thesis as this resembles physiological conditions of immune activation in the presence of a tumor or an infection (Yu *et al.* 2010). Furthermore, this enables the detection of additive or synergistic effects of natural products. For identification of the suboptimal amount of CpG 2216 and LPS that provides the lowest possible concentration with still a detectable increase in IL-12p40/GFP, both TLR stimuli have been titrated on GM-CSF-cultured cells

(Figure 18). At 0.01 µM CpG 2216 or 0.1 ng/ml LPS no increase in IL-12p40/GFP could be measured. With ten-fold higher concentrations, 0.1 µM CpG 2216 and 1 ng/ml LPS, respectively, an approximately three-fold increase in IL-12p40/GFP was detectable which even increased with increasing concentrations of the stimuli. Consequently, the second highest concentrations were chosen to be applied for the analysis of natural products.

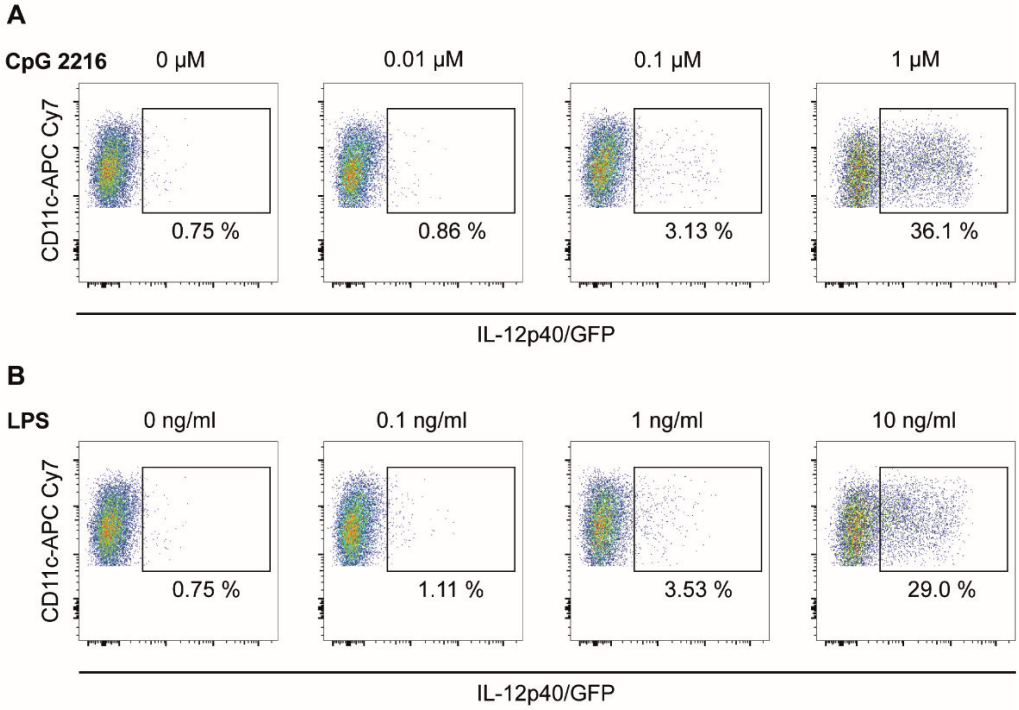

Figure 18: CpG 2216 and LPS titration. GM-CSF-cultured cells were treated with varying concentrations of CpG 2216 (A) or LPS (B) and analyzed for IL-12p40/GFP$^+$ cells pre-gated on single, live, CD11c$^+$ MHCII$^+$ cells. Percentages indicate the frequencies of the parental populations. This figure has been modified from Richter *et al.* (2019).

In the initial screening of the 41 natural products that were non-toxic to the immune target cells and exhibited additional beneficial bioactivities, twelve compounds showed immune activating properties (Figure 19). Natural products were defined to be immune activating if they induced an at least two-fold increase in IL-12p40 compared to the respective control. The twelve immune activating compounds found in the initial experiment included natural products that either induced IL-12p40 production without additional TLR stimulation, with either CpG 2216 or LPS or in both conditions with TLR ligands present. As presented in Figure 19, two natural products, isosulochrin and manzamine J *N*-oxide were the only compounds inducing IL-12p40 at 10 µM without an additional stimulus. Isosulochrin furthermore showed an increase in IL-12p40 at any concentration when stimulated with CpG 2216 with simultaneous decrease after addition of LPS. Similarly,

manzamine J *N*-oxide induced enhanced IL-12p40 levels in the presence of CpG 2216 at 0.1 and 1 µM but not at 10 µM. Its derivative manzamine F on the other hand did not exhibit IL-12p40-inducing potential without an additional stimulus but triggered IL-12p40 production when simultaneously incubated with CpG 2216. One cytochalasin, 18-dehydroxycytochalasin H, caused an increase in IL-12p40 at both CpG 2216 or LPS stimulation, while its derivative cytochalasin D also responded to both stimuli but with a strong decrease at 10 µM in the presence of CpG 2216. Furthermore, several natural products triggered IL-12p40 production by $MHCII^+$ $CD11c^+$ cells in the presence of LPS. Besides the aforementioned, these compounds included bionectriamide A with a peak at 1 µM, neobavaisoflavone which showed promising effects at any concentration, (-) arctigenin with the strongest increase at 10 µM, 3-O-methylgallic acid methyl ester with an optimal concentration of 1 µM, 6-methoxycomaparvin-5-methyl ester which showed immune activating potential especially at 0.1 µM and 3-O-methylgallic acid butyl ester as well as dienone which both exhibited a slight, constant increase in IL-12p40 production with increasing concentrations.

Despite these promising results from pilot experiments, repetitions were performed to validate the findings and to define the robustness of the immune activating characteristics detected here. These results are presented in the following.

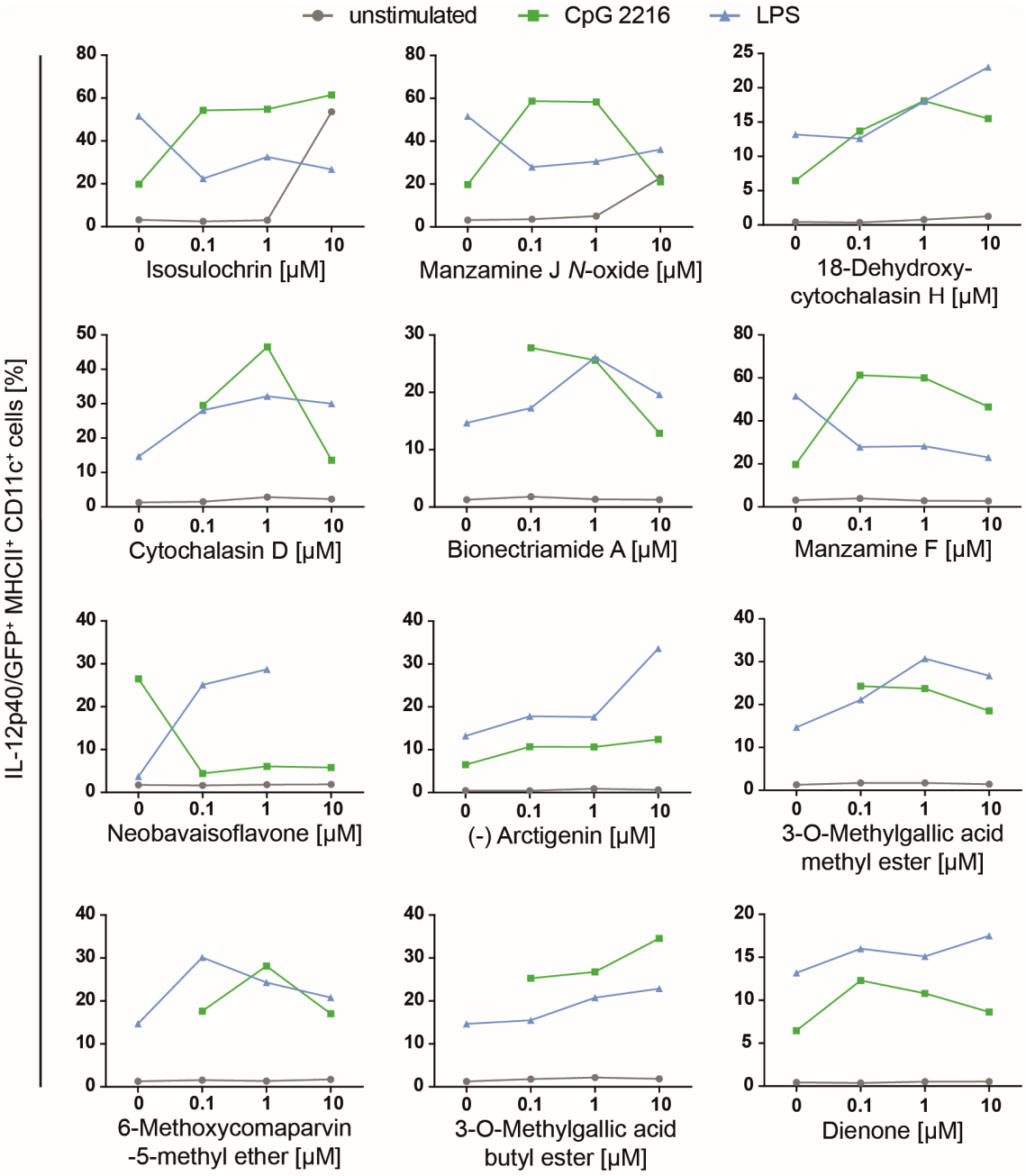

Figure 19: Immune activating properties of twelve natural products in the initial IL-12p40 assay. GM-CSF-cultured cells were incubated with varying concentrations (0.1, 1 and 10 µM) of natural products that were non-toxic to immune target cells and exhibited additional beneficial bioactivities for 16 h. Samples were analyzed via flow cytometry for IL-12p40/GFP$^+$ cells pre-gated on single, live, CD11c$^+$ MHCII$^+$ cells.

Stimulation experiments have been repeated two times with two separately treated mice and independent natural product aliquots. Out of the twelve natural products that were immune activating in the initial screening, three compounds showed reproducible immune activating characteristics in all following experiments. One of those three is manzamine J *N*-oxide. In the initial screening, manzamine J *N*-oxide was one of two

compounds that induced IL-12p40/GFP by MHCII$^+$ CD11c$^+$ cells at 10 µM without an additional TLR stimulus. The second experiment supported these findings but revealed additional features exhibited by this compound (Figure 20). Manzamine J *N*-oxide again induced IL-12p40 production by MHCII$^+$ CD11c$^+$ cells at 10 µM and also a slight increase from 0.1-10 µM when additionally stimulated with LPS but only to the maximum level of the control (Figure 20B). Simultaneously, CD86 expression on MHCII$^+$ CD11c$^+$ cells increased with increasing concentrations under all stimulation conditions (Figure 20C). Nevertheless, ELISAs for the analysis of the amount of secreted IL-12p40 revealed a strong decrease in IL-12p40 at 10 µM under all stimulation conditions (Figure 20D). The first promising results were furthermore impacted by the recognition of the strong cytotoxicity of manzamine J *N*-oxide at 10 µM that was not detected in the initial screenings for cytotoxicity (Figure 20A; see section 3.2 Cytotoxicity assays).

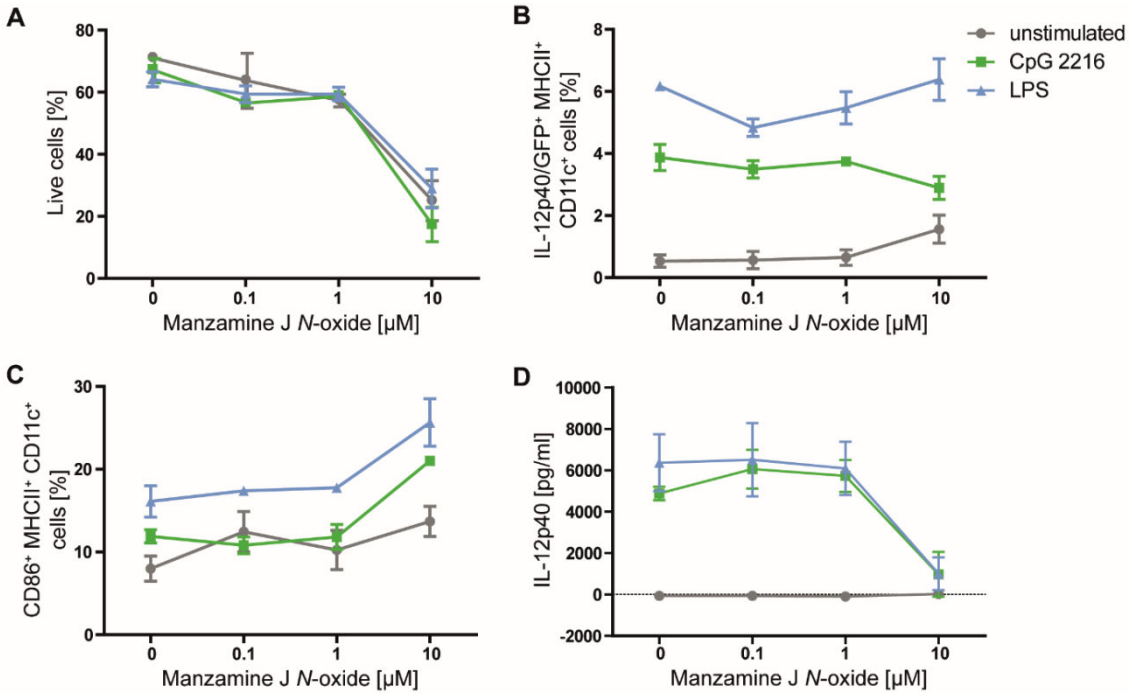

Figure 20: Immune activating properties of manzamine J *N*-oxide in the second experiment. GM-CSF-cultured cells were incubated with varying concentrations (0.1, 1 and 10 µM) of manzamine J *N*-oxide for 16 h. Samples were analyzed via flow cytometry for live cells (A), IL-12p40/GFP$^+$ DCs pre-gated on single, live, CD11c$^+$ MHCII$^+$ cells (B), CD86$^+$ DCs pre-gated on single, live, CD11c$^+$ MHCII$^+$ cells (C) or by ELISA for the amount of secreted IL-12p40 (D). Error bars indicate SDs of two biological replicates.

Similar results could be observed in the third experiment (Figure 21). Manzamine J *N*-oxide induced an increase in IL-12p40 production by MHCII$^+$ CD11c$^+$ cells at 10 µM without additional TLR stimulation but a decrease in combination with either CpG 2216

or LPS (Figure 21B). In contrast to the previous experiment, CD86 expression on MHCII$^+$ CD11c$^+$ cells did not increase in any condition but revealed a strong decrease at 10 µM in the presence of CpG 2216 (Figure 21C). Furthermore, ELISAs demonstrated elevated IL-12p40 levels at 1 and 10 µM without additional TLR stimulation, thus supporting the flow cytometry results (Figure 21D). However, IL-12p40 secretion after CpG 2216 or LPS stimulation was decreased and the frequency of live cells was impacted at 10 µM (Figure 21D and Figure 21A). Moreover, the higher frequencies of IL-12p40$^+$ MHCII$^+$ CD11c$^+$ and CD86$^+$ MHCII$^+$ CD11c$^+$ cells as well as IL-12p40 levels can be explained with the change of the culture dishes used for cultivation of GM-CSF cells (see section 2.2.1 GM-CSF cultures).

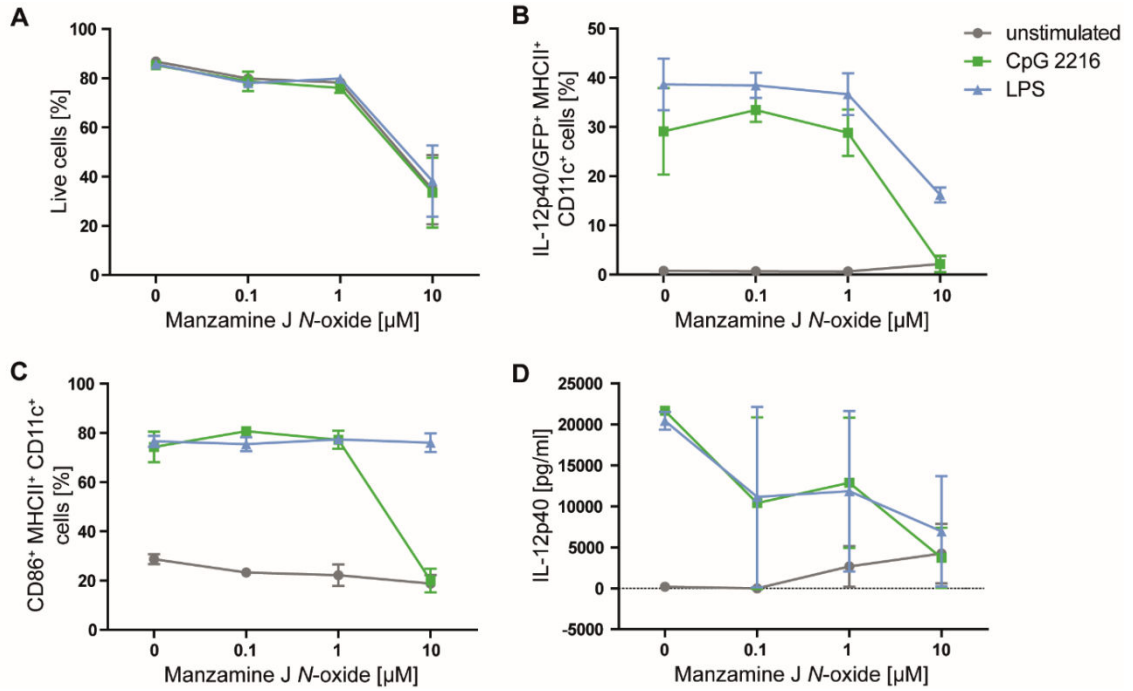

Figure 21: Immune activating properties of manzamine J *N*-oxide in the third experiment. GM-CSF-cultured cells were incubated with varying concentrations (0.1, 1 and 10 µM) of manzamine J *N*-oxide for 16 h. Samples were analyzed as described in Figure 20 for live cells (A), IL-12p40/GFP$^+$ DCs (B), CD86$^+$ DCs (C) or by ELISA for the amount of secreted IL-12p40 (D). Error bars indicate SDs of two biological replicates.

Taken together, manzamine J *N*-oxide indeed induced IL-12p40 production by MHCII$^+$ CD11c$^+$ cells but simultaneously exhibited strong cytotoxic effects at this concentration. Besides manzamine J *N*-oxide, the promising results obtained from 18-dehydroxycytochalasin H stimulation could be validated in the second experiment (Figure 22). In contrast to manzamine J *N*-oxide, 18-dehydroxycytochalasin H was non-toxic to GM-CSF-cultured cells (Figure 22A). In the first screening, the compound

showed increased IL-12p40 production by MHCII$^+$ CD11c$^+$ cells after CpG 2216 as well as LPS stimulation. Here, 18-dehydroxycytochalasin H showed the strongest increase in IL-12p40 production at 1 µM with additional CpG 2216 or LPS stimulation with the best induction of IL-12p40 detected for the CpG 2216 sample (Figure 22B). Similarly, CD86 expression by MHCII$^+$ CD11c$^+$ cells was increased at 1 µM for all TLR stimulation conditions (Figure 22C). Both, IL-12p40 and CD86 expression declined at 10 µM. Analysis of the supernatant supported the observed findings and revealed a strong induction of IL-12p40 secretion at 0.1, 1 and 10 µM 18-dehydroxycytochalasin H in addition to CpG 2216 stimulation (Figure 22D). ELISAs validated an optimal immunostimulatory concentration of 1 µM for 18-dehydroxycytochalasin H.

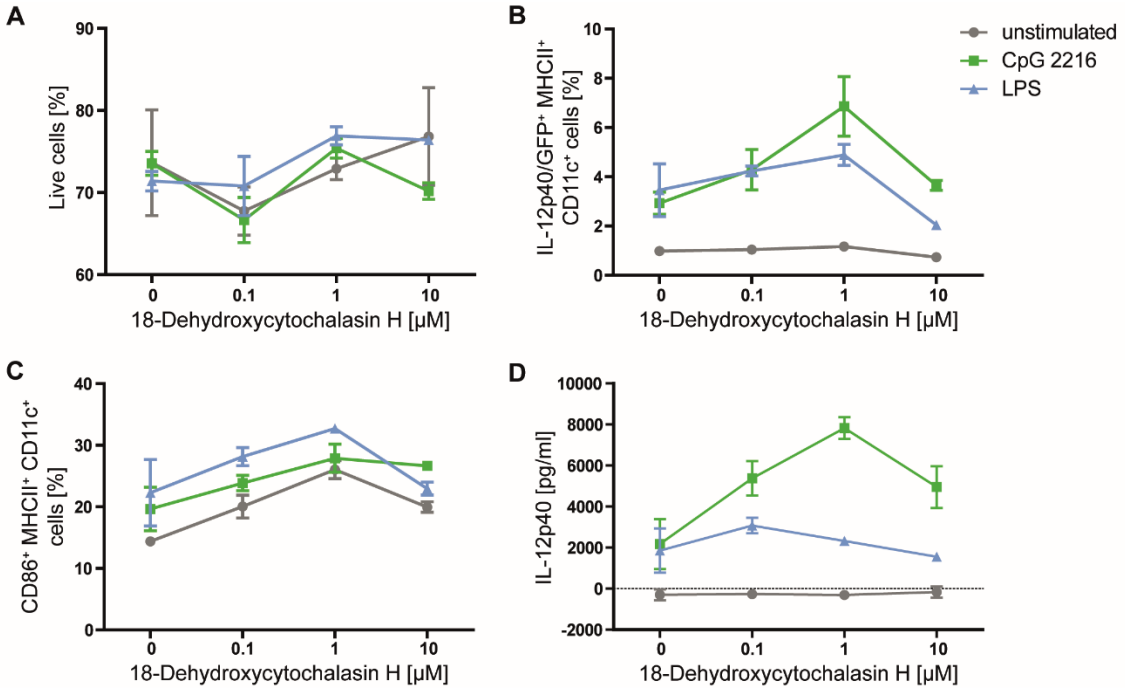

Figure 22: Immune activating properties of 18-dehydroxycytochalasin H in the second experiment. GM-CSF-cultured cells were incubated with varying concentrations (0.1, 1 and 10 µM) of 18-dehydroxycytochalasin H with or without CpG 2216 or LPS for 16 h. Samples were analyzed as described in Figure 20 for live cells (A), IL-12p40/GFP$^+$ DCs (B), CD86$^+$ DCs (C) or by ELISA for the amount of secreted IL-12p40 (D). Error bars indicate SDs of two biological replicates.

In the third experiment, similar results could be observed (Figure 23). IL-12p40 production by MHCII$^+$ CD11c$^+$ cells clearly peaked at 1 µM after additional stimulation with CpG 2216 (Figure 23B). However, a slight cytotoxic tendency was detected at 10 µM (Figure 23A). In contrast to the second experiment, CD86 expression increased with increasing concentrations (Figure 23C). Nevertheless, ELISAs supported the

assumption of an optimal concentration of 1 µM although demonstrating lower differences of IL-12p40 levels (Figure 23D). Like for manzamine J *N*-oxide, the increase in IL-12p40 frequencies and levels can be explained by the change in cell culture dishes.

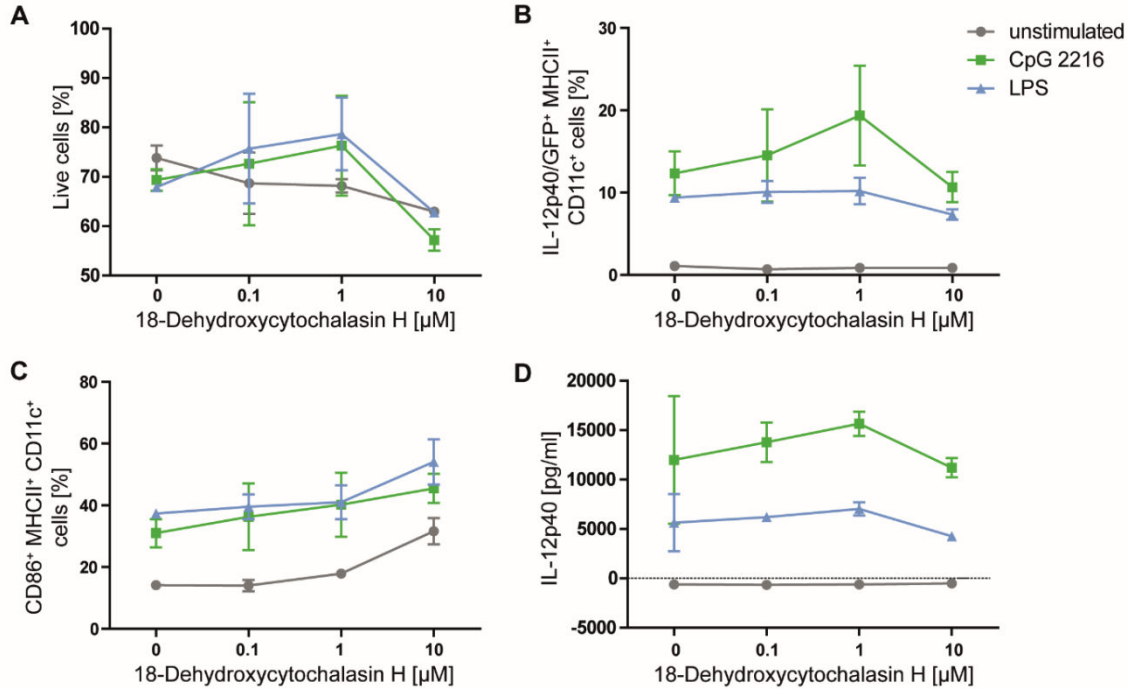

Figure 23: Immune activating properties of 18-dehydroxycytochalasin H in the third experiment. GM-CSF-cultured cells were incubated with varying concentrations (0.1, 1 and 10 µM) of 18-dehydroxycytochalasin H with or without CpG 2216 or LPS for 16 h. Samples were analyzed as described in Figure 20 for live cells (A), IL-12p40/GFP$^+$ DCs (B), CD86$^+$ DCs (C) or by ELISA for the amount of secreted IL-12p40 (D). Error bars indicate SDs of two biological replicates.

In summary, results obtained in the first screening could be validated. In all repetitions, 18-dehydroxycytochalasin H exhibited distinct immune activating capacities with an assumed optimal concentration of 1 µM at additional stimulation with CpG 2216.

Similar to 18-dehydroxycytochalasin H, a second cytochalasin, cytochalasin D, demonstrated advantageous results in the initial screening which were recapitulated in the following experiments (Figure 24 and Figure 25). In the second experiment, cytochalasin D exhibited a strong increase in IL-12p40 production by MHCII$^+$ CD11c$^+$ cells at 1 µM with additional CpG 2216 stimulation. Interestingly, an induction of IL-12p40 at 0.1 µM without an additional TLR stimulus could be detected (Figure 24B). Furthermore, elevated levels of CD86 expression by MHCII$^+$ CD11c$^+$ cells were observed at stimulation with CpG 2216 or LPS with the strongest increase measured at 10 µM with additional LPS treatment (Figure 24C). Analysis of the supernatant showed a clear

enhancement in IL-12p40 secretion at 1 µM in addition to CpG 2216 stimulation and no change in the sample without a TLR stimulus or with LPS (Figure 24D). Auspiciously, cytochalasin D was non-toxic to the GM-CSF-cultured cells and induced an increase in live cells with increasing concentrations (Figure 24A).

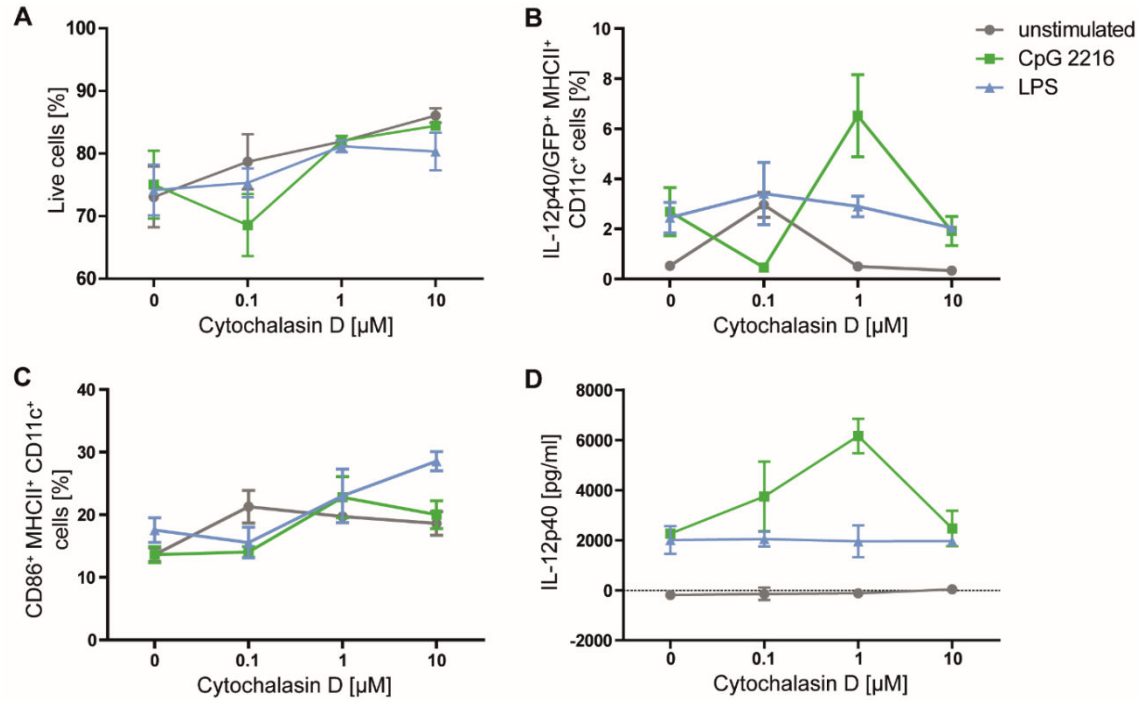

Figure 24: Immune activating properties of cytochalasin D in the second experiment. GM-CSF-cultured cells were incubated with varying concentrations (0.1, 1 and 10 µM) of cytochalasin D with or without CpG 2216 or LPS for 16 h. Samples were analyzed as described in Figure 20 for live cells (A), IL-12p40/GFP$^+$ DCs (B), CD86$^+$ DCs (C) or by ELISA for the amount of secreted IL-12p40 (D). Error bars indicate SDs of two biological replicates.

The results from the third experiment with cytochalasin D largely supported the results obtained from the previous experiments (Figure 25). The strongest increase in IL-12p40 production by MHCII$^+$ CD11c$^+$ cells was detected at 1 µM with additional CpG 2216 stimulation (Figure 25B). However, CD86 expression levels changed only slightly with CpG 2216 or LPS treatment but strongly increased without an additional stimulus at 1 or 10 µM cytochalasin D (Figure 25C). In contrast, in the third experiment, ELISAs did not reveal a change in IL-12p40 levels in any condition (Figure 25D). Moreover, cytochalasin D showed slight decreases in viability for the samples with all stimulation treatments instead of an increase in live cells like observed before (Figure 25A).

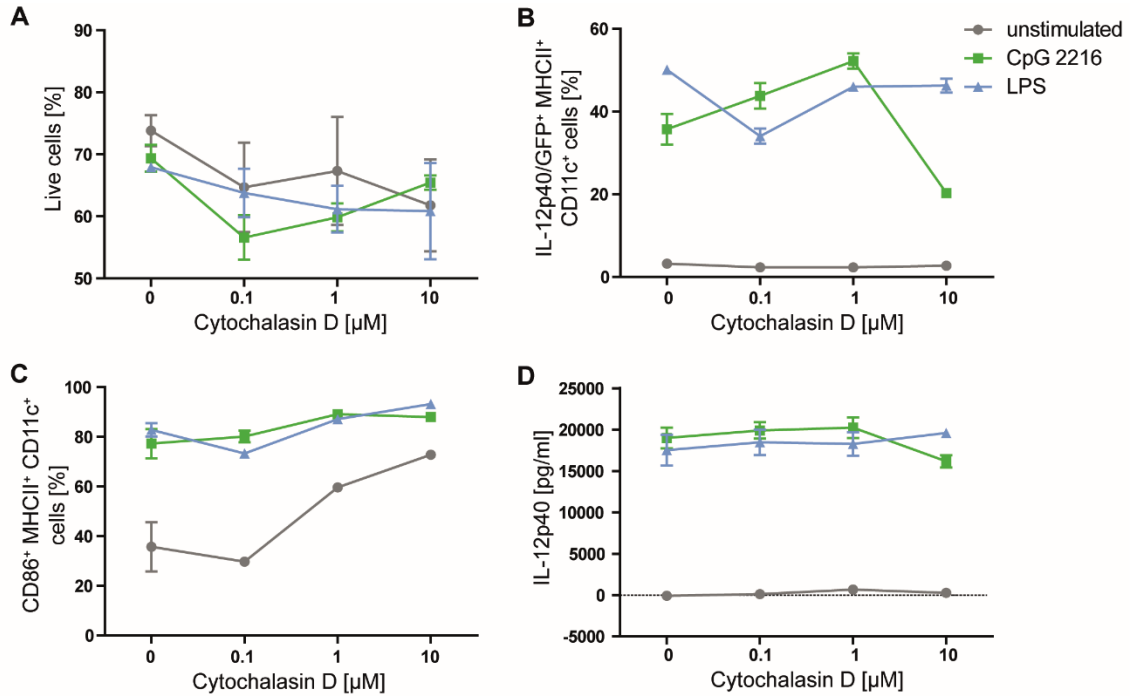

Figure 25: Immune activating properties of cytochalasin D in the third experiment. GM-CSF-cultured cells were incubated with varying concentrations (0.1, 1 and 10 µM) of cytochalasin D with or without CpG 2216 or LPS for 16 h. Samples were analyzed as described in Figure 20 for live cells (A), IL-12p40/GFP$^+$ DCs (B), CD86$^+$ DCs (C) or by ELISA for the amount of secreted IL-12p40 (D). Error bars indicate SDs of two biological replicates.

In brief, results of cytochalasin D obtained in the first screening could be verified in the second and third experiment. Cytochalasin D clearly induced IL-12p40 production by MHCII$^+$ CD11c$^+$ cells at 1 µM with additional CpG 2216 stimulation.

Taken together, 41 natural products were initially analyzed for immune activating properties via induction of IL-12p40. In the first screenings, twelve compounds were identified that enhanced IL-12p40$^+$ MHCII$^+$ CD11c$^+$ cells either alone or when additionally treated with the TLR stimuli CpG 2216 or LPS. To verify the robustness of these results, the experiments have been repeated and revealed the three reproducibly immunostimulatory natural products manzamine J *N*-oxide, 18-dehydroxycytochalasin H and cytochalasin D which were further analyzed in T cell activation assays (see section 3.5 T cell activation assays).

3.5 T cell activation assays

To evaluate if the identified promising natural products are not only capable of activating innate immune cells but also of inducing an effective adaptive immune response, T cell

activation assays were performed. IL-12 is a cytokine that is recognized by T cells and induces their differentiation and proliferation, thus IL-12p40 inducing natural products should also trigger T cell activation (Abdi and Singh 2015; Zundler and Neurath 2015). For T cell activation assays, natural product-stimulated GM-CSF-cultured cells were incubated with $CD4^+$ cells from OTII mice in the presence of OVA peptide. As readout, IL-2 was chosen as it is produced by activated $CD4^+$ T cells upon antigen presentation by DCs (Boyman and Sprent 2012).

For assessment of T cell activation, a protocol according to Reinhardt *et al*. was adapted with initial determination of the optimal GM-CSF cell count (Reinhardt *et al.* 2006) (Figure 26). Similar to the titration of CpG 2216 and LPS in the IL-12p40 assays, a cell count of 10^4 cells/well was chosen that allows the detection of additive or synergistic effects on IL-2 secretion after natural product stimulation and co-cultivation with $CD4^+$ cells.

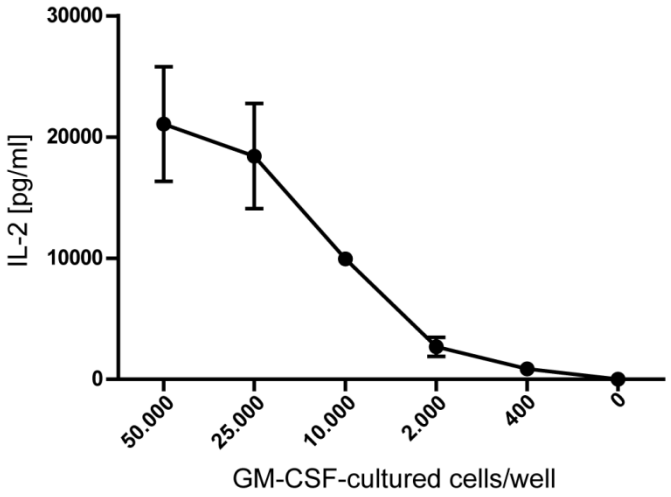

Figure 26: Optimal cell counts of GM-CSF-cultured cells for T cell activation assays. CpG 2216-stimulated GM-CSF-cultured cells were titrated prior to analysis of natural products and co-cultured with $CD4^+$ cells obtained from OTII mice. The amount of secreted IL-2 secretion was analyzed by ELISA on day five of co-culture. Error bars indicate SDs of one biological replicate measured as technical triplicates. This figure has been modified from (Richter *et al.* 2019).

The three most promising natural products identified in the IL-12p40 assays, manzamine J *N*-oxide, 18-dehydroxycytochalasin H and cytochalasin D, were analyzed for their effects in T cell activation assays. To ensure the reproducibility of the results, T cell activation assays were performed thrice with two independently treated mice each and independent natural product aliquots. In the IL-12p40 assays, manzamine J *N*-oxide was found to induce immune activation of GM-CSF-derived DCs at 10 µM without any additional stimulus. Here, no T cell activation measured as IL-2 production by $CD4^+$ cells

was detectable (Figure 27A). IL-2 was lowest at 2.5 µM and slightly increased with increasing concentrations but did not exceed levels of IL-2 production induced by the controls. Because of that and because of its toxicity at 10 µM as presented before, manzamine J *N*-oxide was excluded from further analyses. In contrast to that, 18-dehydroxycytochalasin H triggered IL-2 secretion by $CD4^+$ cells in the first experiment (Figure 27B). In IL-12p40 assays, 18-dehydroxycytochalasin H exhibited an optimal concentration of 1 µM in combination with CpG 2216. Here, IL-2 production was induced already in the samples without additional TLR stimulation. IL-2 levels increased up to a concentration of 5 µM and decreased at 10 µM. A similar tendency could be observed at simultaneous stimulation with LPS with a clear optimal concentration of 5 µM. Additional stimulation with CpG 2216 revealed increases in IL-2 at 1 and 5 µM but both did not exceed IL-2 levels of the control. The second cytochalasin, cytochalasin D, also induced IL-2 secretion by $CD4^+$ cells (Figure 27C). Similar to 18-dehydroxycytochalasin H, cytochalasin D triggered T cell activation at conditions without additional TLR stimulation and with LPS. Here, an optimal concentration of 1 µM could be identified. In contrast to IL-12p40 assays in which the best IL-12p40 induction could be observed at 1 µM in the presence of CpG 2216, samples treated simultaneously with cytochalasin D and CpG 2216 showed a concentration-dependent decrease in IL-2 production by $CD4^+$ cells. Strikingly, IL-2 levels strongly decreased at increasing concentrations with no detectable IL-2 production at 10 µM.

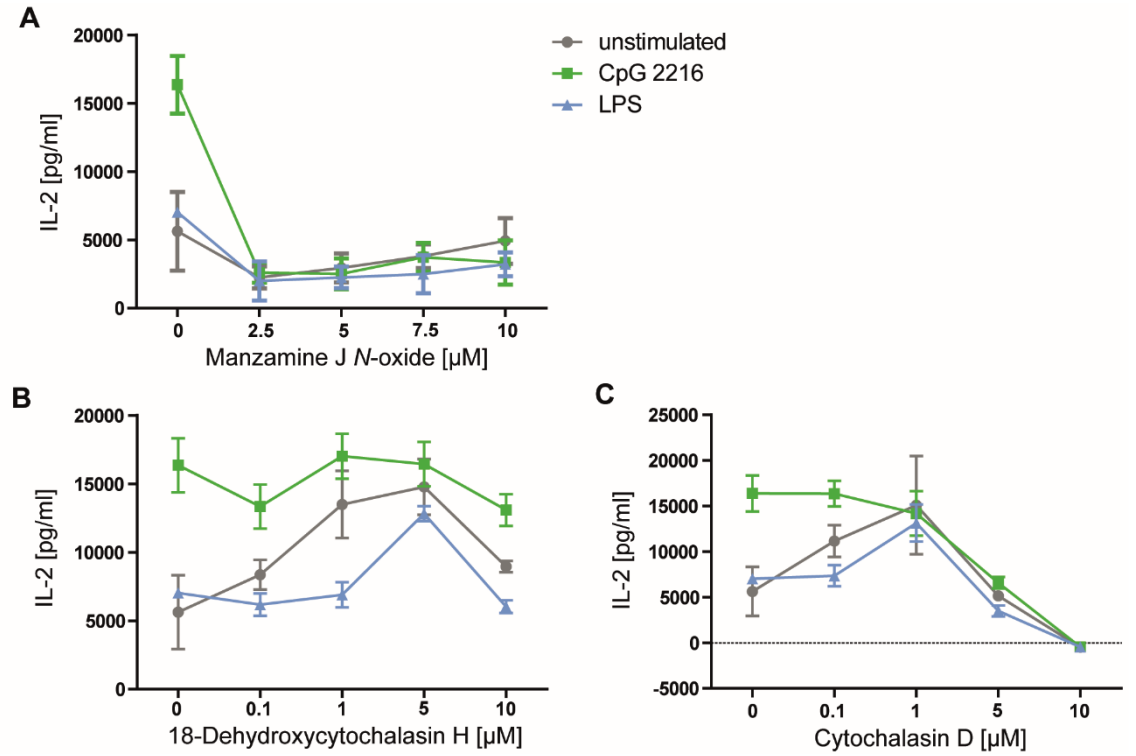

Figure 27: T cell activating properties of selected natural products in the first experiment. GM-CSF-cultured cells were incubated with varying concentrations of manzamine J *N*-oxide (A; 0.1, 1 and 10 µM), 18-dehydroxycytochalasin H (B; 0.1, 1, 5 and 10 µM) or cytochalasin D from the natural product library (C; 0.1, 1, 5 and 10 µM) with or without CpG 2216 or LPS for 24 h, co-cultured with CD4⁺ cells obtained from OTII mice and pulsed with $OVA_{323-339}$ peptide. The supernatant was analyzed for IL-2 by ELISA on day five. Error bars indicate SDs of two biological replicates measured as technical duplicates.

In the second experiment it should be determined whether results obtained in the first experiment could be verified. Additionally, besides analysis of the effects of natural product-stimulated cells on T cells, direct effects of the two natural products on CD4⁺ cells in the absence of DCs should be examined to ensure the detection of DC-dependent effects (Figure 28). In comparison to the first experiment, both cytochalasins exhibited sharper effects in the second. 18-Dehydroxycytochalasin H induced IL-2 production by CD4⁺ cells after co-cultivation with DCs at 5 µM independently of the presence of TLR stimuli (Figure 28A). IL-2 levels increased with increasing concentrations of up to 5 µM and dropped at 10 µM. CD4⁺ cells only did not show an elevation in IL-2 in any of the samples. Similarly, samples stimulated with cytochalasin D increased in IL-2 secretion up to an optimal concentration of 1 µM and decreased with higher concentrations (Figure 28B). Similar to 18-dehydroxycytochalasin H, no change in IL-2 levels with CD4⁺ cells only could be observed.

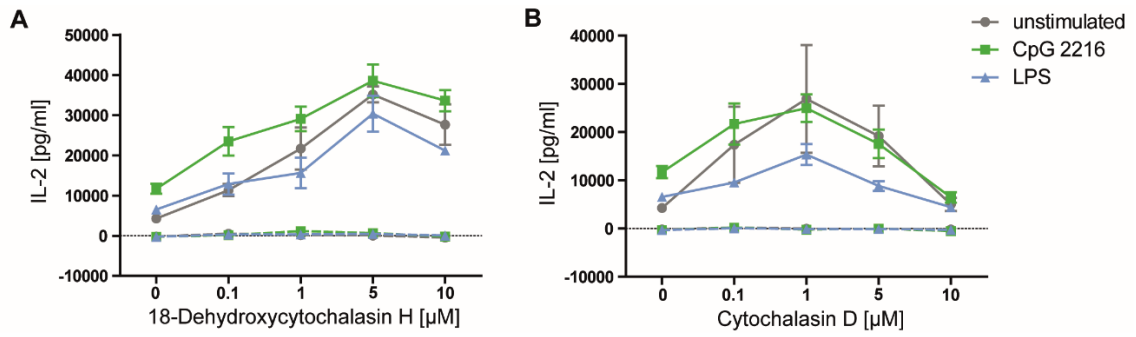

Figure 28: T cell activating properties of selected natural products in the second experiment. GM-CSF-cultured cells were incubated with varying concentrations of 18-dehydroxycytochalasin H (A; 0.1, 1, 5 and 10 µM) or cytochalasin D from the natural product library (B; 0.1, 1, 5 and 10 µM) with or without CpG 2216 or LPS for 24 h and co-cultured with CD4⁺ cells as described in Figure 27. Solid lines indicate samples with co-cultures of DCs and CD4⁺ cells while dashed lines represent samples with T cells only. Error bars indicate SDs of two biological replicates measured as technical duplicates.

In the third experiment, a commercially available sample of cytochalasin D was tested in parallel (Figure 29). As seen in the first and second experiment, 18-dehydroxycytochalasin H induced the strongest increase in IL-2 production by CD4⁺ cells at 5 µM although not as distinct (Figure 29A). In presence of LPS, 10 µM triggered similar IL-2 production like 5 µM while CpG 2216-stimulated samples did not exceed the levels of the control. Contrary to the second experiment, a slight increase in IL-2 secretion by CD4⁺ cells only could be detected at 5 µM. Results from cytochalasin D from the natural product library supported the results obtained in the previous analyses (Figure 29B). An optimal concentration of 1 µM independent of TLR stimulation could be validated. As observed before, higher concentrations of cytochalasin D induced strong decreases in IL-2 secretion CD4⁺ cells. Similar to 18-dehydroxycytochalasin H, stimulation of CD4⁺ cells only induced slight elevations in IL-2 at 1 and 5 µM. In comparison to this, the purchased cytochalasin D caused an increase in IL-2 with increasing concentrations (Figure 29C). Thus, the highest levels in IL-2 were detected at 10 µM without an additional TLR stimulus as well as with CpG 2216 or LPS indicating that the optimal concentration was not yet reached. The strongest increase in IL-2 production by CD4⁺ cells could be observed for the samples without additional TLR stimulation. Moreover, a slight increase in IL-2 secretion by CD4⁺ cells only could be observed at 10 µM.

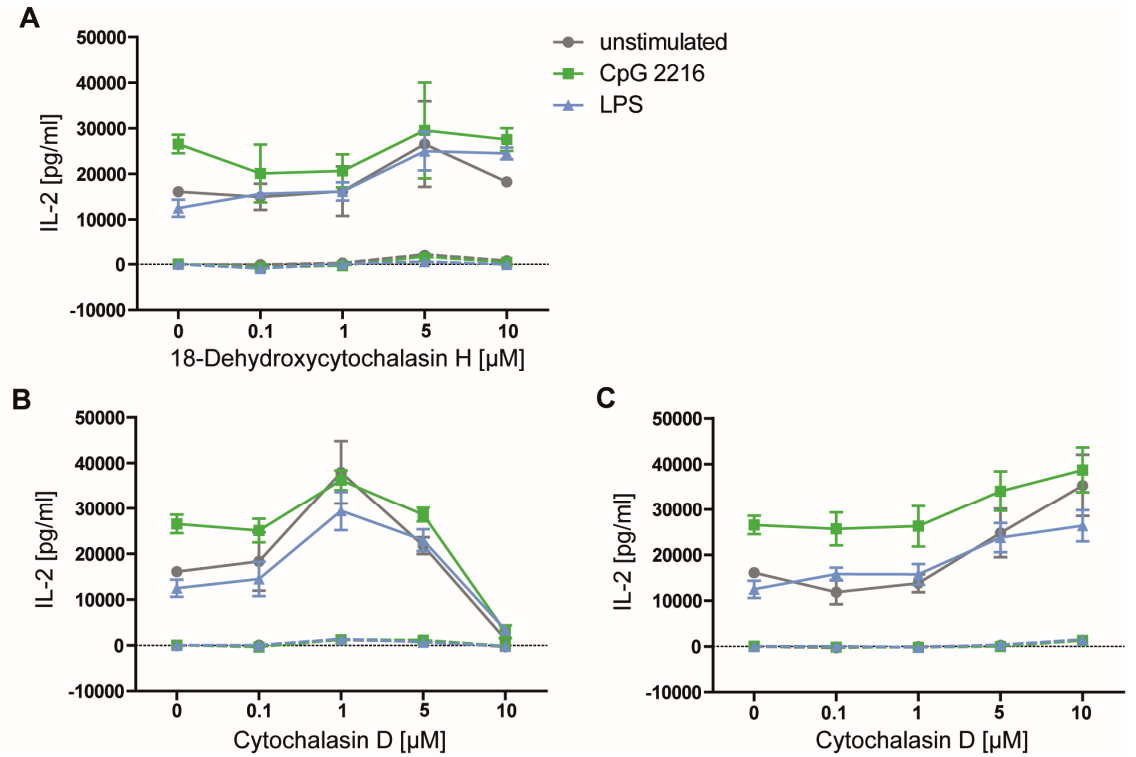

Figure 29: T cell activating properties of selected natural products in the third experiment. GM-CSF-cultured cells were incubated with varying concentrations of 18-dehydroxycytochalasin H (A; 0.1, 1, 5 and 10 µM), cytochalasin D from the natural product library (B; 0.1, 1, 5 and 10 µM)) or purchased cytochalasin D (C; 0.1, 1, 5 and 10 µM) with or without CpG 2216 or LPS for 24 h and co-cultured with $CD4^+$ cells as described in Figure 27. Solid lines indicate samples with co-cultures of DCs and $CD4^+$ cells while dashed lines represent samples with T cells only. Error bars indicate SDs of two biological replicates measured as technical duplicates.

Taken together, out of the three natural products identified as promising compounds in the IL-12p40 assays, only 18-dehydroxycytochalasin H and cytochalasin D were capable of also effectively inducing T cell activation. Here, 18-dehydroxycytochalasin H exhibited an optimal concentration of 5 µM instead of 1 µM in the IL-12p40 while cytochalasin D was constantly most activating at 1 µM. In the T cell activation assays, these effects largely happened independently of an additional TLR stimulus. In contrast to cytochalasin D from the natural product library, the optimal concentration of purchased cytochalasin D was not yet reached in our experiment. These different effects might be explained by varying concentrations of the used natural product aliquots or their contamination with TLR ligands during extraction and preparation of the compounds. Nevertheless, both compounds successfully induced T cell activation.

3.6 Histone deacetylase inhibitors

HDACi are promising candidates for immunotherapeutic drug development (Banik *et al.* 2019). Treatment with specific HDACi with a limited range of targets instead of pan HDACi that cause inconsistent cellular effects is thought to be an alternative opportunity for cancer therapy (Knox *et al.* 2019). In this thesis, the effect of HDACi stimulation of pDCs on IFNβ production was analyzed. Besides treatments with HDACi, pDCs were additionally incubated with the synthetic dsRNA analog poly I:C. For this experimental approach, bone marrow cultures from mob mice were set up which allow the detection of YFP as a reporter molecule for IFNβ expression (Scheu *et al.* 2008). In other approaches, pDCs have been defined to be CD11c^{int} B220^{+} CD317^{+} CD11b^{-} (Bauer *et al.* 2016). Here, pDCs were gated on single, live cells negative for T and B cell markers, defined to be CD11c^{+} CD11b^{-} B220^{+} and analyzed for IFNβ/YFP production as well as for CD86 surface expression (Figure 30).

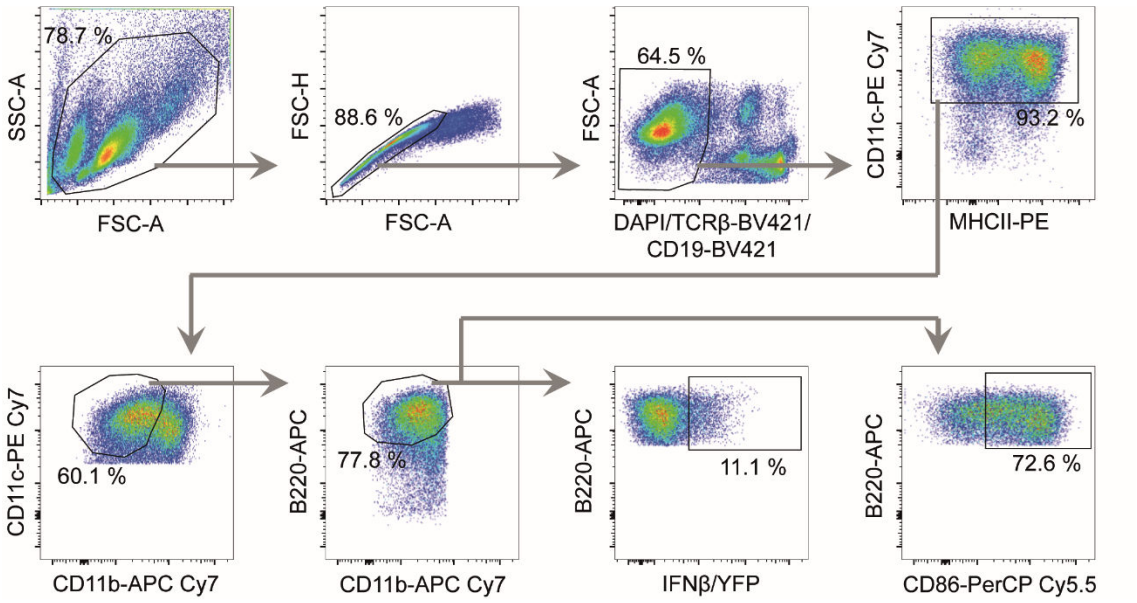

Figure 30: Gating strategy for Flt3L-cultured cells. Samples were measured using a BD FACSCanto II and subsequently analyzed via FlowJo 10.5.3. Samples were initially gated for cells, single and live TCRβ^{-} CD19^{-} cells. Live cells were further gated on CD11c^{+}CD11b^{-} B220^{+} cells for the analysis of IFNβ/YFP and CD86 expression by pDCs. Percentages indicate the frequencies of the parental populations.

In pilot experiments it could be shown that a pan HDACi induced IFNβ secretion by poly I:C-stimulated pDCs leading to the conclusion that HDACi are capable of inducing type I IFN expression of pDCs. This is especially surprising due to the fact that pDCs

lack TLR3 for poly I:C sensing. In this thesis, the effects of two HDACi with preferences for HDAC6 and HDAC1 (KSK64) or HDAC6 (MPK264) were tested.

The first HDACi, KSK64, was non-toxic to pDCs for a concentration range of 1-100 nM (Figure 31A). Higher concentrations showed toxic effects (data not shown). With KSK64 alone, no IFNβ$^+$ pDCs could be detected (Figure 31B). Similarly, at stimulation only with poly I:C a comparable slight increase was observed. At co-stimulation with both, HDACi and poly I:C, analysis of the frequency of IFNβ$^+$ pDCs revealed an increase with increasing concentrations, indicating 100 nM with 11% IFNβ$^+$ pDCs to be the optimal concentration. This observation was supported by the calculation of the mean fluorescence intensities (MFIs; Figure 31C). By calculation of the MFI, the mean expression strength of a marker can be determined and enables direct conclusions on expression levels. Like IFNβ/YFP frequencies, IFNβ/YFP MFIs increased with increasing concentrations. Besides IFNβ, the surface activation marker CD86, which is important for T cell activation, was increased simultaneously (Figure 31D & E).

In brief, the HDACi KSK64 caused IFNβ production by pDCs upon treatment of Flt3L-cultured cells at following stimulation with poly I:C.

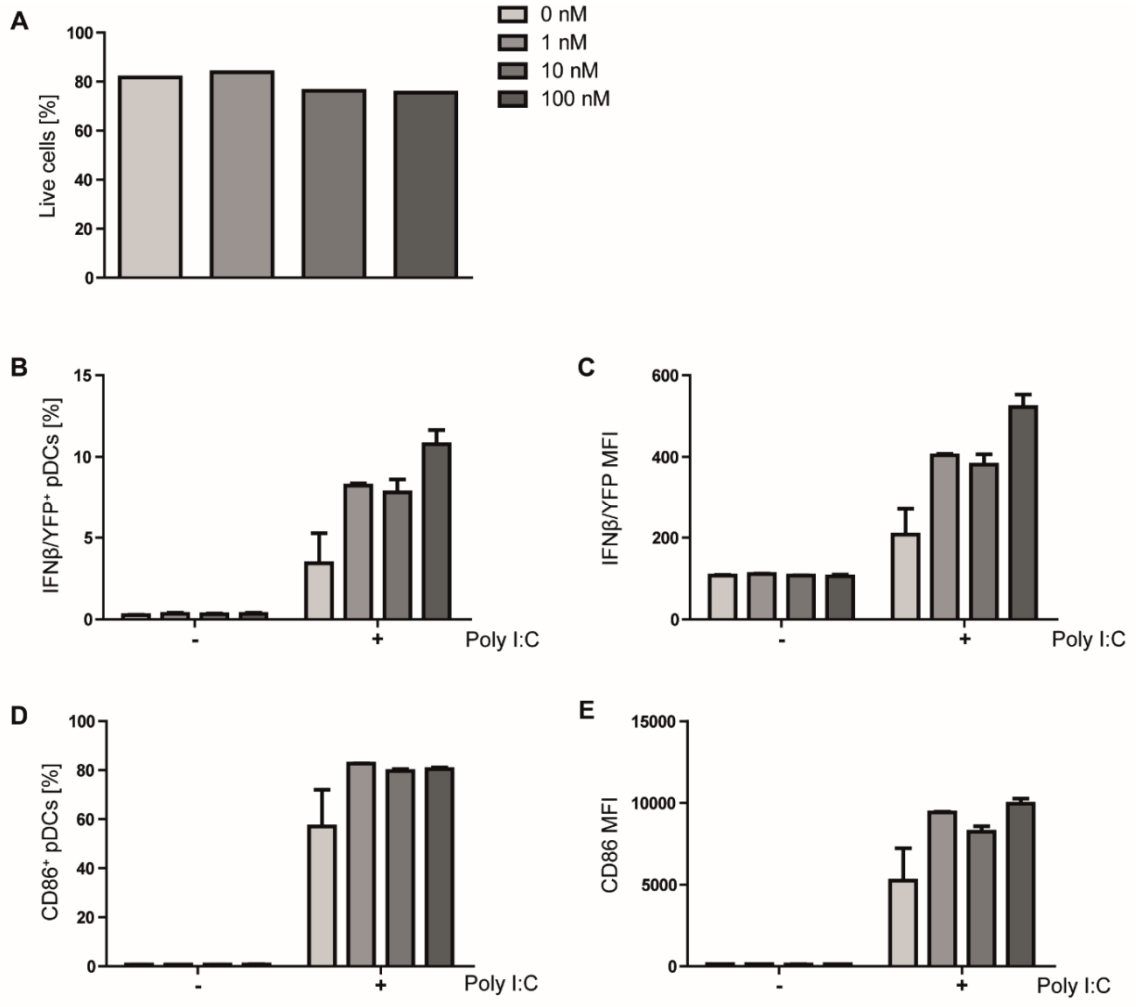

Figure 31: Immune stimulating effects of KSK64. Flt3L-cultured cells were incubated with varying concentrations (1, 10 and 100 nM) of KSK64 for 24 h with following stimulation with poly I:C for additional 24 h. Samples were analyzed via flow cytometry for live cells (A), IFNβ/YFP$^+$ pDCs (B) or IFNβ/YFP MFI (C), CD86$^+$ pDCs (D) or CD86 MFI (E) with pre-gating on single, live, CD11c$^+$ CD11b$^-$ B220$^+$ cells. Percentages indicate the frequencies of the parental populations. Error bars indicate SDs of technical triplicates of the poly I:C stimulation. Shown is one representative experiment out of three.

Treatment with the second HDACi MPK264 revealed a slight increase in live cells with increasing concentrations of up to 2 µM (Figure 32A). Frequency of IFNβ$^+$ pDCs increased with increasing concentrations of MPK264 when additionally stimulated with poly I:C (Figure 32B). Poly I:C stimulation of MPK264-treated pDCs induced an increase in IFNβ$^+$ pDCs of 17% for the highest concentration, thus inducing a stronger enhancement than after treatment with KSK64. This observation is additionally supported by calculation of MFIs which increased with increasing concentrations but displayed an optimal concentration of 1 µM (Figure 32C). Moreover, frequency of CD86$^+$ pDCs increased after combination treatment (Figure 32D). However, analysis of the MFI

revealed stronger increases in CD86 expression levels with the highest increase observed at 2 µM (Figure 32E).

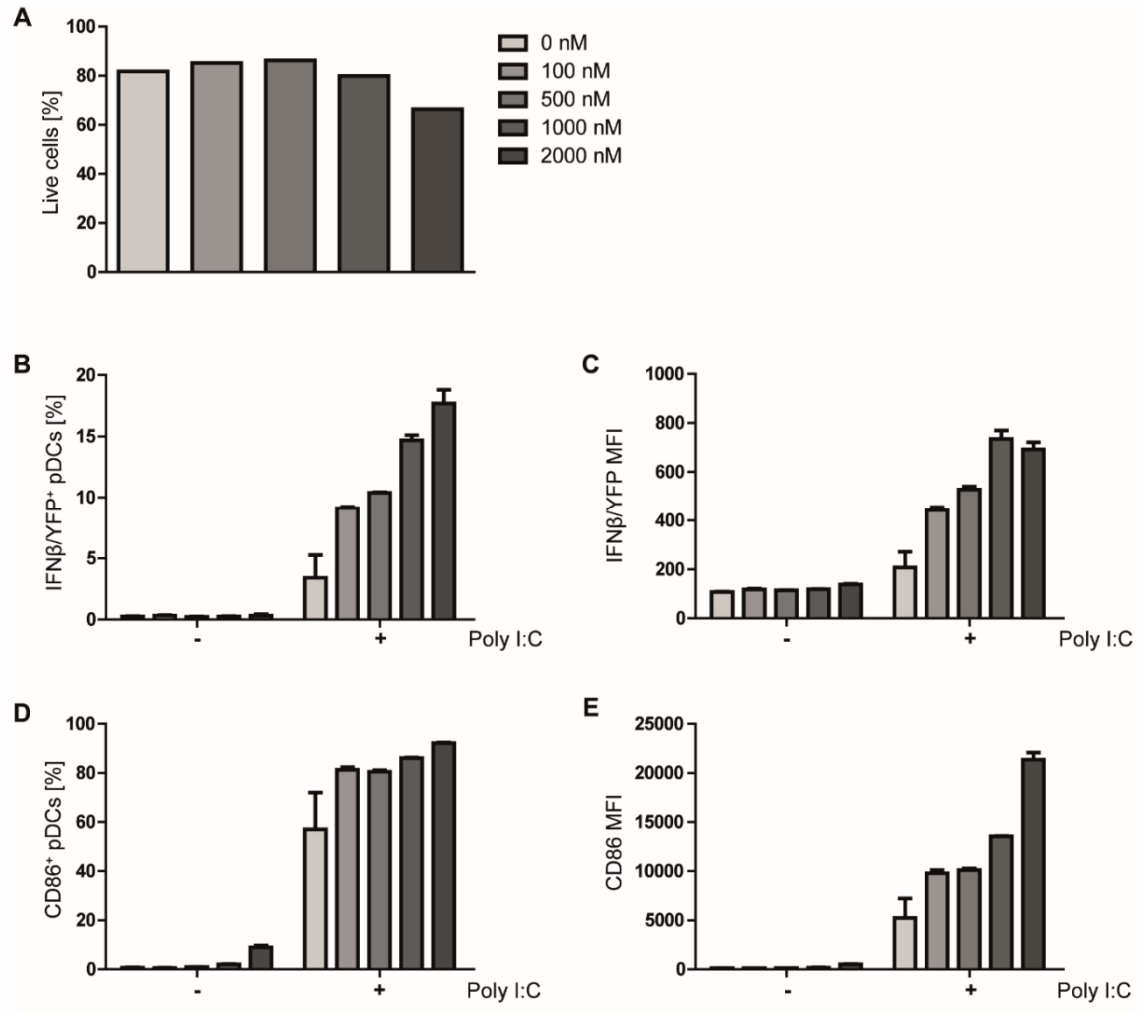

Figure 32: Immune stimulating effects of MPK264. Flt3L-cultured cells were incubated with varying concentrations (100, 500, 1000 and 2000 nM) of MPK264 for 24 h with following stimulation with poly I:C for additional 24 h. Samples were analyzed as described in Figure 31 for live cells (A), IFNβ/YFP$^+$ pDCs (B) or IFNβ/YFP MFI (C), CD86$^+$ pDCs (D) or CD86 MFI (E). Percentages indicate the frequencies of the parental populations. Error bars indicate SDs of technical triplicates of the poly I:C stimulation. Shown is one representative experiment out of three.

Thus, MPK264 like KSK64 was capable of inducing IFNβ production by pDCs.

Taken together, both HDACi significantly induced IFNβ expression by pDCs when additionally treated with poly I:C. The experiments were performed thrice with one experiment independently performed by our bachelor student Azlan Nisar. The hypothesis regarding the underlying mechanism and opportunities for HDAC6i in cancer therapy are discussed in the following sections.

4. Discussion and outlook

Natural products as well as HDACi provide promising tools for the treatment of cancers but also of diseases caused by bacterial infections. In this thesis, novel screening guidelines for the identification of immune activating natural products suitable for immunotherapy have been defined and tested by screening a library comprising 240 natural products. Moreover, two HDACi have been analyzed for their capacity to induce type I IFN production by pDCs. The respective results are discussed in the following sections. An outlook is provided on how to integrate these results in future experiments and on how to proceed with promising candidates as drugs inspiring immunotherapeutic drug development.

4.1 Natural products as immune activating compounds

The current lack of universally valid guidelines for determination of immune activating properties of compounds led to the definition of new screening guidelines in this thesis. These guidelines enable the screening for advantageous properties of compounds such as natural products and their suitability for further immunotherapeutic drug development. According to these guidelines, natural products have to be non-toxic for immune target cells, here comprising cDCs, pDCs and macrophages, to exhibit additional beneficial bioactivities for the treatment of cancer or infections and to induce immune activation. For evaluation and establishment of these guidelines, 240 natural products have been analyzed. The screening results and the characteristics of the most promising natural products are discussed in the following sections and an outlook on further optimization of screening conditions is given.

4.1.1 Characteristics of the three most promising natural products

Three out of 240 natural products in the natural product library were found to be non-toxic to immune target cells in the initial screenings for cytotoxicity, to exhibit additional beneficial bioactivities and to be immune activating, thus fulfilling the guidelines. The first natural product, manzamine J *N*-oxide, showed encouraging results in the comparative analyses as it was the only compound displaying four additional beneficial bioactivities. It was directly active against tumor cell lines and bacteria as well as it showed the potential to modulate autophagic mechanisms. In IL-12p40 assays, manzamine J *N*-oxide alone among 41 natural products tested was capable of inducing an increase in IL-12p40 of up to 4-fold at 10 µM compared to the unstimulated controls. Surprisingly, it

also displayed high toxicity at 10 µM which had not been detected in MTT assays before. These opposing effects observed in MTT and IL-12p40 assays regarding toxicity might be caused by freeze and thaw cycles that have been avoided by usage of independent natural product aliquots beginning with the immune activation experiments. Despite the promising first results, manzamine J *N*-oxide did not exhibit any T cell activating potential. Based on this observation, an explanation for the toxic but immune stimulating effects at 10 µM might be the emergence of DAMPs from dying cells. It has been shown previously that IL-12p40 can be produced as a reaction to toxicity-associated DAMP formation (Piccinini and Midwood 2010). In the natural product library analyzed in this thesis, the manzamine J *N*-oxide derivative manzamine F has also been tested (Figure 33). Both derivatives share the same basic structure.

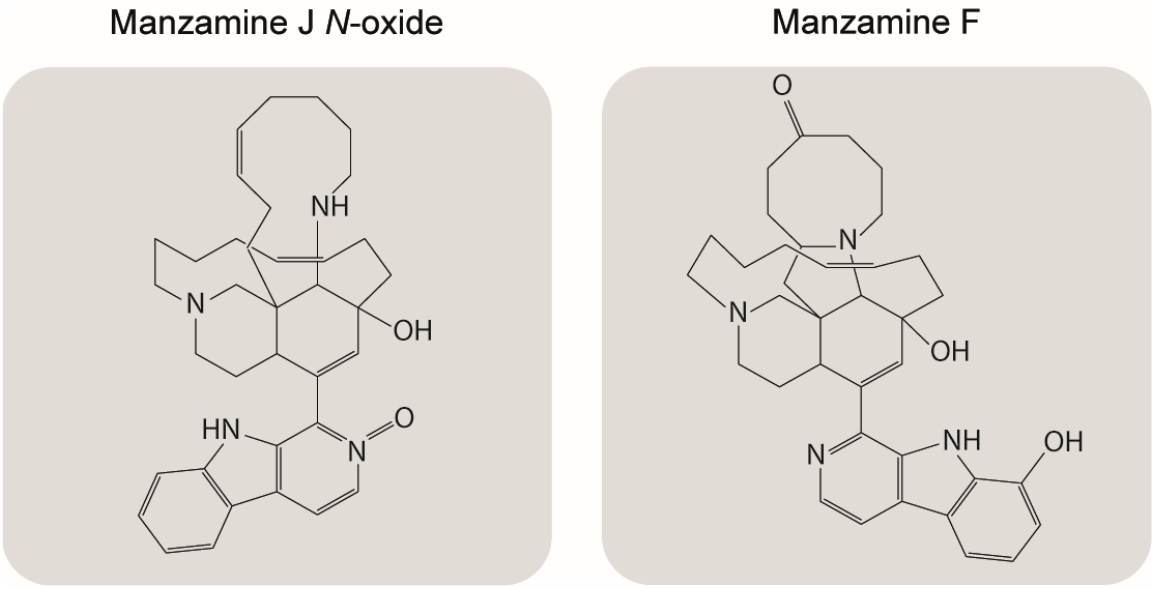

Figure 33: Structures of the two manzamine derivatives manzamine J *N*-oxide and manzamine F.

Like its derivative, Manzamine F was non-toxic to all immune target cells, did exhibit toxicity for lymphoma cells and showed autophagy-modulating potential. However, manzamine F did not exert any immune activating characteristics. In literature, various other manzamines have been analyzed and are in discussion for drug development. For example, manzamine A has potential as anti-cancer drug while other manzamines exhibit anti-bacterial, anti-viral and anti-parasitic capacities (Guzman *et al.* 2011; Song *et al.* 2018; Rao *et al.* 2004). Contrary to this, in this thesis, manzamine A and 8-O-manzamine A were excluded as candidates initially due to cytotoxicity detected in MTT assays (see Appendix). Taken together, manzamine J *N*-oxide itself is unsuitable

for further drug development but biochemically optimized derivatives could prove promising. This is further discussed in section 4.3.2 Biochemical optimization.

The two cytochalasins 18-dehydroxycytochalasin H and cytochalasin D also belong to the most promising natural products identified in this thesis. Both compounds have been shown to be non-toxic to target immune cells, to possess additional beneficial bioactivities and to induce immune activation via enhancement of IL-12p40 as well as T cell activation. In comparative analyses conducted by cooperation partners, cytochalasin D exhibited direct toxicity against lymphoma cells and p53-mutated pancreatic cancer cells, while 18-dehydroxycytochalasin H was toxic against lymphoma cells solely.

Cytochalasins are fungal toxins, potent inhibitors of actin polymerization and frequently used in experiments exploring cytoskeletal functions (Sampath and Pollard 1991). Actin polymerization is an essential mechanism for cellular movement processes including angiogenesis, immune surveillance and endocytic events. The course of actin polymerization is dependent on ATP. Monomeric ATP-bound actin is added to the fast-growing end of actin filaments. After conversion of ATP to ADP, actin detaches from the filaments. Actin-binding proteins support this process by e.g. capping of actin filaments (Lee and Dominguez 2010). Cytochalasins have been shown to interfere with several steps of actin polymerization. For example, cytochalasin D is able to stimulate the hydrolysis of ATP, thus accelerating the release of actin from filaments. Cytochalasin B on the other side has been shown to bind the fast-growing end of actin filaments, thereby inhibiting their elongation (Trendowski 2015). Moreover, it is known from literature that several cytochalasins including cytochalasin D show anti-tumor effects which probably can be explained by the rapid proliferation cycle of cancer cells and a consequently stronger inhibition of actin polymerization (Trendowski 2015; Bousquet *et al.* 1990; Udagawa *et al.* 2000; Huang *et al.* 2012). In this thesis, the immune activating effects of both cytochalasins 18-dehydroxycytochalasin H and cytochalasin D were especially prominent at additional stimulation with the TLR ligand CpG 2216. Thus, we hypothesize that cytochalasins induce a concentration-dependent retention of CpG 2216 in the endosome and a longer exposition of TLR9 to this stimulus. Actin itself plays an essential role in endocytic processes as it regulates the formation of vesicles and the detachment of vesicles from the cell membrane (Mooren *et al.* 2012). The hypothesis underlying immune stimulation by cytochalasins is supported by the knowledge that cytochalasin D is capable of forming actin aggregates associated with endosomal proteins (Mortensen and Larsson 2003). Following this hypothesis, a specific concentration range is necessary for retention of CpG 2216 in the cytosol with 10 µM already being too high. Thus, the next step would be to further elucidate this hypothesis via, for example, staining

of the actin cytoskeleton with phalloidin after cytochalasin and CpG 2216 treatment to visualize changes in actin arrangement. For comparison purposes, other actin-disrupting agents can be used.

In the course of this thesis, 18-dehydroxycytochalasin H exhibited an optimal concentration of 1 µM in the IL-12p40 assays and of 5 µM in the T cell activation assays. As 5 µM was not tested in the IL-12p40 assays, the optimal concentration probably could not be detected here. Cytochalasin D on the other hand showed the best effects at 1 µM in both IL-12p40 and T cell activation experiments. Interestingly, both compounds depended on CpG 2216 stimulation in the IL-12p40 assays but exhibited potent T cell activation potential independently of additional TLR stimulation. These observations might be explained by the usage of different natural product aliquots. However, 18-dehydroxycytochalasin H and cytochalasin D might induce DC activation independently of simultaneous TLR stimulation without a distinct increase in IL-12p40 production that nevertheless causes activation of T cells. Furthermore, the differences in IL-2 production by $CD4^+$ cells only from the second and third T cell activation experiment might be explained by a different composition of $CD4^+$ cells obtained from MACS. Presumably, $CD4^+$ cells in the third experiment comprised more cells with a higher memory status that those in the second experiment.

In general, cytochalasins might prove promising as chemotherapeutic drugs in combination with other cytoskeleton-modulating drugs that target, for example, microtubules (Trendowski 2015). Moreover, particularly cytochalasin D has already been shown to have a positive impact on anti-infection immune responses exhibited by macrophages in combination treatment with antibiotics (Dey *et al.* 2015). Thus, cytochalasins might also be advantageous for immunotherapeutic drug development and the prevention of resistances especially when used in combination with other direct tumor- or infection-targeting drugs.

4.1.2 Optimization of screening conditions

In this thesis, the cytokines IL-12p40 and IL-2 were chosen as readouts for immune activation of DCs or T cells, respectively. IL-12 itself, which is necessary for the differentiation of T helper 1 cells, is still in discussion for immunotherapeutic approaches despite conflicting results in clinical trials (Garris *et al.* 2018; Lasek *et al.* 2014). New applications and routes of administration are tested and might prove beneficial in combination therapies with activating natural products. IL-2 is secreted by activated T cells and is essential for the differentiation of $CD4^+$ T cells into effector T cells after antigen presentation (Jiang *et al.* 2016). Here, in the T cell activation assays, $CD4^+$ cells

have been incubated with GM-CSF-derived cells. Thus, these $CD4^+$ cells include naïve but potentially also memory T cells that might be sensitive to natural product stimulation also in the absence of antigen presentation. This could be prevented by using naïve cells only. T cell activation could furthermore be confirmed by analysis of T cell proliferation by e.g. [^{3}H] thymidine incorporation. IL-2 is approved by the U.S. Food and Drug Administration (FDA) for the treatment of metastatic renal cell carcinoma and metastatic melanoma but due to the occurrence of side effects it appears to be inappropriate in monotherapy and should rather be used in combination therapies (Jiang *et al.* 2016). Natural products that are capable of inducing effective T cell activation and thus IL-2 secretion as well as following immune reactions thus might be promising as agents supporting other immunotherapeutic approaches.

In this thesis, immune activating effects of natural products alone or in combination with TLR ligands have been explored. Because it cannot be ruled out that those compounds were contaminated with TLR ligands, application of adequate controls is crucial like also performed in this thesis. Prospectively, further immune stimulating agents could be applied.

In the presented screening pipeline, the focus was set on compounds that are non-toxic and activate immune cells, but also toxic and inhibitory natural products could be interesting for different applications in drug development and diseases that are accompanied by malfunctions of distinct immune cell types. It was decided to only continue working with compounds that are non-toxic to all cell types at all concentrations which led to the consequence that some compounds that induced a high metabolic activity of one cell type but were toxic to another were excluded from further analyses. Similarly, only GM-CSF-derived cells as very potent APCs were analyzed for immune activation whereas distinct natural products might be stimulatory (or inhibitory) for pDCs or macrophages. Distinct cell subtypes could also be analyzed in greater detail, e.g. cDCs from GM-CSF-cultured cells could additionally be stained for Flt3/CD135 as a cDC marker and CD115 for exclusion of macrophages (Helft *et al.* 2015). This would allow a more accurate determination of cell types responsible for IL-12p40 production, however, mixed cultures with different cell types are closer to physiological conditions. In general, the usage of primary murine cells is advantageous over the use of human cells as mouse strains could also easily be used in *in vivo* mouse experiments (see section 4.3.3 *In vivo* mouse models), thus allowing better transition of experimental setups.

The presented screening platform has been established using robust assay setups and is useful particularly for application in academic environments. These institutions usually do not have access to industrial high throughput facilities. For HTS, assays can be validated by the Z-factor which provides advantages over simple signal-to-background

or signal-to-noise ratio calculations. Due to its high sensitivity to variability a large bulk of data is obligate for usage of the Z-factor (Zhang *et al.* 1999). Instead, here appropriate controls have been carefully chosen and sample data have been normalized to these results in the applied assays. Where possible, background data have been subtracted. Biological replicates including separate samples from more than one animal in at least three independent replicates ensured that the depicted assays are robust and provide stable results.

In summary, the presented screening guidelines were applied for the detection of immune activating natural products but can furthermore be applied for other settings that aim e.g. at the identification of inhibitory compounds or that use other cell types. This might require the analysis of different cytokines as markers for immune suppression or activation of distinct cell types. However, natural products provide a wide variety of molecules with the potential to inspire medical drug development. Application of natural products alone or in combination with existing therapies might be a promising approach as they augur more targeted therapies with less side effects for patients and avoidance of resistances.

4.2 HDAC6i as immune activating compounds

HDACs are often misregulated in the context of cancer and thus serve as promising targets for therapy. HDACi such as the pan HDACi vorinostat are already used in clinics to treat cutaneous T cell lymphoma and other cancer types while often accompanied by severe side effects therapy due to the unspecific targeting of HDACs (Banik *et al.* 2019). Specific HDACi including HDAC6i have already shown promising results for the treatment of cancer (Woan *et al.* 2015). Nevertheless, balanced type I IFN levels are required for successful therapy (Budhwani *et al.* 2018). Here, the results obtained from the two HDAC6i KSK64 and MPK264 tested in this thesis are discussed and a hypothesis regarding underlying mechanisms is postulated.

4.2.1 Combinatorial HDAC6i and poly I:C treatment induces IFNβ production by pDCs

In this thesis, two HDACi that preferentially target HDAC6 or HDAC6 and 1 have been tested for immunostimulatory functions in pDCs. HDAC6 has previously been shown to regulate immune functions and hamper tumor growth *in vivo* (Cosenza and Pozzi 2018; Knox *et al.* 2019). pDCs are promising target cells due to their eminent capacity to produce type I IFNs upon stimulation. IFNβ expression triggers activation of surrounding

cells and thus is essential for the activation of effective adaptive immune responses by e.g. T and NK cells (Lee and Ashkar 2018). Type I IFNs have previously been shown to be essential for most cancer immunotherapeutic approaches. Insufficient type I IFN secretion might induce resistance, thus making pDCs auspicious targets for immune activation (Budhwani *et al.* 2018). In this thesis, pDCs have additionally been incubated with poly I:C after HDACi treatment. Poly I:C is a TLR ligand that usually signals via TLR3. pDCs lack this receptor and alternatively recognize poly I:C via the RIG-I-like receptor MDA5, thus inducing lower levels of type I IFN compared to TLR7/9 stimulation by other ligands such as CpG 2216 (Matsumoto and Seya 2008; Ali *et al.* 2019; Takeuchi and Akira 2008). Here, combinatorial treatment with the two HDAC6i KSK64 and MPK264 and additional poly I:C stimulation induced a concentration-dependent secretion of IFNβ by pDCs.

So far it is known that HDAC6 is capable of forming complexes with STAT3, thus regulating the STAT3/IL-10 pathway in APCs (Cheng *et al.* 2014). STAT3 is one of seven proteins belonging to the STAT family of proteins. Recognition of cytokines by receptors in the cell membrane triggers phosphorylation and thus activation and homodimerization of STAT3. The following signaling cascade ultimately leads to the expression of genes involved in a vast variety of processes such as cell proliferation, immune responses but also metastasis. As elevated levels of STAT3 are often found in the context of cancer and are associated with bad prognosis, the protein is discussed as target for cancer treatment (Johnston and Grandis 2011). Additionally, STAT3 has been shown to negatively regulate type I IFN expression. In STAT3 knockout mouse embryonic fibroblasts, MDA5 mRNA is upregulated upon viral infection leading to increased production of type I IFNs (Wang *et al.* 2011). In the context of this work, this knowledge led to the hypothesis, that treatment with KSK64 or MPK264 at first disrupts STAT3-HDAC6 complexes, consequently inactivating STAT3 and enabling IFNβ expression which otherwise would have been negatively regulated by STAT3 (Figure 34). This capacity to produce IFNβ is further potentiated by increased MDA5 expression due to STAT3 inactivity. Thus, STAT3 inactivation and upregulation of MDA5 expression pave the way for enhanced recognition of poly I:C stimulation and subsequently higher IFNβ expression.

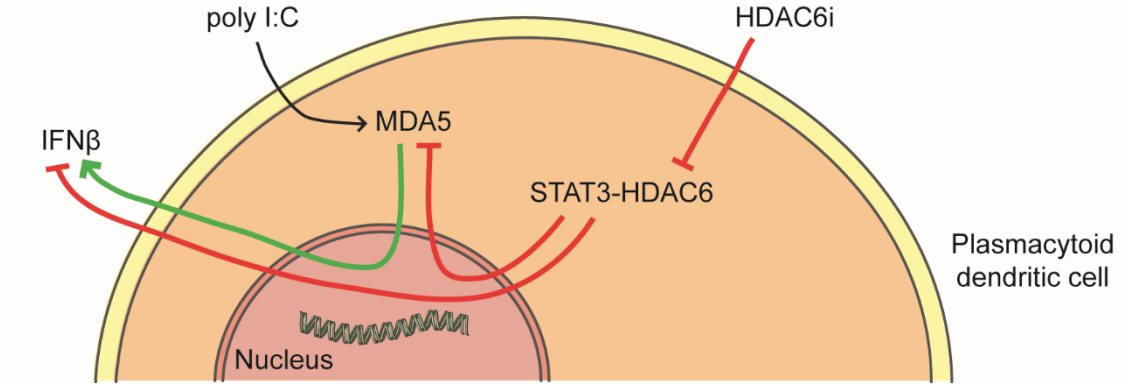

Figure 34: Proposed mechanism behind the observed increased IFNβ secretion by pDCs after HDAC6i and poly I:C treatment. HDAC6i such as KSK64 and MPK264 disrupt the STAT3-HDAC6 complexes which otherwise inhibit MDA5 and IFNβ expression. Increased expression of MDA5 enables enhanced recognition of poly I:C and consequently higher levels of IFNβ. Red lines indicate inhibitory and the green line activating mechanisms.

Following this hypothesis, the next steps comprise experiments to assess whether these conditions also pertain to pDCs. For this, sorted pDCs instead of whole cell cultures could be used for stimulation to eliminate the influence of other cell types and to determine if this process is solely pDC-dependent. Initially, it has to be evaluated if STAT3 and HDAC6 also form complexes in pDCs and modulate IL-10 expression. To determine whether STAT3 is active or inactive upon treatment of pDCs with HDAC6i, the phosphorylation status of STAT3 can be examined. Here it would be interesting to further analyze if deacetylation and dephosphorylation of STAT3 act dependently or independently of each other. Modified STAT3 functions could moreover be explained by changed suppressor of cytokine 3 signaling (SOCS3) levels. SOCS3 is an indirect inhibitor of STAT3 (Carow and Rottenberg 2014). Further analysis of STAT3 function in this context can be performed by usage of STAT3 knockout pDCs. This way, it can be evaluated whether MDA5 levels are modified upon STAT3 inhibition or knockout in pDCs and give insights to determine whether STAT3 directly represses MDA5.

4.2.2 Opportunities for HDAC6i in cancer therapy

Abnormally high expression of HDAC6 often is associated with tumor growth and survival. Consequently, increased levels of HDAC6 can serve as markers for disease progression in several cancer types (Aldana-Masangkay and Sakamoto 2011). Treatment of pDCs with HDAC6i might be a promising approach for future cancer therapies, thus combining epigenetic and immune stimulating effects. Especially in regard to the development of immunotherapeutic drugs which often only help a restricted

number of patients, such combination therapies using specific drugs could prove helpful in overcoming resistances. The only HDAC6i in clinical trials so far are ricolinostat and citarinostat. Ricolinostat was tested as monotherapy but showed more promising effects in combination with additional drugs such as the proteasome inhibitor bortezomib which is FDA-approved for the treatment of multiple myeloma. Their synergistic activity is supposed to be caused by simultaneous inhibition of proteasome and aggresome components (Cosenza and Pozzi 2018). Citarinostat, on the other hand, has been shown to increase immune functions by upregulation of MHCI and MHCII as well as several other activation markers such as CD86 on tumor cells and DCs, thereby promoting anti-tumor immune responses (Bae *et al.* 2018). Further preclinical studies currently analyze effects of ricolinostat and citarinostat in combination therapies involving, for example, immune checkpoint inhibitors, antibodies or the immunomodulator dexamethasone (Cosenza and Pozzi 2018). Two other HDAC6i, tubacin and tubastatin A, have been determined as unsuitable for clinical trials due to ineffective oral delivery of the agents (Cosenza and Pozzi 2018).
Usage of specific HDACi instead of pan HDACi and potential application in combination approaches might represent promising opportunities for future cancer treatment. Compounds are urgently needed that help overcoming resistances toward traditional treatment options and that exhibit less side effects accompanied by additional advantageous characteristics like reduced treatment times and doses.

4.3 Outlook

Compounds that have been defined promising for further drug development in the presented screenings have to be analyzed for responsible modes of action, interaction partners and possible optimization opportunities. Applicable approaches for target finding, biochemical optimization and useful mouse models are presented in the following sections.

4.3.1 Target finding

A first step for the identification of possible targets in general includes the comparison of the compound of interest with derivatives or similar structures and their targets to narrow down the range of possible targets. For that, computational approaches can be used. If targets of a compound are already known, they can be found via the Binding Database (Gilson *et al.* 2016). The Binding Database gathers information on interactions of proteins and small molecules obtained from research papers and patents and is open to public,

thus allowing analysis especially of known compounds. If no targets are known yet, an alternative method is presented by the Similarity Ensemble Approach (SEA) which predicts possible targets by comparing simplified molecular input line entry system (SMILES) codes of the compound of interest to similar structures with known targets (Keiser *et al.* 2007). Similarly, the molecular pathway predictor PathwayMap can be used for definition of the association of a compound with molecular pathways. PathwayMap is a machine learning approach based on neural networks and draws on data from the pathway databases KEGG and Reactome (Jimenez *et al.* 2019). Computational target finding approaches can be extended by application of biological methods. These approaches can be divided into two categories: Direct and indirect. In the latter one, gene expression profiles, for example, of the compound of interest are compared to those of known compounds via next generation sequencing (Chengalvala *et al.* 2007; Lamb *et al.* 2006; Woollard *et al.* 2011). Consequently, indirect approaches can give hints on involved pathways but require compounds with similar phenotypes. Direct approaches, in contrast, are more straightforward as they identify protein targets directly interacting with the compound of interest (Kubota *et al.* 2019). For this, possible protein targets can be overexpressed, purified, assigned to protein microarrays and examined for compound binding affinities (Schirle and Jenkins 2016; Kubota *et al.* 2019).

Supplementary or alternatively to computational target deconvolution, *in vitro* approaches can be applied. A helpful method for target identification is the functional tagging of natural products e.g. by “minimalist” small molecule tagging (MSMT). Natural products get converted into affinity-based probes, incubated with target proteins and made usable for visualization for example via Western Blot analyses or microscopy for location studies (Lang *et al.* 2019; Kubota *et al.* 2019). A detailed example for application of functional tagging of compounds is represented by photoaffinity labeling. Photoaffinity labeling is an unbiased method for the identification of binding partners as well as unknown binding sites. For this, the compound of interest is labelled with a photoreactive group which reacts with nearby molecules upon irradiation with light (Smith and Collins 2015). Frequently used representatives of photoreactive groups are benzophenones, aryl azides and alkyl or aryl diazirines (Wright and Sieber 2016). Additional labeling with fluorophores or radioactive isotopes can be used to visualize compound-target interactions via e.g. fluorescence microscopy or radiation measuring devices (Smith and Collins 2015; Lang *et al.* 2019; Kubota *et al.* 2019). The application of mass spectrometry further supports the elucidation of bound proteins (Lang *et al.* 2019).

After identification of possible targets, target confirmation is the next step. If antibodies against the protein of interest are available, target confirmation can simply take place via analysis in Western Blots (Wright and Sieber 2016). In general, the usage of small tags

is more straightforward as they are expected to interfere less with biological functions of the molecule but nevertheless compounds have to be highly active to visualize them. Ligands of compounds with known mechanisms can further be confirmed by measurement of enzyme educts and products such as ATP or by usage of specific inhibitors.
Taken together, a vast diversity of possible methods exists and the choice of the appropriate target finding approach always depends on the structure and chemical characteristics of the compound.

4.3.2 Biochemical optimization

To be applicable as drugs, natural products often have to be biochemically modified. Moreover, they can serve as lead compounds inspiring drug development based on their high structural diversity and novelty. Optimization of compounds aims to enhance the efficacy of the drug, to improve its chemical accessibility and to promote absorption, distribution, metabolism, excretion and toxicity (ADMET) profiles of a compound (Xiao *et al.* 2016). For determination of the bioavailability of orally administered drugs, Lipinski *et al*. defined the rule of five. Accordingly, orally administered drugs should have a maximum of five hydrogen bond donors and ten hydrogen bond acceptors, a molecular weight less than 500 and a partition coefficient between octanol and water below five (Lipinski *et al.* 2001). Nevertheless, natural products frequently are excepted from this rule presumably caused by intramolecular hydrogen bonding (Lipinski 2016).
Optimization strategies for compounds involve the direct alteration of functional groups of compounds by addition or substitution to synthesize derivatives and the alteration of ring systems also by modification, addition or removal of ring structures or isosteric substitutes. These approaches do not cause a change in the basic structure of the compound and are intended to keep its advantageous activities (Xiao *et al.* 2016). Alternatively, structure-activity relationships can be determined which aim at the identification of the molecular structures responsible for an exhibited bioactivity. Based on this, optimization can take place without alteration of structures associated with desirable activities (Xiao *et al.* 2016; Guha 2013). Similarly, in pharmacophore-oriented design, pharmacophoric characteristics of the compound are defined and subsequently novel structures are designed with possibly modified basic structures (Xiao *et al.* 2016). A pharmacophore is an abstract model defined by the IUPAC as an “[…] ensemble of steric and electronic features that is necessary to ensure the optimal supramolecular interactions with a specific biological target structure and to trigger (or to block) its biological response” (Wermuth *et al.* 1998). Taken together, all these approaches are

applied for improvement of the efficacy of a compound, its pharmacokinetic and safety properties and its chemical accessibility (Xiao *et al.* 2016). Similar to target finding approaches, the decision for appropriate methods for biochemical optimization depends on the structure causing the desired activities of the compound of interest. Here, an extended literature research could help as natural products such as manzamines and cytochalasins are already widely used and various derivatives exist. Modified compounds would have to be tested again in the presented screenings to ensure they still exhibit their desired bioactivities and immune activating capacities.

4.3.3 *In vivo* mouse models

After examination of the molecular mechanisms underlying immune activating properties of natural products and HDACi as well as eventual biochemical optimization, the compounds can be applied in *in vivo* mouse models. Those models have to be carefully chosen in regard to a specific research question and the ADMET profile which has been determined or modified in advance via biochemical optimization.

Initially in mouse experiments, the general susceptibility of the animals towards a potential drug has to be evaluated. For that, *in vivo* toxicity and optimal dosing are determined before analysis of effects on e.g. tumor size or bacterial load (Hu-Lieskovan *et al.* 2015; Garris *et al.* 2018). For examination of immune activation as previously illustrated, the same reporter mouse models can be used to figure out if capacities of the tested compounds also hold true *in vivo*. In this thesis, get40 mice for tracking IL-12p40/GFP after stimulation with natural products and mob mice for analysis of IFNβ/YFP after incubation with HDAC6i and poly I:C have been used. Moreover, a reporter mouse model combining both cytokines and thus allowing simultaneous analysis of IL-12p40/GFP and IFNβ/YFP is available. Administration of promising compounds to these mice could reveal systemic or distinct immune activating effects.

For examination of immune modulating effects, humanized mouse models are frequently applied. Here, human cells such as peripheral blood mononuclear cells (PBMCs), hematopoietic stem cells or tissue cells are transferred into immunodeficient mice. These models aim at the resemblance of the human immune system but often face the problem of, for example, different cytokine microenvironments and the absence or presence of specific growth factors. Nevertheless, such models are often used to study the efficacy of immunotherapeutic drugs and have already been applied in several infection models such as *Salmonella* infections (Walsh *et al.* 2017). For the analysis of infections with bacteria but also with parasites like *Toxoplasma gondii* it can be necessary to replace

human-infecting strains with other strains because the human pathogen might not be infectious in mice (Swearengen 2018).

For studying drug efficacy against cancer, three models are established for different cancer types. They can be used to examine drug efficacy as well as general tumor biology. Firstly, like for analyses of infection, humanized mouse models can be used. Secondly, in xenograft models, transplantable tumors or human tumor cell lines are implanted into immunodeficient mice which do not reject the tumor and facilitate examination of direct anti-tumor effects. A wide variety of tumor cell lines is available which allows evaluation of the drug efficacy on a diverse set of human cancers. For complete assessment of immune functions, immunocompetent mice can be used. Transplantable tumor models are time-saving and suitable for fast screening of potential drugs but also do not reflect the natural tumor microenvironment (Budhu *et al.* 2014). Lastly, transgenic mouse models can be applied. Here, genes are modified to allow, for example, overexpression of tumor-promoting oncogenes or the inactivation of suppressor genes. In contrast to human cancers, those genetic modifications are continuously present. Transgenic mouse models in general are more time-consuming and can be less efficient for evaluation of immunotherapeutic drugs than transplantable tumor models (Budhu *et al.* 2014). Usage of these mouse models enables the evaluation of immune modulating and anti-tumor effects of a compound such as the analysis of IL-12p40^{+} tumor-infiltrating cells.

In case that underlying mechanisms of immune activating drugs are known, specific mouse models can be used that are genetically modified and lack one protein in specific cell types or allow tracking of another. For deeper analysis of the modes of action of HDAC6i, specific HDAC6-deficient mice are available. These mice show hyperacetylated tubulin but nevertheless develop normally thus indicating important but not crucial roles of HDAC6 for survival. In terms of the immune system, HDAC6-deficient mice do not display a change in immune cell numbers but slightly impacted antibody production and higher HIV infection levels (Zhang *et al.* 2008). Usage of these mice in the experimental approaches illustrated in this thesis could facilitate the examination of whether the effects observed after treatment of pDCs with HDAC6i and poly I:C are due to deacetylation of HDAC6 itself or of any other proteins.

For translation of the results obtained in mouse models to humans, disadvantages and deficiencies of the mouse models have to be evaluated as animal models should be close to humans but never can completely mimic the human biology (Swearengen 2018). Promising compounds can subsequently be analyzed in clinical trials.

4.3.4 Additional remarks

Natural products provide an inestimable number of bioactive compounds with diverse structures and innovative modes of action that are promising for drug development for a wide variety of diseases. Screening of compound libraries with natural products from various sources consequently allows an unbiased analysis and the detection of unexpected mechanisms. In any case, the setup of a database that collects all data obtained from screenings is highly helpful especially in the case of research consortia (Xie *et al.* 2015). Research consortia can gather a high level of knowledge and provide exchange if they are comprised of scientists from various disciplines such as biology, pharmaceutics, computer science and chemistry. Furthermore, the screening guidelines presented in this thesis provide screening conditions that allow evaluation of compound libraries especially for academic institutions. These institutions usually do not have access to high throughput facilities, thus alternatives with low financial burden and a high probability of success are advantageous. Consequently, analyses of natural product libraries from different angles enable the prosperous identification of compounds with the potential for subsequent drug development and the timely detection of resistances.

5. Conclusions

In this thesis, 240 natural products and two HDACi have been analyzed for immune modulating activities. Two cytochalasins, namely 18-dehydroxycytochalasin H and cytochalasin D, have been found to be non-toxic to immune target cells, to display additional beneficial bioactivities against tumors or infections and to exhibit immune activating properties regarding IL-12p40 production by DCs and T cell activation. The two HDACi KSK64 and MPK264 preferentially target HDAC6 and HDAC1 or HDAC6, respectively, and have been proven to induce IFNβ production by pDCs when additionally stimulated with poly I:C. All four compounds show promising features especially for anti-cancer drug development. They exhibit characteristics that can inspire immunotherapy, but the underlying mechanisms remain to be elucidated. Immunotherapy represents a novel, innovative method to treat cancer and infections alternatively to the common treatment options and is prominent to the public at the latest since the allocation of the Nobel Prize 2018 for Medicine or Physiology. It represents a promising approach that hopefully can be advanced by the application of natural products that activate immune cells for targeting tumors or infections. The methodical approaches presented in this thesis especially facilitate screening of natural products for academic institutions without access to high throughput facilities. All assays used are relatively simple, well accepted assays and provide robust results at low financial burden. Moreover, the presented experiments aim to provide a first step for the identification of promising compounds that are specific, avoid the emergence of resistances and minimize side effects for patients. Drugs with innovative modes of action are needed that increase the activity of anti-tumor and anti-infection immune effector cells and simultaneously counteract resistance mechanisms of tumors and pathogens.

6. References

Abdi, K. and Singh, N. J. 2015. 'Making many from few: IL-12p40 as a model for the combinatorial assembly of heterodimeric cytokines', Cytokine, 76: 53-7.

Aldana-Masangkay, G. I. and Sakamoto, K. M. 2011. 'The role of HDAC6 in cancer', J Biomed Biotechnol, 2011: 875824.

Ali, S., Hoven, A., Dress, R. J., Schaal, H., Alferink, J. and Scheu, S. 2018. 'Identification of a novel Dlg2 isoform differentially expressed in IFNbeta-producing plasmacytoid dendritic cells', BMC Genomics, 19: 194.

Ali, S., Mann-Nüttel, R., Schulze, A., Richter, L., Alferink, J. and Scheu, S. 2019. 'Sources of Type I Interferons in Infectious Immunity: Plasmacytoid Dendritic Cells Not Always in the Driver's Seat', Front Immunol, 10: 778.

American Association for Cancer Research. 2018. 'Cancer Progress Report 2018', Accessed 26 March 2019. https://www.cancerprogressreport.org/PAGES/CPR18-CONTENTS.ASPX.

Anguille, S., Smits, E. L., Bryant, C., Van Acker, H. H., Goossens, H., Lion, E., Fromm, P. D., Hart, D. N., Van Tendeloo, V. F. and Berneman, Z. N. 2015. 'Dendritic Cells as Pharmacological Tools for Cancer Immunotherapy', Pharmacol Rev, 67: 731-53.

Bae, J., Hideshima, T., Tai, Y. T., Song, Y., Richardson, P., Raje, N., Munshi, N. C. and Anderson, K. C. 2018. 'Histone deacetylase (HDAC) inhibitor ACY241 enhances anti-tumor activities of antigen-specific central memory cytotoxic T lymphocytes against multiple myeloma and solid tumors', Leukemia, 32: 1932-47.

Bahrami, A., Fereidouni, M., Pirro, M., Bianconi, V. and Sahebkar, A. 2019. 'Modulation of regulatory T cells by natural products in cancer', Cancer Lett, 459: 72-85.

Banchereau, J., Briere, F., Caux, C., Davoust, J., Lebecque, S., Liu, Y. J., Pulendran, B. and Palucka, K. 2000. 'Immunobiology of dendritic cells', Annu Rev Immunol, 18: 767-811.

Banik, D., Moufarrij, S. and Villagra, A. 2019. 'Immunoepigenetics Combination Therapies: An Overview of the Role of HDACs in Cancer Immunotherapy', Int J Mol Sci, 20.

Baraya, Y. S., Wong, K. K. and Yaacob, N. S. 2017. 'The Immunomodulatory Potential of Selected Bioactive Plant-Based Compounds in Breast Cancer: A Review', Anticancer Agents Med Chem, 17: 770-83.

Barnden, M. J., Allison, J., Heath, W. R. and Carbone, F. R. 1998. 'Defective TCR expression in transgenic mice constructed using cDNA-based alpha- and beta-chain genes under the control of heterologous regulatory elements', Immunol Cell Biol, 76: 34-40.

Barrat, F. J. and Su, L. 2019. 'A pathogenic role of plasmacytoid dendritic cells in autoimmunity and chronic viral infection', J Exp Med, 216: 1974-85.

Bauer, J., Dress, R. J., Schulze, A., Dresing, P., Ali, S., Deenen, R., Alferink, J. and Scheu, S. 2016. 'Cutting Edge: IFN-beta Expression in the Spleen Is Restricted to a Subpopulation of Plasmacytoid Dendritic Cells Exhibiting a Specific Immune Modulatory Transcriptome Signature', J Immunol, 196: 4447-51.

Blair, J. M., Webber, M. A., Baylay, A. J., Ogbolu, D. O. and Piddock, L. J. 2015. 'Molecular mechanisms of antibiotic resistance', Nat Rev Microbiol, 13: 42-51.

Bousquet, P. F., Paulsen, L. A., Fondy, C., Lipski, K. M., Loucy, K. J. and Fondy, T. P. 1990. 'Effects of cytochalasin B in culture and in vivo on murine Madison 109 lung carcinoma and on B16 melanoma', Cancer Res, 50: 1431-9.

Boyman, O. and Sprent, J. 2012. 'The role of interleukin-2 during homeostasis and activation of the immune system', Nat Rev Immunol, 12: 180-90.

Budhu, S., Wolchok, J. and Merghoub, T. 2014. 'The importance of animal models in tumor immunity and immunotherapy', Curr Opin Genet Dev, 24: 46-51.

Budhwani, M., Mazzieri, R. and Dolcetti, R. 2018. 'Plasticity of Type I Interferon-Mediated Responses in Cancer Therapy: From Anti-tumor Immunity to Resistance', Front Oncol, 8: 322.

Butler, M. S. 2004. 'The role of natural product chemistry in drug discovery', J Nat Prod, 67: 2141-53.

Butler, M. S., Robertson, A. A. and Cooper, M. A. 2014. 'Natural product and natural product derived drugs in clinical trials', Nat Prod Rep, 31: 1612-61.

Carow, B. and Rottenberg, M. E. 2014. 'SOCS3, a Major Regulator of Infection and Inflammation', Front Immunol, 5: 58.

Cheng, F., Lienlaf, M., Wang, H. W., Perez-Villarroel, P., Lee, C., Woan, K., Rock-Klotz, J., Sahakian, E., Woods, D., Pinilla-Ibarz, J., Kalin, J., Tao, J., Hancock, W., Kozikowski, A., Seto, E., Villagra, A. and Sotomayor, E. M. 2014. 'A novel role for histone deacetylase 6 in the regulation of the tolerogenic STAT3/IL-10 pathway in APCs', J Immunol, 193: 2850-62.

Chengalvala, M. V., Chennathukuzhi, V. M., Johnston, D. S., Stevis, P. E. and Kopf, G. S. 2007. 'Gene expression profiling and its practice in drug development', Curr Genomics, 8: 262-70.

Chow, J. C., Young, D. W., Golenbock, D. T., Christ, W. J. and Gusovsky, F. 1999. 'Toll-like receptor-4 mediates lipopolysaccharide-induced signal transduction', J Biol Chem, 274: 10689-92.

Cosenza, M. and Pozzi, S. 2018. 'The Therapeutic Strategy of HDAC6 Inhibitors in Lymphoproliferative Disease', Int J Mol Sci, 19.

Croxford, A. L., Kulig, P. and Becher, B. 2014. 'IL-12-and IL-23 in health and disease', Cytokine Growth Factor Rev, 25: 415-21.

Cruz, F. M., Colbert, J. D., Merino, E., Kriegsman, B. A. and Rock, K. L. 2017. 'The Biology and Underlying Mechanisms of Cross-Presentation of Exogenous Antigens on MHC-I Molecules', Annu Rev Immunol, 35: 149-76.

D'Andrea, A., Rengaraju, M., Valiante, N. M., Chehimi, J., Kubin, M., Aste, M., Chan, S. H., Kobayashi, M., Young, D., Nickbarg, E. and et al. 1992. 'Production of natural killer cell stimulatory factor (interleukin 12) by peripheral blood mononuclear cells', J Exp Med, 176: 1387-98.

de Zoeten, E. F., Wang, L., Butler, K., Beier, U. H., Akimova, T., Sai, H., Bradner, J. E., Mazitschek, R., Kozikowski, A. P., Matthias, P. and Hancock, W. W. 2011. 'Histone deacetylase 6 and heat shock protein 90 control the functions of Foxp3(+) T-regulatory cells', Mol Cell Biol, 31: 2066-78.

Dey, S., Majhi, A., Mahanti, S., Dey, I. and Bishayi, B. 2015. 'In Vitro Anti-inflammatory and Immunomodulatory Effects of Ciprofloxacin or Azithromycin in Staphylococcus aureus-Stimulated Murine Macrophages are Beneficial in the Presence of Cytochalasin D', Inflammation, 38: 1050-69.

Dias Junior, A. G., Sampaio, N. G. and Rehwinkel, J. 2019. 'A Balancing Act: MDA5 in Antiviral Immunity and Autoinflammation', Trends Microbiol, 27: 75-85.

Garris, C. S., Arlauckas, S. P., Kohler, R. H., Trefny, M. P., Garren, S., Piot, C., Engblom, C., Pfirschke, C., Siwicki, M., Gungabeesoon, J., Freeman, G. J., Warren, S. E., Ong, S., Browning, E., Twitty, C. G., Pierce, R. H., Le, M. H., Algazi, A. P., Daud, A. I., Pai, S. I., Zippelius, A., Weissleder, R. and Pittet, M. J. 2018. 'Successful Anti-PD-1 Cancer Immunotherapy Requires T Cell-Dendritic Cell Crosstalk Involving the Cytokines IFN-gamma and IL-12', Immunity, 49: 1148-61 e7.

Gilson, M. K., Liu, T., Baitaluk, M., Nicola, G., Hwang, L. and Chong, J. 2016. 'BindingDB in 2015: A public database for medicinal chemistry, computational chemistry and systems pharmacology', Nucleic Acids Res, 44: D1045-53.

Gordon, S. and Pluddemann, A. 2017. 'Tissue macrophages: heterogeneity and functions', BMC Biol, 15: 53.

Granucci, F., Feau, S., Angeli, V., Trottein, F. and Ricciardi-Castagnoli, P. 2003. 'Early IL-2 production by mouse dendritic cells is the result of microbial-induced priming', J Immunol, 170: 5075-81.

Guha, R. 2013. 'On exploring structure-activity relationships', Methods Mol Biol, 993: 81-94.

Guzman, E. A., Johnson, J. D., Linley, P. A., Gunasekera, S. E. and Wright, A. E. 2011. 'A novel activity from an old compound: Manzamine A reduces the metastatic potential of AsPC-1 pancreatic cancer cells and sensitizes them to TRAIL-induced apoptosis', Invest New Drugs, 29: 777-85.

Haefner, B. 2003. 'Drugs from the deep: marine natural products as drug candidates', Drug Discov Today, 8: 536-44.

Halili, M. A., Andrews, M. R., Labzin, L. I., Schroder, K., Matthias, G., Cao, C., Lovelace, E., Reid, R. C., Le, G. T., Hume, D. A., Irvine, K. M., Matthias, P., Fairlie, D. P. and Sweet, M. J. 2010. 'Differential effects of selective HDAC inhibitors on macrophage inflammatory responses to the Toll-like receptor 4 agonist LPS', J Leukoc Biol, 87: 1103-14.

Helft, J., Bottcher, J., Chakravarty, P., Zelenay, S., Huotari, J., Schraml, B. U., Goubau, D. and Reis e Sousa, C. 2015. 'GM-CSF Mouse Bone Marrow Cultures Comprise a Heterogeneous Population of CD11c(+)MHCII(+) Macrophages and Dendritic Cells', Immunity, 42: 1197-211.

Hemann, E. A. and Legge, K. L. 2014. 'Peripheral regulation of T cells by dendritic cells during infection', Immunol Res, 59: 66-72.

Hemmi, H., Takeuchi, O., Kawai, T., Kaisho, T., Sato, S., Sanjo, H., Matsumoto, M., Hoshino, K., Wagner, H., Takeda, K. and Akira, S. 2000. 'A Toll-like receptor recognizes bacterial DNA', Nature, 408: 740-5.

Hu-Lieskovan, S., Mok, S., Homet Moreno, B., Tsoi, J., Robert, L., Goedert, L., Pinheiro, E. M., Koya, R. C., Graeber, T. G., Comin-Anduix, B. and Ribas, A. 2015. 'Improved antitumor activity of immunotherapy with BRAF and MEK inhibitors in BRAF(V600E) melanoma', Sci Transl Med, 7: 279ra41.

Huang, F. Y., Mei, W. L., Li, Y. N., Tan, G. H., Dai, H. F., Guo, J. L., Wang, H., Huang, Y. H., Zhao, H. G., Zhou, S. L., Li, L. and Lin, Y. Y. 2012. 'The antitumour activities induced by pegylated liposomal cytochalasin D in murine models', Eur J Cancer, 48: 2260-9.

Iwamoto, T. 2013. 'Clinical application of drug delivery systems in cancer chemotherapy: review of the efficacy and side effects of approved drugs', Biol Pharm Bull, 36: 715-8.

Iwasaki, A. and Medzhitov, R. 2010. 'Regulation of adaptive immunity by the innate immune system', Science, 327: 291-5.

Jelinek, I., Leonard, J. N., Price, G. E., Brown, K. N., Meyer-Manlapat, A., Goldsmith, P. K., Wang, Y., Venzon, D., Epstein, S. L. and Segal, D. M. 2011. 'TLR3-specific double-stranded RNA oligonucleotide adjuvants induce dendritic cell cross-presentation, CTL responses, and antiviral protection', J Immunol, 186: 2422-9.

Jiang, T., Zhou, C. and Ren, S. 2016. 'Role of IL-2 in cancer immunotherapy', Oncoimmunology, 5: e1163462.

Jimenez, J., Sabbadin, D., Cuzzolin, A., Martinez-Rosell, G., Gora, J., Manchester, J., Duca, J. and De Fabritiis, G. 2019. 'PathwayMap: Molecular Pathway Association with Self-Normalizing Neural Networks', J Chem Inf Model, 59: 1172-81.

Johnston, P. A. and Grandis, J. R. 2011. 'STAT3 signaling: anticancer strategies and challenges', Mol Interv, 11: 18-26.

Kawasaki, T. and Kawai, T. 2014. 'Toll-like receptor signaling pathways', Front Immunol, 5: 461.

Keiser, M. J., Roth, B. L., Armbruster, B. N., Ernsberger, P., Irwin, J. J. and Shoichet, B. K. 2007. 'Relating protein pharmacology by ligand chemistry', Nat Biotechnol, 25: 197-206.

Klatzmann, D. and Abbas, A. K. 2015. 'The promise of low-dose interleukin-2 therapy for autoimmune and inflammatory diseases', Nat Rev Immunol, 15: 283-94.

Knox, T., Sahakian, E., Banik, D., Hadley, M., Palmer, E., Noonepalle, S., Kim, J., Powers, J., Gracia-Hernandez, M., Oliveira, V., Cheng, F., Chen, J., Barinka, C., Pinilla-Ibarz, J., Lee, N. H., Kozikowski, A. and Villagra, A. 2019. 'Selective HDAC6 inhibitors improve anti-PD-1 immune checkpoint blockade therapy by decreasing the anti-inflammatory phenotype of macrophages and down-regulation of immunosuppressive proteins in tumor cells', Sci Rep, 9: 6136.

Kontis, V., Bennett, J. E., Mathers, C. D., Li, G., Foreman, K. and Ezzati, M. 2017. 'Future life expectancy in 35 industrialised countries: projections with a Bayesian model ensemble', Lancet, 389: 1323-35.

Krieg, A. M. 2002. 'CpG motifs in bacterial DNA and their immune effects', Annu Rev Immunol, 20: 709-60.

Kubota, K., Funabashi, M. and Ogura, Y. 2019. 'Target deconvolution from phenotype-based drug discovery by using chemical proteomics approaches', Biochim Biophys Acta Proteins Proteom, 1867: 22-27.

Labidi-Galy, S. I., Treilleux, I., Goddard-Leon, S., Combes, J. D., Blay, J. Y., Ray-Coquard, I., Caux, C. and Bendriss-Vermare, N. 2012. 'Plasmacytoid dendritic cells infiltrating ovarian cancer are associated with poor prognosis', Oncoimmunology, 1: 380-82.

Lamb, J., Crawford, E. D., Peck, D., Modell, J. W., Blat, I. C., Wrobel, M. J., Lerner, J., Brunet, J. P., Subramanian, A., Ross, K. N., Reich, M., Hieronymus, H., Wei, G., Armstrong, S. A., Haggarty, S. J., Clemons, P. A., Wei, R., Carr, S. A., Lander, E. S. and Golub, T. R. 2006. 'The Connectivity Map: using gene-expression signatures to connect small molecules, genes, and disease', Science, 313: 1929-35.

Lambert, G., Estevez-Salmeron, L., Oh, S., Liao, D., Emerson, B. M., Tlsty, T. D. and Austin, R. H. 2011. 'An analogy between the evolution of drug resistance in bacterial communities and malignant tissues', Nat Rev Cancer, 11: 375-82.

Lang, W., Yuan, C., Zhu, B., Pan, S., Liu, J., Luo, J., Nie, S., Zhu, Q., Lee, J. S. and Ge, J. 2019. 'Expanding the "minimalist" small molecule tagging approach to different bioactive compounds', Org Biomol Chem, 17: 3010-17.

Lasek, W., Zagozdzon, R. and Jakobisiak, M. 2014. 'Interleukin 12: still a promising candidate for tumor immunotherapy?', Cancer Immunol Immunother, 63: 419-35.

Lee, A. J. and Ashkar, A. A. 2018. 'The Dual Nature of Type I and Type II Interferons', Front Immunol, 9: 2061.

Lee, S. H. and Dominguez, R. 2010. 'Regulation of actin cytoskeleton dynamics in cells', Mol Cells, 29: 311-25.

Li, Y. and Seto, E. 2016. 'HDACs and HDAC Inhibitors in Cancer Development and Therapy', Cold Spring Harb Perspect Med, 6.

Liechtenstein, T., Dufait, I., Lanna, A., Breckpot, K. and Escors, D. 2012. 'Modulating Co-Stimulation during Antigen Presentation to Enhance Cancer Immunotherapy', Immunol Endocr Metab Agents Med Chem, 12: 224-35.

Lipinski, C. A. 2016. 'Rule of five in 2015 and beyond: Target and ligand structural limitations, ligand chemistry structure and drug discovery project decisions', Adv Drug Deliv Rev, 101: 34-41.

Lipinski, C. A., Lombardo, F., Dominy, B. W. and Feeney, P. J. 2001. 'Experimental and computational approaches to estimate solubility and permeability in drug discovery and development settings', Adv Drug Deliv Rev, 46: 3-26.

Luckheeram, R. V., Zhou, R., Verma, A. D. and Xia, B. 2012. 'CD4(+)T cells: differentiation and functions', Clin Dev Immunol, 2012: 925135.

Mansoori, B., Mohammadi, A., Davudian, S., Shirjang, S. and Baradaran, B. 2017. 'The Different Mechanisms of Cancer Drug Resistance: A Brief Review', Adv Pharm Bull, 7: 339-48.

Mantovani, A., Marchesi, F., Malesci, A., Laghi, L. and Allavena, P. 2017. 'Tumour-associated macrophages as treatment targets in oncology', Nat Rev Clin Oncol, 14: 399-416.

Matsumoto, M. and Seya, T. 2008. 'TLR3: interferon induction by double-stranded RNA including poly(I:C)', Adv Drug Deliv Rev, 60: 805-12.

Merad, M., Sathe, P., Helft, J., Miller, J. and Mortha, A. 2013. 'The dendritic cell lineage: ontogeny and function of dendritic cells and their subsets in the steady state and the inflamed setting', Annu Rev Immunol, 31: 563-604.

Mitchell, D., Chintala, S. and Dey, M. 2018. 'Plasmacytoid dendritic cell in immunity and cancer', J Neuroimmunol, 322: 63-73.

Mo, X., Tang, C., Niu, Q., Ma, T., Du, Y. and Fu, H. 2019. 'HTiP: High-Throughput Immunomodulator Phenotypic Screening Platform to Reveal IAP Antagonists as Anti-cancer Immune Enhancers', Cell Chem Biol, 26: 331-39 e3.

Mohammad, H. P., Barbash, O. and Creasy, C. L. 2019. 'Targeting epigenetic modifications in cancer therapy: erasing the roadmap to cancer', Nat Med, 25: 403-18.

Mooren, O. L., Galletta, B. J. and Cooper, J. A. 2012. 'Roles for actin assembly in endocytosis', Annu Rev Biochem, 81: 661-86.

Mortensen, K. and Larsson, L. I. 2003. 'Effects of cytochalasin D on the actin cytoskeleton: association of neoformed actin aggregates with proteins involved in signaling and endocytosis', Cell Mol Life Sci, 60: 1007-12.

Musumeci, A., Lutz, K., Winheim, E. and Krug, A. B. 2019. 'What Makes a pDC: Recent Advances in Understanding Plasmacytoid DC Development and Heterogeneity', Front Immunol, 10: 1222.

Naran, K., Nundalall, T., Chetty, S. and Barth, S. 2018. 'Principles of Immunotherapy: Implications for Treatment Strategies in Cancer and Infectious Diseases', Front Microbiol, 9: 3158.

Newman, D. J. and Cragg, G. M. 2016. 'Natural Products as Sources of New Drugs from 1981 to 2014', J Nat Prod, 79: 629-61.

Oppmann, B., Lesley, R., Blom, B., Timans, J. C., Xu, Y., Hunte, B., Vega, F., Yu, N., Wang, J., Singh, K., Zonin, F., Vaisberg, E., Churakova, T., Liu, M., Gorman, D., Wagner, J., Zurawski, S., Liu, Y., Abrams, J. S., Moore, K. W., Rennick, D., de Waal-Malefyt, R., Hannum, C., Bazan, J. F. and Kastelein, R. A. 2000. 'Novel p19 protein engages IL-12p40 to form a cytokine, IL-23, with biological activities similar as well as distinct from IL-12', Immunity, 13: 715-25.

Papaioannou, N. E., Beniata, O. V., Vitsos, P., Tsitsilonis, O. and Samara, P. 2016. 'Harnessing the immune system to improve cancer therapy', Ann Transl Med, 4: 261.

Perez Del Palacio, J., Diaz, C., de la Cruz, M., Annang, F., Martin, J., Perez-Victoria, I., Gonzalez-Menendez, V., de Pedro, N., Tormo, J. R., Algieri, F., Rodriguez-Nogales, A., Rodriguez-Cabezas, M. E., Reyes, F., Genilloud, O., Vicente, F. and Galvez, J. 2016. 'High-Throughput Screening Platform for the Discovery of New Immunomodulator Molecules from Natural Product Extract Libraries', J Biomol Screen, 21: 567-78.

Piccinini, A. M. and Midwood, K. S. 2010. 'DAMPening inflammation by modulating TLR signalling', Mediat Inflamm, 2010.

Postow, M. A. 2015. 'Managing immune checkpoint-blocking antibody side effects', Am Soc Clin Oncol Educ Book: 76-83.

Quante, A. S., Ming, C., Rottmann, M., Engel, J., Boeck, S., Heinemann, V., Westphalen, C. B. and Strauch, K. 2016. 'Projections of cancer incidence and cancer-related deaths in Germany by 2020 and 2030', Cancer Med, 5: 2649-56.

Rao, K. V., Kasanah, N., Wahyuono, S., Tekwani, B. L., Schinazi, R. F. and Hamann, M. T. 2004. 'Three new manzamine alkaloids from a common Indonesian sponge and their activity against infectious and tropical parasitic diseases', J Nat Prod, 67: 1314-8.

Rebecca, V. W. and Amaravadi, R. K. 2016. 'Emerging strategies to effectively target autophagy in cancer', Oncogene, 35: 1-11.

Reinhardt, R. L., Hong, S., Kang, S. J., Wang, Z. E. and Locksley, R. M. 2006. 'Visualization of IL-12/23p40 in vivo reveals immunostimulatory dendritic cell migrants that promote Th1 differentiation', J Immunol, 177: 1618-27.

Reizis, B. 2019. 'Plasmacytoid Dendritic Cells: Development, Regulation, and Function', Immunity, 50: 37-50.

Richter, L., Kropp, S., Proksch, P. and Scheu, S. 2019. 'A mouse model-based screening platform for the identification of immune activating compounds such as natural products for novel cancer immunotherapies', Bioorg Med Chem: 115145.

Riss, T. L., Moravec, R. A., Niles, A. L., Benink, H. A., Worzella, T. J. and Minor, L. 2004. 'Cell Viability Assays.' in G. S. Sittampalam, N. P. Coussens, H. Nelson, M. Arkin, D. Auld, C. Austin, B. Bejcek, M. Glicksman, J. Inglese, P. W. Iversen, Z. Li, J. McGee, O. McManus, L. Minor, A. Napper, J. M. Peltier, T. Riss, O. J. Trask, Jr. and J. Weidner (eds.), Assay Guidance Manual (Bethesda (MD)).

Rock, K. L., Reits, E. and Neefjes, J. 2016. 'Present Yourself! By MHC Class I and MHC Class II Molecules', Trends Immunol, 37: 724-37.

Rönsberg, D., Debbab, A., Mandi, A., Vasylyeva, V., Bohler, P., Stork, B., Engelke, L., Hamacher, A., Sawadogo, R., Diederich, M., Wray, V., Lin, W., Kassack, M. U., Janiak, C., Scheu, S., Wesselborg, S., Kurtan, T., Aly, A. H. and Proksch, P. 2013. 'Pro-apoptotic and immunostimulatory tetrahydroxanthone dimers from the endophytic fungus Phomopsis longicolla', J Org Chem, 78: 12409-25.

Sampath, P. and Pollard, T. D. 1991. 'Effects of cytochalasin, phalloidin, and pH on the elongation of actin filaments', Biochemistry, 30: 1973-80.

Scheu, S., Dresing, P. and Locksley, R. M. 2008. 'Visualization of IFNbeta production by plasmacytoid versus conventional dendritic cells under specific stimulation conditions in vivo', Proc Natl Acad Sci USA, 105: 20416-21.

Schirle, M. and Jenkins, J. L. 2016. 'Identifying compound efficacy targets in phenotypic drug discovery', Drug Discov Today, 21: 82-89.

Schopf, F. H., Biebl, M. M. and Buchner, J. 2017. 'The HSP90 chaperone machinery', Nat Rev Mol Cell Biol, 18: 345-60.

Serrador, J. M., Cabrero, J. R., Sancho, D., Mittelbrunn, M., Urzainqui, A. and Sanchez-Madrid, F. 2004. 'HDAC6 deacetylase activity links the tubulin cytoskeleton with immune synapse organization', Immunity, 20: 417-28.

Sharma, P., Hu-Lieskovan, S., Wargo, J. A. and Ribas, A. 2017. 'Primary, Adaptive, and Acquired Resistance to Cancer Immunotherapy', Cell, 168: 707-23.

Shen, L., Orillion, A. and Pili, R. 2016. 'Histone deacetylase inhibitors as immunomodulators in cancer therapeutics', Epigenomics, 8: 415-28.

Smith, E. and Collins, I. 2015. 'Photoaffinity labeling in target- and binding-site identification', Future Med Chem, 7: 159-83.

Song, W., Tai, Y. T., Tian, Z., Hideshima, T., Chauhan, D., Nanjappa, P., Exley, M. A., Anderson, K. C. and Munshi, N. C. 2011. 'HDAC inhibition by LBH589 affects the phenotype and function of human myeloid dendritic cells', Leukemia, 25: 161-8.

Song, X., Xiong, Y., Qi, X., Tang, W., Dai, J., Gu, Q. and Li, J. 2018. 'Molecular Targets of Active Anticancer Compounds Derived from Marine Sources', Mar Drugs, 16.

Swearengen, J. R. 2018. 'Choosing the right animal model for infectious disease research', Animal Model Exp Med, 1: 100-08.

Swiecki, M. and Colonna, M. 2011. 'Type I interferons: diversity of sources, production pathways and effects on immune responses', Curr Opin Virol, 1: 463-75.

Swiecki, M. and Colonna, M. 2015. 'The multifaceted biology of plasmacytoid dendritic cells', Nat Rev Immunol, 15: 471-85.

Tacken, P. J., de Vries, I. J., Torensma, R. and Figdor, C. G. 2007. 'Dendritic-cell immunotherapy: from ex vivo loading to in vivo targeting', Nat Rev Immunol, 7: 790-802.

Tait Wojno, E. D., Hunter, C. A. and Stumhofer, J. S. 2019. 'The Immunobiology of the Interleukin-12 Family: Room for Discovery', Immunity, 50: 851-70.

Takeuchi, O. and Akira, S. 2008. 'MDA5/RIG-I and virus recognition', Curr Opin Immunol, 20: 17-22.

Tewary, P., Gunatilaka, A. A. and Sayers, T. J. 2017. 'Using natural products to promote caspase-8-dependent cancer cell death', Cancer Immunol Immunother, 66: 223-31.

The Nobel Prize in Physiology or Medicine. 2011. Accessed 06 November 2019. https://www.nobelprize.org/prizes/medicine/2011/steinman/facts/.

The Nobel Prize in Physiology or Medicine. 2018. Accessed 26 March 2019. https://www.nobelprize.org/prizes/medicine/2018/press-release/.

Trendowski, M. 2015. 'Using cytochalasins to improve current chemotherapeutic approaches', Anticancer Agents Med Chem, 15: 327-35.

Udagawa, T., Yuan, J., Panigrahy, D., Chang, Y. H., Shah, J. and D'Amato, R. J. 2000. 'Cytochalasin E, an epoxide containing Aspergillus-derived fungal metabolite, inhibits angiogenesis and tumor growth', J Pharmacol Exp Ther, 294: 421-7.

Valenzuela-Fernandez, A., Cabrero, J. R., Serrador, J. M. and Sanchez-Madrid, F. 2008. 'HDAC6: a key regulator of cytoskeleton, cell migration and cell-cell interactions', Trends Cell Biol, 18: 291-7.

van Gulijk, M., Dammeijer, F., Aerts, Jgjv and Vroman, H. 2018. 'Combination Strategies to Optimize Efficacy of Dendritic Cell-Based Immunotherapy', Front Immunol, 9: 2759.

Walsh, N. C., Kenney, L. L., Jangalwe, S., Aryee, K. E., Greiner, D. L., Brehm, M. A. and Shultz, L. D. 2017. 'Humanized Mouse Models of Clinical Disease', Annu Rev Pathol, 12: 187-215.

Wang, C., Engelke, L., Bickel, D., Hamacher, A., Frank, M., Proksch, P., Gohlke, H. and Kassack, M. U. 2019. 'The tetrahydroxanthone-dimer phomoxanthone A is a strong inducer of apoptosis in cisplatin-resistant solid cancer cells', Bioorg Med Chem, 27: 115044.

Wang, W. B., Levy, D. E. and Lee, C. K. 2011. 'STAT3 negatively regulates type I IFN-mediated antiviral response', J Immunol, 187: 2578-85.

Wculek, S. K., Cueto, F. J., Mujal, A. M., Melero, I., Krummel, M. F. and Sancho, D. 2019. 'Dendritic cells in cancer immunology and immunotherapy', Nat Rev Immunol.

Wei, S. C., Duffy, C. R. and Allison, J. P. 2018. 'Fundamental Mechanisms of Immune Checkpoint Blockade Therapy', Cancer Discov, 8: 1069-86.

Wermuth, C.G., Ganellin, C.R., Lindberg, P. and Mitscher, L.A. 1998. 'Glossary of terms used in medicinal chemistry (IUPAC Recommendations 1998)', Pure and Applied Chemistry, 70: 1129–43.

Wherry, E. J. and Kurachi, M. 2015. 'Molecular and cellular insights into T cell exhaustion', Nat Rev Immunol, 15: 486-99.

Woan, K. V., Lienlaf, M., Perez-Villaroel, P., Lee, C., Cheng, F., Knox, T., Woods, D. M., Barrios, K., Powers, J., Sahakian, E., Wang, H. W., Canales, J., Marante, D., Smalley, K. S. M., Bergman, J., Seto, E., Kozikowski, A., Pinilla-Ibarz, J., Sarnaik, A., Celis, E., Weber, J., Sotomayor, E. M. and Villagra, A. 2015. 'Targeting histone deacetylase 6 mediates a dual anti-melanoma effect: Enhanced antitumor immunity and impaired cell proliferation', Mol Oncol, 9: 1447-57.

Woollard, P. M., Mehta, N. A., Vamathevan, J. J., Van Horn, S., Bonde, B. K. and Dow, D. J. 2011. 'The application of next-generation sequencing technologies to drug discovery and development', Drug Discov Today, 16: 512-9.

World Health Organization. 2018. 'World health statistics 2018: Monitoring health for the SDGs, sustainable development goals.', Accessed 26 March 2019. https://www.who.int/gho/publications/world_health_statistics/2018/en/.

Wright, G. D. 2017. 'Opportunities for natural products in 21(st) century antibiotic discovery', Nat Prod Rep, 34: 694-701.

Wright, M. H. and Sieber, S. A. 2016. 'Chemical proteomics approaches for identifying the cellular targets of natural products', Nat Prod Rep, 33: 681-708.

Xiao, Z., Morris-Natschke, S. L. and Lee, K. H. 2016. 'Strategies for the Optimization of Natural Leads to Anticancer Drugs or Drug Candidates', Med Res Rev, 36: 32-91.

Xie, T., Song, S., Li, S., Ouyang, L., Xia, L. and Huang, J. 2015. 'Review of natural product databases', Cell Prolif, 48: 398-404.

Yang, L., Wen, K. S., Ruan, X., Zhao, Y. X., Wei, F. and Wang, Q. 2018. 'Response of Plant Secondary Metabolites to Environmental Factors', Molecules, 23.

Yang, M., McKay, D., Pollard, J. W. and Lewis, C. E. 2018. 'Diverse Functions of Macrophages in Different Tumor Microenvironments', Cancer Res, 78: 5492-503.

Yu, L., Wang, L. and Chen, S. 2010. 'Endogenous toll-like receptor ligands and their biological significance', J Cell Mol Med, 14: 2592-603.

Zhang, J. H., Chung, T. D. and Oldenburg, K. R. 1999. 'A Simple Statistical Parameter for Use in Evaluation and Validation of High Throughput Screening Assays', J Biomol Screen, 4: 67-73.

Zhang, Y., Kwon, S., Yamaguchi, T., Cubizolles, F., Rousseaux, S., Kneissel, M., Cao, C., Li, N., Cheng, H. L., Chua, K., Lombard, D., Mizeracki, A., Matthias, G., Alt, F. W., Khochbin, S. and Matthias, P. 2008. 'Mice lacking histone deacetylase 6 have hyperacetylated tubulin but are viable and develop normally', Mol Cell Biol, 28: 1688-701.

Zheng, W., Thorne, N. and McKew, J. C. 2013. 'Phenotypic screens as a renewed approach for drug discovery', Drug Discov Today, 18: 1067-73.

Zhong, Z., Sanchez-Lopez, E. and Karin, M. 2016. 'Autophagy, Inflammation, and Immunity: A Troika Governing Cancer and Its Treatment', Cell, 166: 288-98.

Zhu, J., Yamane, H. and Paul, W. E. 2010. 'Differentiation of effector CD4 T cell populations (*)', Annu Rev Immunol, 28: 445-89.

Zitvogel, L., Galluzzi, L., Kepp, O., Smyth, M. J. and Kroemer, G. 2015. 'Type I interferons in anticancer immunity', Nat Rev Immunol, 15: 405-14.

Zundler, S. and Neurath, M. F. 2015. 'Interleukin-12: Functional activities and implications for disease', Cytokine Growth Factor Rev, 26: 559-68.

Appendix

List of figures

List of tables

List of abbreviations

Abbreviation	Meaning
ADMET	Absorption, distribution, metabolism, excretion, toxicity
APC	Antigen-presenting cell
CAR	Chimeric antigen receptor
cDC	Conventional dendritic cell
DAMP	Damage-associated molecular pattern
DC	Dendritic cell
dsRNA	Double-stranded RNA
E. coli	*Escherichia coli*
ELISA	Enzyme-linked immunosorbent assay
EtOH	Ethanol
FDA	U.S. Food and Drug Administration
Flt3L	FMS-like tyrosine kinase ligand
get40 mice	Green-enhanced transcript for *p40* mice; IL-12p40/GFP reporter mice
GM-CSF	Granulocyte-macrophage colony-stimulating factor
HAT	Histone acetylase
HDAC	Histone deacetylase
HDACi	Histone deacetylase inhibitor
HIV	Human immunodeficiency virus
HTS	High throughput screening
IAP	Inhibitor of apoptosis protein
IFN	Interferon
IFNAR	Interferon α receptor
IL	Interleukin
IRF	Interferon-regulatory factor
ISG	Interferon-stimulated gene
JAK	Janus kinase

Abbreviation	Meaning
LPS	Lipopolysaccharide
M. tuberculosis	*Mycobacterium tuberculosis*
M-CSF	Macrophage colony-stimulating factor
MAPK	Mitogen-activated protein kinase
MFI	Mean fluorescence intensity
MHCI	Major histocompatibility complex class I
MHCII	Major histocompatibility complex class II
mob mice	Messenger of interferon β mice; IFNβ/YFP reporter mice
MTT	Thiazolyl blue tetrazolium bromide
MSMT	Minimalist small molecular tagging
MyD88	Myeloid differentiation primary response protein 88
NK cell	Natural killer cell
NFκB	Nuclear factor κ-light-chain-enhancer of activated B cells
OD	Optical density
PAMP	Pathogen-associated molecular pattern
PBMC	Peripheral blood mononuclear cells
pDC	Plasmacytoid dendritic cell
PI3K	Phosphoinositide 3-kinase
PRR	Pattern recognition receptor
RIG-I	Retinoic acid-inducible gene-I
SD	Standard deviation
SEA	Similarity Ensemble Approach
SMILES	Simplified molecular input line entry system
SOCS3	Suppressor of cytokine signaling 3
STAT	Signal transducer and activator of transcription proteins
T. gondii	*Toxoplasma gondii*
TCR	T cell receptor
TLR	Toll-like receptor
TNR	Tumor necrosis factor

Abbreviation	Meaning
TRIF	Toll/IL-1R domain-containing adapter-inducing interferon β
WHO	World Health Organization

Cytotoxicity assays

In the following, the detailed results of the cytotoxicity assays are shown (see section 3.2 Cytotoxicity assays). Green color indicates high viability while red indicates high toxicity. All data were normalized to the DMSO control (= 100%).

		GM-CSF culture			Flt3L culture			M-CSF culture		
Code	**Name**	**0.1 µM**	**1 µM**	**10 µM**	**0.1 µM**	**1 µM**	**10 µM**	**0.1 µM**	**1 µM**	**10 µM**
P01B02	Dibromhemibastadin-1	**97,51**	**96,85**	**95,96**	**104,6**	**113**	**113,3**	**95,62**	**98,95**	**109,9**
P01B03	Oximester	**95,25**	**95,11**	**93,66**	**113,1**	**109,2**	**115,2**	**86,63**	**86,2**	**90,8**
P01B04	(-) α-Bisabolol	**77,68**	**74,72**	**62,55**	**108,1**	**107,7**	**102,2**	**98,3**	**94,18**	**87,58**
P01B05	Nor-Bromhemibastadin	**58,83**	**59,77**	**68,09**	**110,2**	**108,2**	**118**	**93,14**	**91,63**	**94,58**
P01B06	Cinnamic acid	**55,78**	**50,85**	**63,72**	**109,1**	**114,7**	**111,8**	**97,19**	**90,98**	**85,16**
P01B07	Visnagin	**64,99**	**61,33**	**54,65**	**109,1**	**95,58**	**107**	**95,1**	**102,3**	**96,47**
P01B08	Oxim acid	**59,21**	**78,38**	**74,39**	**95,9**	**102,1**	**97,73**	**92,55**	**103,5**	**105,8**
P01B09	Phomoxanthone A	**80,12**	**74,77**	**78,24**	**104**	**100,1**	**91,5**	**91,83**	**74,97**	**49,74**
P01B10	5,5'-dibromohemibastadin-1	**81,86**	**83,27**	**74,25**	**80,27**	**99,33**	**99,5**	**97,45**	**97,84**	**96,41**
P01B11	Helenalin	**129,9**	**127,8**	**21,07**	**98,38**	**80,83**	**18,22**	**123,5**	**124,2**	**5,49**
P01C02	Agelasine D	**64,14**	**64,76**	**64,66**	**101,4**	**99,72**	**90,05**	**84,71**	**81,5**	**99,79**
P01C03	Ester-Br2	**59,3**	**67,62**	**66,73**	**96,15**	**93,95**	**108**	**97,52**	**91,05**	**88,1**
P01C04	Aeroplysinin	**59,87**	**66,35**	**68,09**	**89,04**	**95,14**	**111,8**	**84,6**	**84,28**	**93,16**
P01C05	Berberin hemisulfat	**57,71**	**39,9**	**71,62**	**102,4**	**96,59**	**102,7**	**96,86**	**102,1**	**113,6**
P01C06	Manzamine A	**70,35**	**64,43**	**65,6**	**89,21**	**90,05**	**68,36**	**97,12**	**97,39**	**67,58**
P01C07	W493 B	**114,2**	**110**	**127,2**	**95,47**	**101,1**	**101,7**	**100,5**	**104**	**105,4**
P01C08	Cholest-5-en-3β-ol/(22E, 24S)-24-Methylcholesta-5,22-dien-3β-ol	**144,6**	**96,95**	**106**	**111,3**	**92,92**	**102,6**	**95,64**	**102,6**	**103,3**
P01C09	Aerothionin	**103,1**	**112,6**	**126,3**	**108,4**	**105,4**	**108,2**	**106,9**	**103**	**110,8**
P01C10	24-Ethylcholesta-5-en-3β-ol	**107,8**	**104,9**	**104,1**	**89,12**	**82,41**	**87,24**	**104,1**	**94,36**	**90,84**
P01C11	Benzylnitrile	**93,61**	**99,43**	**101,5**	**88,63**	**93,4**	**85,15**	**82,78**	**78,72**	**81,07**
P01D02	Debromhymenialdisin	**94,57**	**101,1**	**85,99**	**91,42**	**80,91**	**69,49**	**96,99**	**89,17**	**86,55**
P01D03	Aloesin	**102,3**	**97,9**	**101,2**	**84,24**	**81,55**	**79,89**	**105,8**	**95,52**	**88,34**
P01D04	Hydroxydienone acid	**107,2**	**102,9**	**105,4**	**82,25**	**82,36**	**86,6**	**99,23**	**95,96**	**88,73**
P01D05	Bakuchiol	**100,1**	**103,7**	**5,43**	**71,1**	**77,05**	**85,47**	**91,67**	**99,81**	**120,6**
P01D06	Macrosporin	**96,95**	**102,7**	**93,9**	**81,61**	**67,56**	**81,45**	**95,32**	**91,42**	**99,1**

		GM-CSF culture			Flt3L culture			M-CSF culture		
Code	**Name**	**0.1 µM**	**1 µM**	**10 µM**	**0.1 µM**	**1 µM**	**10 µM**	**0.1 µM**	**1 µM**	**10 µM**
P01D07	Tetrahydroxybostricin	**95,9**	**105,2**	**105,7**	**84,61**	**83**	**67,67**	**89,56**	**90,9**	**96,99**
P01D08	Isobavachalcone	**95,9**	**97,62**	**118,5**	**78,71**	**80,8**	**80,8**	**99,74**	**96,03**	**124,7**
P01D09	Alternariol	**96,38**	**94,76**	**109,6**	**66,49**	**79,95**	**77,05**	**92,7**	**103,7**	**79,88**
P01D10	Roquefortin C	**95,14**	**88,94**	**93,61**	**76,51**	**66,17**	**77,69**	**97,12**	**87,89**	**85,84**
P01D11	Chlorogenic acid	**107,5**	**121,6**	**71,91**	**77,64**	**81,18**	**73,08**	**88,53**	**84,88**	**84,18**
P01E02	Aloeemodin	**97,01**	**106,7**	**97,86**	**115,1**	**104,4**	**102,8**	**75,61**	**80,53**	**71,12**
P01E03	Midpacamide	**77,73**	**80,59**	**77,64**	**103,7**	**98,42**	**97,26**	**79,14**	**76,47**	**75,19**
P01E04	Embeurekol B	**93,35**	**77,51**	**77,29**	**106,5**	**105,3**	**95,31**	**90,34**	**87,94**	**82,24**
P01E05	(+) Aeroplysinin-1	**86,76**	**80,73**	**116**	**97,84**	**99,31**	**93,14**	**101,8**	**88,89**	**54,89**
P01E06	Br2 hydroxyethylamide	**77,47**	**77,87**	**77,55**	**93,25**	**103**	**96,31**	**87,38**	**95,25**	**84,25**
P01E07	Corynesidone A	**70,77**	**82,91**	**72,87**	**103,5**	**91,51**	**92,72**	**84,53**	**92,57**	**111,8**
P01E08	7-O-Methylaloeresin A	**73,54**	**74,21**	**69,08**	**99,58**	**103,4**	**89,14**	**81,8**	**77,44**	**87,05**
P01E09	4-(4,5-dibromo-1-methyl-1H-pyrrole-2-carboxamido) butanoic acid	**72,82**	**78,67**	**80,32**	**95,25**	**92,35**	**91,77**	**82,03**	**77,54**	**82,99**
P01E10	Ergosterol	**108**	**100,9**	**79,22**	**94,41**	**94,57**	**95,41**	**94,97**	**97,93**	**80,12**
P01E11	Emb-peptide = WLIP	**70,68**	**67,69**	**74,88**	**98,23**	**111,3**	**142,5**	**85,09**	**81,91**	**98,44**
P01F02	Wortmannin A	**77,73**	**75,77**	**76,75**	**77,16**	**61,5**	**52,27**	**87,05**	**72,03**	**69,01**
P01F03	4,6-dibromo-2-(2´,4´-dibromophenoxy)phenol	**110,6**	**117,6**	**96,34**	**97,1**	**92,72**	**93,25**	**104,5**	**92,29**	**65,33**
P01F04	Citrinin	**73,27**	**66**	**70,55**	**98,84**	**93,88**	**93,62**	**98,44**	**105,5**	**105,8**
P01F05	Aloeresin A	**80,62**	**108,7**	**102,6**	**105,5**	**106,7**	**78,22**	**82,25**	**82,78**	**83,21**
P01F06	Demethoxyencecalin	**96,88**	**93,22**	**105,6**	**96,72**	**104,7**	**102,1**	**85,13**	**86,52**	**84,28**
P01F07	3,5-dibromo-2-hydroxy-4-methoxyphenylacetonitril	**99,46**	**106,5**	**102,7**	**99,43**	**104,9**	**115,5**	**89,31**	**102,4**	**115,5**
P01F08	3,4,6-tribromo-2-(2´,4´-dibromophenoxy)phenol	**105,4**	**106,8**	**111,2**	**94,15**	**98,49**	**68,2**	**103,1**	**86,09**	**71,38**
P01F09	Isovitexin	**92,47**	**107,6**	**92,47**	**97,17**	**94,22**	**92,9**	**99,77**	**90,38**	**76,07**
P01F10	Catechin	**75**	**77,3**	**91,25**	**100,4**	**95,41**	**93,71**	**78,73**	**72,23**	**76,87**
P01F11	Dienone	**80,04**	**83,83**	**81,98**	**89,69**	**104,9**	**87,37**	**81,05**	**87,56**	**83,2**

		GM-CSF culture			Flt3L culture			M-CSF culture		
Code	**Name**	**0.1 µM**	**1 µM**	**10 µM**	**0.1 µM**	**1 µM**	**10 µM**	**0.1 µM**	**1 µM**	**10 µM**
P01G02	Sclerotiorin	**95,59**	**98,06**	**112,4**	**88,06**	**90,19**	**98,99**	**82,58**	**76,81**	**87,56**
P01G03	(-) Ageloxime D	**100,5**	**99,14**	**89,02**	**91,45**	**87,05**	**78,25**	**87,56**	**87,22**	**84,62**
P01G04	Enniatin B	**72,97**	**90,46**	**87,15**	**99,06**	**89,19**	**51,54**	**100,7**	**91,29**	**76,07**
P01G05	Aranorosinol B	**73,45**	**97,97**	**78,05**	**76,87**	**103,7**	**96,1**	**92,31**	**97,34**	**91,86**
P01G06	Sekikaic acid	**76,5**	**65,95**	**83,88**	**97,8**	**78,25**	**98,87**	**103,9**	**79,92**	**91,46**
P01G07	Cyclopenol	**110**	**93,11**	**93,97**	**92,77**	**89,38**	**80,26**	**91,46**	**85,58**	**78,9**
P01G08	(-) Matairesinol	**89,22**	**82,33**	**73,1**	**88,87**	**87,24**	**80,2**	**99,43**	**97,79**	**64,59**
P01G09	Homosekikaic Acid	**64,4**	**82,38**	**90,11**	**80,26**	**90,89**	**98,55**	**94,06**	**87,9**	**83,94**
P01G10	N-Methyl-4,5-dibromopyrrole-2-carboxylic acid	**82,82**	**76,63**	**71,86**	**93,78**	**81,77**	**99,5**	**89,2**	**79,24**	**87,73**
P01G11	Meleagrin	**88,48**	**99,03**	**100**	**100,3**	**106**	**89,94**	**88,91**	**83,14**	**85,46**
P02B02	Neobavaisoflavone	**111,5**	**104,4**	**109,2**	**100,4**	**105**	**121,8**	**91,43**	**114,6**	**133,4**
P02B03	(-) Arctigenin	**97,15**	**98,4**	**111,3**	**97**	**101,4**	**98,62**	**109,5**	**84,54**	**104,8**
P02B04	Kojic acid	**89,61**	**89,96**	**78,21**	**98,04**	**99,83**	**91,88**	**108,3**	**104,1**	**72,1**
P02B05	Stemphyperylenol	**82,3**	**84,2**	**71,97**	**94,12**	**91,71**	**80,99**	**94,52**	**82,22**	**82,8**
P02B06	2,2-Dimethylchroman-3,6-diol	**83,61**	**82,72**	**77,32**	**91,82**	**95,33**	**90,15**	**86,15**	**82,28**	**81,38**
P02B07	Avaron	**79,69**	**79,45**	**86,58**	**89,11**	**98,62**	**89,11**	**88,64**	**97,61**	**155,3**
P02B08	(E)-Methyl-3-(-4-methoxyphenoxy)propenoat	**77,08**	**76,43**	**82,07**	**90,78**	**97**	**97,29**	**84,34**	**87,69**	**71,97**
P02B09	Hydroxysydon acid	**84,56**	**79,04**	**79,93**	**98,62**	**98,1**	**93,66**	**94,39**	**88,14**	**81,31**
P02B10	Alternariol monomethyl ether	**83,85**	**85,27**	**83,49**	**93,78**	**97,75**	**93,09**	**88,07**	**86,14**	**72,73**
P02B11	BrPhenethylamide	**83,61**	**86,34**	**87,59**	**91,99**	**95,45**	**100,4**	**83,83**	**78,54**	**79,38**
P02C02	BrIsobutylamide	**80,76**	**82,96**	**76,78**	**90,5**	**95,62**	**87,9**	**91,37**	**82,47**	**85,18**
P02C03	Phenol A acid	**78,56**	**80,58**	**80,82**	**93,49**	**86,87**	**89,46**	**87,37**	**92,72**	**96,46**
P02C04	Xanthorrhizol	**77,67**	**76,13**	**88,72**	**95,74**	**90,96**	**93,89**	**95,68**	**90,79**	**94,52**
P02C05	Waol acid	**88,72**	**83,43**	**83,85**	**94,59**	**95,79**	**94,59**	**103,7**	**75,32**	**81,44**
P02C06	4,5-dibromo-1H-pyrrol-2-carboxyamide	**93,47**	**91,92**	**86,52**	**80,41**	**92,86**	**81,22**	**92,65**	**80,54**	**80,35**

		GM-CSF culture			Flt3L culture			M-CSF culture		
Code	**Name**	**0.1 µM**	**1 µM**	**10 µM**	**0.1 µM**	**1 µM**	**10 µM**	**0.1 µM**	**1 µM**	**10 µM**
P02C07	Kahalalide F	**112,6**	**105,9**	**76,79**	**84,95**	**88,87**	**110,2**	**109,7**	**104,4**	**19,57**
P02C08	Wortmannin	**100,6**	**103,3**	**105,5**	**67,14**	**54,37**	**46,48**	**114,6**	**78,12**	**82,99**
P02C09	Skyrin	**103,4**	**103,9**	**128,3**	**89,03**	**83,73**	**78,43**	**108,8**	**118,6**	**128,6**
P02C10	Hymenidin	**99,58**	**97,21**	**86,2**	**88,29**	**87,6**	**83,94**	**115,3**	**106,4**	**108,2**
P02C11	(+) Avarol	**90,45**	**97,91**	**132,1**	**85,74**	**83,2**	**66,14**	**110,5**	**117,2**	**141,5**
P02D02	Hexylamide	**102,1**	**110,5**	**114,3**	**87,28**	**82,3**	**86,75**	**89,43**	**90,91**	**108,9**
P02D03	Kuanoniamin D	**91,43**	**88,57**	**54,77**	**83,68**	**77,53**	**52,52**	**108,1**	**92,65**	**28,99**
P02D04	Altersolanol A	**104,3**	**106,1**	**113,2**	**87,39**	**87,49**	**88,66**	**113,7**	**112,9**	**5,19**
P02D05	Isofistularin 3	**100,4**	**103,6**	**147,8**	**70,22**	**84,37**	**102,8**	**99,44**	**112,3**	**161,5**
P02D06	Br2Tyrosin	**91,5**	**94,7**	**102,7**	**74,14**	**72,92**	**80,5**	**113,9**	**102,7**	**101,9**
P02D07	Br2Hexylamide	**106,1**	**94,15**	**110,4**	**84,95**	**83,36**	**86,06**	**92,33**	**102,8**	**87,62**
P02D08	4,5-Dibromo-1H-pyrrol-2-carbon acid ethyl ester	**120,1**	**104,5**	**107,1**	**77,37**	**80,07**	**74,03**	**105,3**	**98,64**	**101,6**
P02D09	Dihydrogeodin	**91,92**	**105,6**	**100,4**	**76,95**	**78,27**	**80,45**	**110,5**	**112,3**	**98**
P02D10	3,5-Dibromo-1H-pyrrole-2-carboxylic acid	**89,83**	**87,32**	**86,69**	**72,92**	**79,01**	**83,57**	**114,4**	**109,4**	**86,02**
P02D11	Mauritamide B	**94,36**	**103,4**	**95,54**	**82,62**	**90,62**	**88,92**	**106,8**	**107,8**	**107,8**
P02E02	Indole-3-carboxylic acid	**99,81**	**89,5**	**103,6**	**107,6**	**111**	**104,4**	**109,7**	**114,2**	**105,8**
P02E03	Dasyclamide	**97,8**	**102,3**	**94,04**	**103,2**	**107**	**100,9**	**111**	**101,3**	**110,6**
P02E04	Aranorosin	**80,23**	**94,82**	**70,12**	**100,3**	**98,9**	**43,02**	**124,1**	**100,9**	**2,91**
P02E05	Viridicatin	**90,34**	**96,11**	**90,02**	**99,45**	**102,1**	**108,3**	**111**	**87,57**	**99,27**
P02E06	Enniatin A1	**103,2**	**97,15**	**139,9**	**100,4**	**102,3**	**38,09**	**108**	**109,2**	**37,34**
P02E07	Scorzodihydrostilbene B	**97,15**	**112,4**	**89,89**	**97,81**	**96,59**	**89,64**	**94,78**	**105,6**	**99,67**
P02E08	Anomalin A	**88,4**	**85,35**	**103,2**	**94,21**	**99,09**	**94,09**	**88,75**	**93,41**	**118,3**
P02E09	Tetrahydroxystilbene-glucoside	**91,51**	**89,76**	**85,81**	**87,63**	**94,27**	**100,7**	**106,4**	**101,1**	**94,51**
P02E10	4′-O-Methyl norhomosekikaic acid	**92,74**	**82,76**	**74,66**	**88,6**	**92,5**	**100,2**	**96,56**	**102,3**	**100,7**
P02E11	BrHistamide	**101,2**	**95,27**	**92,22**	**101,4**	**72,46**	**95,67**	**88,63**	**90,61**	**94,05**

		GM-CSF culture			Flt3L culture			M-CSF culture		
Code	**Name**	**0.1 µM**	**1 µM**	**10 µM**	**0.1 µM**	**1 µM**	**10 µM**	**0.1 µM**	**1 µM**	**10 µM**
P02F02	Br2Phenethylamide	**85,16**	**98,38**	**105,3**	**90,55**	**99,7**	**81,17**	**97,36**	**83,15**	**80,96**
P02F03	18-Dehydroxycytochalasin H	**102,1**	**94,49**	**124,8**	**86,59**	**88,97**	**82,57**	**106,5**	**84,07**	**104,7**
P02F04	Ilimaquinone = Ilimachinon	**94,36**	**80,43**	**111,3**	**84,34**	**94,21**	**89,09**	**97,69**	**96,5**	**75,81**
P02F05	4´,5,7-trimethoxydihydroflavonol	**82,89**	**80,62**	**108,3**	**90,62**	**81,72**	**77,45**	**91,67**	**102,8**	**62,33**
P02F06	Theonellapeptolide Ie	**92,74**	**92,87**	**92,74**	**93,17**	**96,83**	**57,71**	**106,3**	**80,3**	**95,57**
P02F07	Piperin	**107,9**	**90,97**	**102,1**	**113,4**	**100,9**	**107,4**	**98**	**115,9**	**104,5**
P02F08	Lutein	**110,7**	**99,24**	**107,1**	**95,33**	**103,1**	**118,7**	**109**	**102,5**	**117,2**
P02F09	3,4,5-Tri-O-methylgallic acid butyl ester	**92,15**	**96,94**	**104**	**97,29**	**95,45**	**100,9**	**108,8**	**95,83**	**96,73**
P02F10	3-O-Methylgallic acid butyl ester	**106,9**	**88,13**	**93,26**	**97,87**	**99,14**	**100,4**	**93,41**	**83,3**	**79,43**
P02F11	Dibromohydroxyphakellin	**97,78**	**96,46**	**104,7**	**108,8**	**95,22**	**94,35**	**86,82**	**91,02**	**91,48**
P02G02	(+) Agelasidine C	**94,44**	**96,94**	**97,15**	**96,6**	**101,2**	**98,5**	**83,06**	**68,72**	**84,15**
P02G03	Orientin	**84,86**	**88,4**	**91,39**	**104,9**	**99,52**	**86,16**	**79,92**	**79,25**	**79,55**
P02G04	Tilirosid	**90**	**94,86**	**86,11**	**91,3**	**95,97**	**89,86**	**89,59**	**81,43**	**82,27**
P02G05	Br2Histamide	**92,64**	**93,89**	**85,07**	**93,6**	**88,65**	**88,93**	**86,81**	**87,3**	**82,94**
P02G06	Kaempferol-3,7-O-α-L-dirhamnopyranoside	**83,33**	**92,29**	**84,65**	**98,88**	**101,6**	**89,01**	**91,65**	**81,43**	**88,2**
P02G07	Flavomannin A	**85,56**	**111**	**108,8**	**90,89**	**87,67**	**95,1**	**74,47**	**79,01**	**86,87**
P02G08	Alternarienoic acid	**77,92**	**86,6**	**103,6**	**83,86**	**93,37**	**85,71**	**86,81**	**80,58**	**73,74**
P02G09	Cytochalasin D	**104,8**	**105,6**	**138,1**	**85,19**	**83**	**80,81**	**93,28**	**81,49**	**96,61**
P02G10	Br2Tryptamide	**107,6**	**101,9**	**97,08**	**85,59**	**83,92**	**79,19**	**81,31**	**80,04**	**85,12**
P02G11	Euparin	**97,92**	**97,85**	**97,08**	**90,55**	**86,11**	**94,41**	**80,1**	**85,42**	**67,39**
P03B02	2,3,4-Trimethyl-5,7-dihydroxy-3-dihydrobenzofuran	**111,3**	**108,2**	**100,6**	**98,91**	**102**	**95,91**	**97,64**	**105,2**	**105,7**
P03B03	Pinocembrin	**102,1**	**99,12**	**97,3**	**97,38**	**99,17**	**101,4**	**108,9**	**97,71**	**104,8**
P03B04	Scorzodihydrostilbene A	**96,92**	**83,24**	**100,8**	**95,02**	**91,44**	**89,72**	**96,45**	**91,21**	**93,87**
P03B05	Feralolide	**112,9**	**105,3**	**119,9**	**100,1**	**99,04**	**108,6**	**105,5**	**105,8**	**112,8**
P03B06	8-0-manzamine A	**104**	**99,62**	**68,3**	**89,72**	**88,06**	**20,82**	**96,01**	**102,7**	**11,74**

		GM-CSF culture			Flt3L culture			M-CSF culture		
Code	**Name**	**0.1 µM**	**1 µM**	**10 µM**	**0.1 µM**	**1 µM**	**10 µM**	**0.1 µM**	**1 µM**	**10 µM**
P03B07	N-trans-feruoyltyramine	**93,91**	**93,16**	**96,48**	**88,25**	**86,65**	**99,04**	**100,8**	**91,95**	**108,4**
P03B08	Wortmannin C	**84,43**	**90,46**	**100,8**	**88,7**	**82,25**	**50,89**	**99,93**	**83,38**	**73,93**
P03B09	Aerophobin 2	**98,81**	**94,54**	**90,58**	**104,5**	**95,91**	**94,32**	**115,7**	**97,42**	**101,9**
P03B10	Aposphaerin A	**106,9**	**90,77**	**83,36**	**81,8**	**101,2**	**89,08**	**102,4**	**108,9**	**99,93**
P03B11	Cladosporin	**89,33**	**93,97**	**76,27**	**79,69**	**83,33**	**92,66**	**102,9**	**101,1**	**110,9**
P03C02	W493 A	**81,73**	**87,51**	**91,59**	**90,49**	**95,72**	**90,68**	**108,1**	**98,82**	**94,46**
P03C03	(S)-(-)-Rhodoptilometrin	**86,5**	**79,16**	**84,62**	**100,4**	**90,8**	**95,85**	**117,7**	**107,5**	**114**
P03C04	N-methyl-4,5-dibromopyrrole-2-methylcarboxylate	**81,23**	**82,23**	**82,55**	**80,97**	**91,06**	**88,57**	**106,5**	**110,5**	**94,53**
P03C05	Paxillin	**82,93**	**83,68**	**78,53**	**86,78**	**76,95**	**99,3**	**104,7**	**98,82**	**106,7**
P03C06	Tryptamide	**91,21**	**94,1**	**145,8**	**82,89**	**81,93**	**94,89**	**93,72**	**87,44**	**123,9**
P03C07	Dienone dimethoxyketal	**107,2**	**109,2**	**111,1**	**92,22**	**99,88**	**95,07**	**99,38**	**92,86**	**96,09**
P03C08	Alterporriol D	**84,46**	**91,84**	**99,34**	**90,86**	**87,83**	**93,41**	**103,2**	**97,12**	**100,1**
P03C09	Cyclohexylamide	**91,11**	**102,4**	**85,78**	**89,01**	**88,3**	**90,02**	**107**	**96,43**	**106,1**
P03C10	3-O-Methylgallic acid methyl ester	**98,55**	**87,16**	**89,27**	**99,23**	**96,32**	**90,5**	**112,9**	**100,2**	**94,92**
P03C11	3-O-Methylgallic acid propyl ester	**93,02**	**90,19**	**82,75**	**82,96**	**90,5**	**94,18**	**99,93**	**99,04**	**103,9**
P03D02	Genestein	**88,68**	**91,97**	**97,83**	**83,37**	**89,96**	**86,64**	**108,2**	**97,53**	**103,1**
P03D03	3,5-dicaffeoylquinic acid	**93,09**	**92,23**	**90,52**	**80,29**	**89,96**	**89,9**	**100,8**	**92,31**	**95,4**
P03D04	Resacetophenon	**89,14**	**85,71**	**86,5**	**89,67**	**92,4**	**90,44**	**102,3**	**100,8**	**96,23**
P03D05	Histamide	**83,54**	**86,97**	**94,87**	**83,19**	**95,07**	**93,17**	**106,9**	**108,6**	**98,42**
P03D06	Bionectriamide A	**92,23**	**93,29**	**90,52**	**89,9**	**83,55**	**97,33**	**103,1**	**101,7**	**118,7**
P03D07	Imiquimod	**86,64**	**93,35**	**83,54**	**85,63**	**88,48**	**81,95**	**104,2**	**94,92**	**73,92**
P03D08	Corynesidone C	**91,18**	**92,63**	**89,4**	**90,74**	**82,6**	**87,65**	**109,9**	**97,67**	**101,4**
P03D09	L-Tryptophan	**88,87**	**95,06**	**91,24**	**78,15**	**90,02**	**78,98**	**112,8**	**109,2**	**103,9**
P03D10	Altenusin	**85,91**	**93,55**	**86,18**	**84,98**	**74,35**	**85,99**	**105,8**	**97,8**	**88,74**
P03D11	9,21-didehydroryanodine	**91,77**	**81,44**	**88,08**	**85,75**	**84,44**	**79,57**	**101,9**	**92,93**	**88,54**

		GM-CSF culture			Flt3L culture			M-CSF culture		
Code	**Name**	**0.1 µM**	**1 µM**	**10 µM**	**0.1 µM**	**1 µM**	**10 µM**	**0.1 µM**	**1 µM**	**10 µM**
P03E02	BrCyclohexylamide	**96,23**	**101,4**	**110,1**	**88,61**	**90,17**	**83,29**	**110,3**	**105,1**	**102,5**
P03E03	Isobutylamide	**105,9**	**84,23**	**82,05**	**91,33**	**86,94**	**89,08**	**107,4**	**96,01**	**109,4**
P03E04	3,4,5-O-trimethyl-gallate	**84,55**	**86,25**	**86,25**	**92,31**	**93,58**	**85,49**	**102,9**	**86,7**	**70,41**
P03E05	Lasiodiplodin	**88,42**	**78,76**	**93,15**	**90,58**	**87,86**	**99,42**	**85,57**	**79,65**	**101,2**
P03E06	6-Methoxycomaparvin-5-methyl ether	**93,84**	**84,01**	**92,72**	**82,6**	**88,44**	**85,84**	**80,98**	**82,51**	**84,71**
P03E07	Citreodrimene B	**88,16**	**94,58**	**112,9**	**87,11**	**89,83**	**50,87**	**83,91**	**82,11**	**1,2**
P03E08	Scopularide A	**74,72**	**88,37**	**103,2**	**84,97**	**87,63**	**92,77**	**86,84**	**99,53**	**80,19**
P03E09	5 -(3,5-dibromo-4-) (2-oxooxazolidin-5yl)methoxy phenyl) oxazolidin-2-one	**77,32**	**85,93**	**88,95**	**81,33**	**83,24**	**81,21**	**95,94**	**90,49**	**90,96**
P03E10	Kaempferol 3-O-β-D-glucopyranosyl (1-4) α-L-rhamnopyranosyl-7-O-α-L-rhamnopyranoside	**80,99**	**81,73**	**84,71**	**84,39**	**82,89**	**85,9**	**89,36**	**89,36**	**91,76**
P03E11	Cerebroside D	**89,33**	**79,29**	**77,54**	**90**	**80,64**	**89,83**	**97,14**	**90,09**	**89,23**
P03F02	Warfarin	**88,74**	**90,39**	**81,68**	**87,4**	**82,77**	**77,11**	**91,16**	**83,44**	**80,72**
P03F03	5-epi-Nakijiquinone Q	**75,31**	**76,63**	**100,4**	**81,21**	**81,97**	**102,2**	**102,9**	**87,5**	**94,61**
P03F04	Myrocin A	**77,16**	**79,24**	**75,2**	**78,84**	**80,64**	**82,72**	**90,76**	**92,49**	**95,61**
P03F05	3,5-dibromo-2-benzoyloxy-4-methoxyphenylacetonitril	**87,57**	**69,46**	**73,66**	**84,34**	**76,82**	**76,01**	**99,73**	**88,76**	**91,62**
P03F06	Callyaerin F	**73,66**	**83,32**	**77,75**	**78,5**	**88,61**	**91,68**	**95,81**	**108,5**	**95,15**
P03F07	3-O-Methylgallic acid butyl ester	**103,8**	**111,6**	**107,8**	**94,4**	**99,43**	**97,66**	**112,3**	**104**	**97,87**
P03F08	Viriditoxin	**106,2**	**102,6**	**93,52**	**73,94**	**44,97**	**5,83**	**100,4**	**92,66**	**30,53**
P03F09	Luffariellolid	**107,2**	**108,2**	**84,86**	**99,49**	**95,54**	**76,4**	**102,2**	**96,04**	**75,98**
P03F10	Agelanin B	**106**	**95,31**	**106,3**	**81,6**	**83,26**	**82,97**	**111,4**	**96,51**	**91,42**
P03F11	Eupatoriumchromene 1	**79,14**	**83,76**	**82,14**	**81,66**	**86,34**	**80,86**	**100,6**	**95,56**	**102,3**
P03G02	4-methoxybenzoic acid	**93,48**	**87,81**	**83,57**	**84,91**	**84,11**	**84,23**	**100,1**	**102,4**	**99,11**
P03G03	Isoferulic acid methylester	**79,81**	**82,05**	**79,67**	**86,97**	**89,6**	**80,23**	**93,67**	**87,04**	**93,37**
P03G04	Syringic acid	**79,43**	**81,52**	**82,95**	**85,49**	**86,11**	**86,17**	**93,85**	**84,62**	**83,96**
P03G05	4-Bromopyrrole-2-carboxamide	**77,29**	**81,33**	**79,9**	**83,6**	**82,97**	**80,63**	**86,57**	**113,6**	**93,43**
P03G06	Hyperoside	**101,5**	**95,97**	**99,67**	**87,37**	**74,91**	**80,23**	**101,3**	**84,14**	**97,87**

		GM-CSF culture			Flt3L culture			M-CSF culture		
Code	**Name**	**0.1 µM**	**1 µM**	**10 µM**	**0.1 µM**	**1 µM**	**10 µM**	**0.1 µM**	**1 µM**	**10 µM**
P03G07	2-Hydroxy-4-methoxyphenylacetonitril	**96,18**	**100,1**	**101,7**	**81,77**	**79,09**	**76,57**	**105,9**	**100,7**	**87,4**
P03G08	Acteoside	**75,86**	**79,52**	**85,05**	**87,77**	**77,2**	**80,86**	**115,2**	**97,46**	**107,6**
P03G09	1,3-Dihydro-4-hydroxy-1(1-hydroxyethyl)-3-oxoisobenzofuran-5-carboxylic acid	**99,89**	**101,9**	**105,9**	**76,97**	**87,14**	**75,71**	**100,9**	**109,5**	**102,1**
P03G10	Mauritamide C	**75,57**	**73,86**	**71,38**	**78,97**	**82,74**	**78,46**	**110,2**	**98,34**	**101,9**
P03G11	Atromentine	**72,38**	**69,86**	**57,29**	**75,2**	**77,31**	**69,49**	**110,4**	**88,58**	**71,48**
P04B02	Aaptamine	**112**	**126,4**	**150,6**	**95,27**	**97,31**	**96,79**	**101**	**106,2**	**109,4**
P04B03	Altersolanol C	**122,7**	**124,3**	**120**	**94,45**	**98,19**	**109,4**	**115**	**107,7**	**97,88**
P04B04	Pyrrocidine D	**119**	**112,6**	**2,82**	**96,44**	**90,07**	**37,68**	**103,5**	**104,8**	**36,63**
P04B05	Unguisin E	**129,6**	**121,8**	**120,5**	**96,32**	**89,25**	**88,26**	**109,5**	**101,2**	**107,3**
P04B06	Asterric acid	**129**	**138,8**	**130,1**	**102,1**	**94,6**	**96,96**	**100,4**	**104,9**	**100,8**
P04B07	Beauvericin	**127,8**	**136,6**	**43,17**	**91,65**	**91,82**	**30,84**	**100,7**	**120,7**	**5,07**
P04B08	Butyrolactone II	**126,7**	**136,9**	**124,1**	**88,79**	**97,2**	**91,94**	**106,2**	**96,53**	**106,7**
P04B09	Cochliodinol	**122,3**	**127,6**	**122,5**	**101,6**	**92,29**	**37,09**	**113**	**88,72**	**7,76**
P04B10	4,5-dibromo-1H-pyrrol-2 carboxylic acid	**118,1**	**118,4**	**115,8**	**88,38**	**99,01**	**93,4**	**103,5**	**107,7**	**110,7**
P04B11	Debromsceptrin	**122,8**	**107,8**	**125,2**	**93,46**	**87,56**	**96,67**	**99,79**	**109,8**	**102,6**
P04C02	Enniatin B1	**118,1**	**121,6**	**106,6**	**96,9**	**98,13**	**65,48**	**97,88**	**104,6**	**66,22**
P04C03	Isosulochrin	**117,8**	**109**	**121,1**	**98,54**	**94,68**	**91,06**	**105,3**	**92,71**	**99,28**
P04C04	Galactitol	**121,5**	**119,4**	**125,6**	**88,55**	**97,9**	**89,89**	**102,7**	**102,6**	**101,5**
P04C05	Isoharzianic acid	**131,2**	**111,1**	**121,2**	**96,03**	**88,14**	**92,23**	**94,83**	**95,55**	**101,1**
P04C06	Hexaprenylhydroquinone	**70,91**	**50,16**	**23,36**	**100,8**	**79,44**	**27,8**	**103,5**	**52,72**	**11,95**
P04C07	Kämpferol-3-rutinoside	**104,7**	**97,44**	**89,64**	**100,1**	**101,5**	**92,38**	**92,58**	**96,47**	**106,8**
P04C08	Longamide B	**94,44**	**86,95**	**104,6**	**100**	**96,04**	**104,1**	**106,1**	**93,16**	**98,03**
P04C09	7-O-Methylaloesin	**98,15**	**106,3**	**105,6**	**89,94**	**94,04**	**95,78**	**89,09**	**89,09**	**94,77**
P04C10	Manzamine J N-Oxid	**104,4**	**87,95**	**123**	**101,8**	**95,19**	**131,8**	**98,26**	**106,6**	**156,3**
P04C11	Manzamine F	**95,32**	**94,69**	**97,88**	**90,62**	**92,2**	**110,2**	**96,41**	**110,2**	**120,9**

		GM-CSF culture			Flt3L culture			M-CSF culture		
Code	**Name**	**0.1 µM**	**1 µM**	**10 µM**	**0.1 µM**	**1 µM**	**10 µM**	**0.1 µM**	**1 µM**	**10 µM**
P04D02	Pyrenocine A	**91,57**	**96,69**	**99,75**	**93,85**	**93,48**	**75,93**	**99,94**	**96,87**	**86,5**
P04D03	Rutin	**90,01**	**97,19**	**101,1**	**88,91**	**91,96**	**81,84**	**100,9**	**97,1**	**93,92**
P04D04	12-Carboxyl-paspaline	**99,5**	**99,5**	**109,9**	**100,6**	**95,37**	**94,64**	**104,1**	**101,7**	**104,4**
P04D05	Sarasinoside A1	**95,07**	**100,4**	**113,2**	**98,29**	**107,9**	**108,8**	**90,85**	**107,1**	**106,1**
P04D06	Sceptrin	**91,01**	**93,82**	**87,95**	**87,39**	**92,44**	**92,75**	**95,6**	**93,22**	**115,9**
P04D07	Sulochrin	**86,7**	**91,82**	**99,25**	**96,28**	**92,32**	**86,05**	**102,4**	**91,54**	**87,54**
P04D08	Tenuazon acid	**98,94**	**84,52**	**89,51**	**97,07**	**93,3**	**81,96**	**102,4**	**104,9**	**97,97**
P04D09	Acremonisol	**91,07**	**90,57**	**86,39**	**87,02**	**92,87**	**88,67**	**92,76**	**94,09**	**105,9**
P04D10	Viridicatol	**104,1**	**105,2**	**90,73**	**83,24**	**94,88**	**89,09**	**106,1**	**93,28**	**98,09**
P04D11	5-epi-Nakijiquinone C	**97,25**	**93,38**	**87,45**	**86,53**	**84,83**	**88,91**	**98,03**	**95,31**	**112,6**
P04E02	Dammarenol acid	**91,22**	**94,86**	**91,99**	**104,7**	**100,3**	**107,6**	**106,9**	**110,2**	**103,7**
P04E03	Isospongiaquinone	**90,72**	**89,23**	**113**	**97,64**	**106,1**	**74,6**	**109,6**	**94,54**	**106,9**
P04E04	5-epi-Ilimaquinone	**92,21**	**86,46**	**92,49**	**102,2**	**96,9**	**76,62**	**105,9**	**91,02**	**92,89**
P04E05	Butyrolactone I	**85,86**	**86,57**	**91,88**	**112,8**	**101**	**104,7**	**113,5**	**107,7**	**132**
P04E06	Butyrolactone III	**79,06**	**85,52**	**89,89**	**100**	**110**	**106,3**	**109,5**	**113,7**	**103,1**
P04E07	Terretonin	**81,55**	**76,3**	**75,14**	**103,5**	**104,5**	**106,3**	**116,6**	**106,6**	**112,9**
P04E08	Tenuazonic acid	**81,22**	**93,48**	**91,71**	**99,73**	**96,36**	**91,44**	**102,8**	**111,5**	**99,52**
P04E09	Paspaline	**85,08**	**92,98**	**108,8**	**110**	**103**	**98,38**	**108,5**	**104,3**	**138,7**
P04E10	(+)-Isochromophilone VI	**83,92**	**85,8**	**87,57**	**90,03**	**111,6**	**101**	**89,43**	**88,41**	**104,7**
P04E11	Amorfrutin 4	**87,29**	**76,8**	**79,28**	**91,85**	**96,09**	**102,8**	**111,3**	**107,4**	**121,3**
P04F02	Dukunolide A (LS4E-3)	**82,27**	**81,33**	**71,49**	**98,52**	**91,91**	**87,13**	**101,7**	**111,3**	**102,3**
P04F03	Dukunolide B (LS4E-2)	**80,77**	**80,39**	**75,69**	**102,4**	**98,85**	**91,17**	**109,5**	**104,8**	**110,2**
P04F04	Dukunolide C (LS4E-4)	**75,58**	**75,8**	**77,9**	**97,17**	**104,3**	**101,5**	**93,18**	**88,18**	**102,8**
P04F05	Fusaproliferin	**81,93**	**76,8**	**81,05**	**92,92**	**94,95**	**86,79**	**109,6**	**109,6**	**150,8**
P04F06	Secalonic acid F	**74,09**	**70,22**	**16,57**	**102,9**	**72,71**	**3,57**	**99,03**	**39,85**	**1,04**

		GM-CSF culture			Flt3L culture			M-CSF culture		
Code	**Name**	**0.1 µM**	**1 µM**	**10 µM**	**0.1 µM**	**1 µM**	**10 µM**	**0.1 µM**	**1 µM**	**10 µM**
P04F07	Andrographolide	**92,04**	**120,2**	**104,7**	**99,87**	**103**	**90,9**	**94,12**	**119,5**	**124,7**
P04F08	Precocene II	**98,07**	**94,81**	**90,02**	**93,78**	**101,9**	**108,5**	**94,67**	**100,4**	**97,8**
P04F09	Precocene I	**92,88**	**106**	**93,7**	**95,45**	**109**	**96,52**	**88,79**	**94,49**	**88,36**
P04F10	(R)-(+)-Methylsuccinic acid	**86,58**	**85,01**	**97,02**	**107,2**	**93,98**	**99,8**	**93,94**	**86,41**	**85,92**
P04F11	6,7-dimethoxy-2,2-dimethyl-4-chromanone	**103,6**	**92,65**	**89,21**	**104,6**	**107,8**	**92,1**	**90,32**	**89,47**	**87,32**
P04G02	p-Coumaric acid	**91,95**	**82,15**	**89,38**	**102,8**	**106,6**	**105,1**	**87,32**	**97,67**	**92,47**
P04G03	Piperanine	**86,81**	**95,97**	**95,57**	**94,18**	**97,93**	**86,14**	**87,88**	**87,2**	**105**
P04G04	Chrysin 6-C-(2″-O-α-L-rhamnopyranosyl)-β-D-glucopyranoside	**86,35**	**80,4**	**97,2**	**104,8**	**98,39**	**100,7**	**94,18**	**88,18**	**89,28**
P04G05	Talbutyrolactone A	**73,57**	**82,32**	**79,93**	**94,78**	**106,8**	**97,19**	**99,94**	**94,61**	**86,77**
P04G06	Aristolochic acid	**85,3**	**80,81**	**87,57**	**102,7**	**94,58**	**100**	**84,45**	**105,1**	**100**
P04G07	Xanthoangelol	**86,81**	**92,82**	**94,92**	**101,2**	**105,5**	**128,1**	**90,14**	**96,57**	**147,1**
P04G08	Amorphastilbol	**85,71**	**93,17**	**101**	**96,92**	**97,93**	**104,9**	**93,51**	**89,83**	**114**
P04G09	Dalpanol	**70,6**	**86,76**	**83,49**	**96,59**	**101,5**	**83,47**	**101,3**	**101,2**	**94,98**
P04G10	Chabamide	**84,89**	**71,47**	**92,42**	**95,25**	**84,81**	**105,2**	**101,7**	**103,9**	**128,2**
P04G11	(S)-cis-Resorcylide	**84,19**	**87,4**	**87,51**	**102,5**	**103**	**94,18**	**101**	**99,33**	**141,8**

Original publication

Bioorganic & Medicinal Chemistry 27 (2019) 115145

Contents lists available at ScienceDirect

Bioorganic & Medicinal Chemistry

journal homepage: www.elsevier.com/locate/bmc

A mouse model-based screening platform for the identification of immune activating compounds such as natural products for novel cancer immunotherapies

Lisa Richter[a], Sonja Kropp[a], Peter Proksch[b], Stefanie Scheu[a,*]

[a] Institute of Medical Microbiology and Hospital Hygiene, University of Düsseldorf, 40225 Düsseldorf, Germany
[b] Institute of Pharmaceutical Biology and Biotechnology, University of Düsseldorf, 40225 Düsseldorf, Germany

ARTICLE INFO

Keywords:
Natural products
Drug development
Anti-cancer immunotherapy
Immune activation
Screening guidelines
Mouse models

ABSTRACT

The therapy of cancer continues to be a challenge aggravated by the evolution of resistance against current medications. As an alternative for the traditional tripartite treatment options of surgery, radiation and chemotherapy, immunotherapy is gaining increasing attention due to the opportunity of more targeted approaches. Promising targets are antigen-presenting cells which drive innate and adaptive immune responses. The discovery and emergence of new drugs and lead structures can be inspired by natural products which comprise many highly bioactive molecules. The development of new drugs based on natural products is hampered by the current lack of guidelines for screening these structures for immune activating compounds. In this work, we describe a phenotypic preclinical screening pipeline for first-line identification of promising natural products using the mouse as a model system. Favorable compounds are defined to be non-toxic to immune target cells, to show direct anti-tumor effects and to be immunostimulatory at the same time. The presented screening pipeline constitutes a useful tool and aims to integrate immune activation in experimental approaches early on in drug discovery. It supports the selection of natural products for later chemical optimization, direct application in *in vivo* mouse models and clinical trials and promotes the emergence of new innovative drugs for cancer treatment.

1. Introduction

In 2016 cancers in general caused 22% of deaths worldwide with respiratory cancers alone ranked 6th among the top ten causes of death.[1] Additionally, the American Association for Cancer Research predicts a global increase in cancer prevalence from 15.2 million cases in 2015 to up to 24 million cases in 2035.[2] This indicates a strong need for new treatment approaches. Besides the traditional options of surgery, chemotherapy and radiation, immunotherapy is being applied with increasing success. In the latter case, medications are used to support the immune system to target the cancer without affecting healthy cells. For their pioneering work in this field, James P. Allison and Tasuku Honjo were awarded with the Nobel Prize in Physiology or Medicine in 2018 after discovery of immune checkpoint inhibitors and their usage as anti-cancer drugs.[3] Immune checkpoint proteins are expressed on certain types of immune cells like T cells in order to protect from uncontrolled immune activation. Cancer cells can hijack that mechanism by expressing ligands for these proteins and thus prevent anti-cancer immune responses.[4]

To mount an effective immune response, antigen-presenting cells (APCs) such as dendritic cells (DCs) and macrophages sample non-self antigens e.g. from cancer cells and activate T cells expressing T cell receptors (TCRs) specific for that antigen. In the presence of supportive cytokines such as interleukin-12 (IL-12) these specific T cells differentiate and become capable of targeting the cancer cells. This process defines APCs and T cells as key players in anti-cancer immunity (Figure 1). DCs can be subdivided into plasmacytoid DCs (pDCs) and conventional DCs (cDCs). pDCs are specialized type I interferon (IFN) producers and are important in antiviral immunity.[5] However, their role in cancer development has been increasingly studied in the last few years and pDCs can both promote and inhibit tumor progression.[6,7,8,9] They tend to be tolerogenic but can also be immunogenic under certain stimulation conditions.[10] cDCs on the other hand comprise roughly all other DCs except for monocyte-derived DCs.

DCs have already been intensively investigated for their application in vaccination approaches in which antigen-loaded, activated DCs get injected into patients to induce effective anti-tumor responses. Combinations with for example immune checkpoint therapies seem

* Corresponding author.
E-mail addresses: lisa.richter.14@hhu.de (L. Richter), stefanie.scheu@hhu.de (S. Scheu).

https://doi.org/10.1016/j.bmc.2019.115145
Received 30 March 2019; Received in revised form 19 September 2019; Accepted 28 September 2019
Available online 09 October 2019

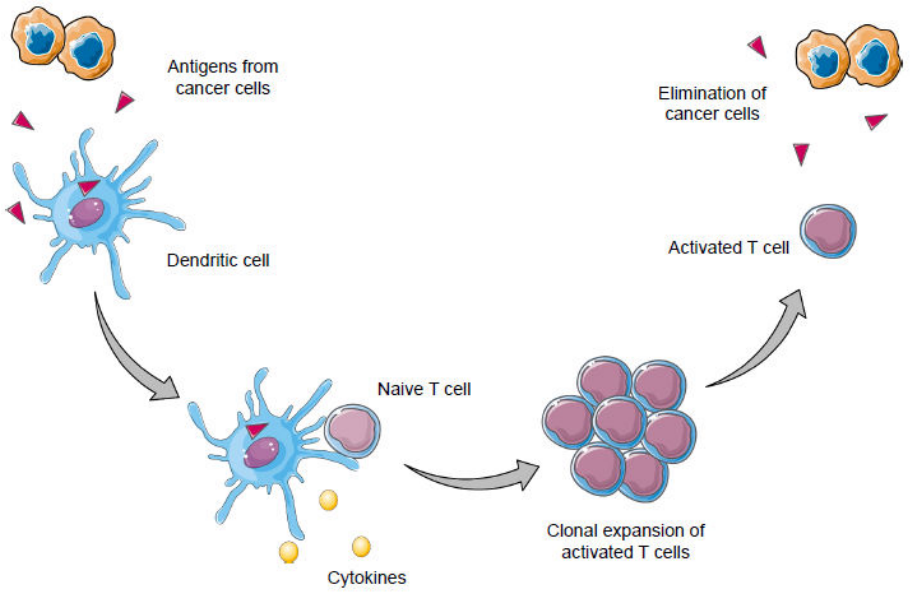

Figure 1. DCs activate T cells. Upon detection of antigens from cancer cells, DCs process and present these antigens as peptides on their cell surface in the context of major histocompatibility complex (MHC) molecules. Naïve T cells with TCRs specific for this antigen interact with the DCs and get activated in the presence of supportive cytokines or chemokines. Consequently, activated T cells start to clonally expand and help in the elimination of cancer cells at the tumor site.

additionally encouraging but the development of resistances against common medications is still a main challenge in drug development.[11,12] Strategies for overcoming intrinsic as well as acquired resistances call for new lead structures. One solution might be provided by natural products. Natural products originate from living organisms which can synthesize secondary metabolites as an adaption to biotic and abiotic stress factors.[13,14,15] They provide a wide variety of bioactive molecules and compounds. Here, penicillin and aspirin are widely known examples for natural product derived drugs.[16]

It can be hypothesized that there are compounds which could serve as immunotherapeutic agents helping the immune system to target the tumor. Natural products are not yet commonly used as immunotherapeutic agents and screening guidelines are lacking. Here we describe a methodical screening pipeline which can be applied to identify immunostimulatory properties of natural products and to select compounds that are promising for further medical research and drug development. We tested natural products for cytotoxic and immunomodulatory characteristics on murine bone marrow-derived cell cultures comprising cDCs, pDCs and macrophages and present an outlook on opportunities to further analyze, develop and optimize such compounds.

2. Material and methods

2.1. Mice

MTT and IL-12p40 experiments were performed with wildtype (WT) or with get40 reporter mice[17] (Figure 2), respectively. OVA-specific, MHC class II-restricted TCR-transgenic mice were used for T cell activation assays.[18] Animals were kept under specific pathogen-free conditions in the animal research facility of the University of Düsseldorf according to German animal welfare guidelines.

2.2. Bone marrow preparation and cell culture conditions

Mice for bone marrow preparation were sacrificed via cervical dislocation. Femurs and tibias were removed from the bodies, kept in PBS (Thermo Fisher Scientific), disinfected in 70% ethanol (VWR Chemicals) for 3 min and washed in PBS again. The ends of the bones were cut off and the bone marrow was flushed out with FCS-containing medium. To remove erythrocytes, the bone marrow was resuspended in 3 ml erylysis buffer (Morphisto). After 3 min incubation erylysis was stopped with 5 ml medium. The cell suspension was filtered through 100 µm cell strainers (Corning). After centrifugation, cells were resuspended in medium and counted for cell culturing.

2.2.1. GM-CSF cultures

For obtaining cultures with high amounts of cDCs, bone marrow cells were cultured in VLE DMEM (Biochrom) containing 10% heat-inactivated FCS (Sigma-Aldrich), 0.1% 2-mercaptoethanol (Thermo Fischer Scientific), and granulocyte–macrophage colony-stimulating factor (GM-CSF). GM-CSF cultures were performed as previously described.[19] In short, 2×10^6 cells in 10 ml medium were added to 94 × 16 mm non-treated petri dishes (Greiner Bio-One) and kept for 10 days. On day 3 of the culture 10 ml GM-CSF containing medium was added to the plates. On day 6 10 ml medium was carefully removed and centrifuged. Supernatant was removed and the remaining cell pellet was resuspended in 10 ml medium and added to the dish again. Stimulation was performed on day 9.

2.2.2. Flt3L cultures

For pDC-rich cultures bone marrow cells were cultured in medium consisting of VLE RPMI (Biochrom) containing 10% heat-inactivated FCS, 0.1% 2-mercaptoethanol, and FMS-like tyrosine kinase 3 ligand (Flt3L) for 8 days. Flt3L cultures were performed as previously described.[19,20,21] In short, 20×10^6 bone marrow cells in 10 ml were added to 94 × 16 mm non-treated petri dishes. On day 5 medium was

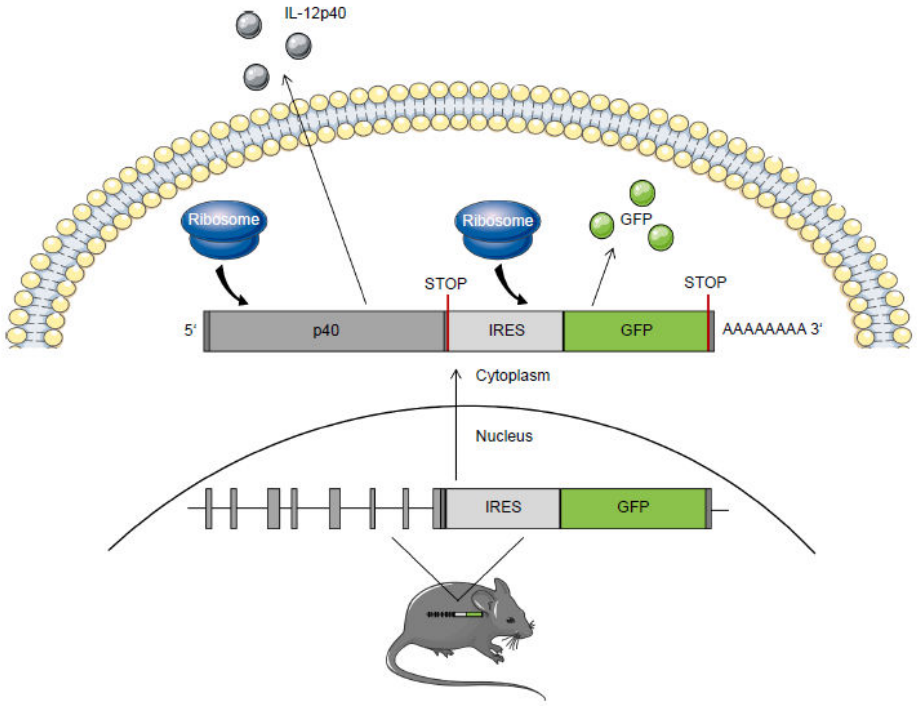

Figure 2. The get40 cytokine reporter mouse model. Get40 mice are knockin reporter mice which express IL-12p40 linked to GFP via an internal ribosomal entry site (IRES).[17] This allows tracking of IL-12p40 by detection of GFP.

refreshed by careful removal of 5 ml medium, centrifugation, resuspension in 5 ml fresh medium and return to the culture dishes. Stimulation was performed on day 7.

2.2.3. M – CSF cultures

Cultures mainly containing macrophages were obtained by culturing bone marrow cells in medium consisting of VLE RPMI containing 10% heat-inactivated FCS, 0.1% 2-mercaptoethanol, and macrophage colony-stimulating factor (M – CSF). M – CSF cultures were performed as previously described.[19] In short, 1.5×10^6 bone marrow cells in 10 ml were added to 94 × 16 mm non-treated petri dishes and cultured for 7 days. On day 3 5 ml fresh medium were added to the cultures. Stimulation was performed on day 6.

2.3. MTT assays

After preparation of cell cultures as described in section 2.2, cells were stored at 4 °C for 30 min and afterwards scraped off the dishes. Cells were centrifuged, resuspended in fresh medium and counted for culturing in non-treated 96-well plates (Sigma-Aldrich). GM-CSF-cultured cells were seeded at a density of 8×10^4 cells/well, Flt3L-cultured cells at 4×10^5 cells/well and M – CSF – cultured cells at 6×10^4 cells/well. Afterwards, cells were stimulated with 0.1, 1 or 10 µM of natural products or as controls with DMSO (Sigma-Aldrich) or staurosporine (AdipoGen Life Sciences) for a final volume of 200 µl and incubated at 37 °C for 24 h.

At the end of stimulation 20 µl of 5 mg/ml thiazolyl blue tetrazolium bromide (MTT; Sigma-Aldrich) were added to each well. Samples were incubated at 37 °C for 3 h. Afterwards, plates were centrifuged, 170 µl of the supernatant was discarded and 100 µl 5% formic acid (Merck) in isopropanol (VWR Chemicals) were added to the wells and mixed carefully. Absorption was measured at a wave length of 570 nm using a microplate reader (Tecan).

2.4. IL-12p40 flow cytometry assays

For determination of IL-12p40 production by activated DCs and macrophages, GM-CSF cultures were set up from get40 mice as described in section 2.2.1. On day 9, cells were stored at 4 °C for 30 min and afterwards scraped off the dishes. Cells were centrifuged, resuspended in fresh medium and counted for culturing in non-treated 12-well plates (Sigma-Aldrich). Cells were seeded at a density of 5×10^5 cells/well for a final volume of 1 ml and initially treated with 5 concentrations of 0–1 µM CpG 2216 (TIB Molbiol) or 0–10 ng/ml lipopolysaccharide (LPS; List Biological Laboratories, Inc.), respectively, for 16 h to determine suboptimal stimulation conditions. For testing of natural compounds, cells were incubated with 0.1, 1 or 10 µM of natural products with or without 0.1 µM CpG 2216 or 1 ng/ml LPS or left untreated at 37 °C for 16 h. Untreated cells or cells treated with 0.1 µM CpG 2216 or 1 ng/ml LPS were used as controls. At the end of stimulation, supernatant was collected for ELISAs before storing the plates at 4 °C for 30 min. After scraping off, cells were distributed to flow cytometry tubes (Corning). Cells were centrifuged to remove the supernatant and Fc binding sites were blocked with an anti-CD16/CD32 antibody (1:50; Thermo Fisher Scientific) at 4 °C for 10 min. Subsequently, cells were stained with anti-CD11b APC (1:200; BD Pharmingen), anti-CD11c APC-Cy7 (1:100; Biolegend), anti-CD86 PE-Cy7 (1:200; Biolegend) and anti-MHCII biotin (1:400; BD Pharmingen) at 4 °C for 30 min. After washing the cells with PBS containing 2% heat-inactivated FCS and 2 mM EDTA (Invitrogen), they were stained with streptavidin PerCP-Cy5.5 (1:300; BD Pharmingen). After another washing step, cells were resuspended in DAPI (Sigma-Aldrich)

containing buffer. Following this, samples were kept on ice in the dark and measurement was performed at a BDFACS Canto II. Mean fluorescence intensities (MFIs) were calculated by FlowJo version 10.5.3.

2.5. T cell activation assay

To test whether IL-12p40-producing DCs are also capable of sufficient T cell priming T cell activation assays were performed. For the initial test experiment GM-CSF cultures were set up and stimulated with 1 μM CpG 2216 on day 9. On day 10 OT-II mice were sacrificed by cervical dislocation and mesenterial, axial, brachial, inguinal, paraaortal and submandibular lymph nodes (LNs) were removed and collectively kept in PBS for further processing. LNs were then put onto 70 μm cell strainers (Corning) in a small petri dish filled with 3 ml OT-II medium consisting of RPMI 1640 (Thermo Fisher Scientific) containing 10% heat-inactivated FCS. Organs were homogenized by pressure applied via a syringe plug (Braun). Following, cells were counted and $CD4^+$ cells were separated by MACS (Miltenyi Biotec) according to the supplier's protocol. In short, cells were Fc-blocked as described in section 2.4 and incubated with biotinylated anti-CD4 antibodies (BD Pharmingen). Subsequently, magnetic anti-biotin beads (Miltenyi Biotec) were added and $CD4^+$ cells were positively selected by running cells along a MACS magnet. $CD4^+$ cells were afterwards added to non-treated 96-V-bottom plates in an amount of 2×10^4 cells/well according to Reinhardt *et al.*[17] GM-CSF-cultured cells were put at 4 °C for 30 min and afterwards scraped off the dishes. Samples were centrifuged, resuspended in OT-II medium and added to the wells at 5×10^4, 2.5×10^4, 1×10^4, 2×10^3, 4×10^2 or 0 cells/well in triplicates. Lastly, cells were pulsed with 300 nM $OVA_{323-339}$ peptide (Sigma-Aldrich). Samples were incubated for 5 days before analysis of the supernatant for IL-2 amount by ELISA (R&D Systems). Analysis of natural products was performed accordingly: 1×10^4 GM-CSF-cultured cells were incubated in technical duplicates with cytochalasin D or 18-dehydroxycytochalasin (0.1, 1, 5 or 10 μM) or manzamine J *N*-oxide (2.5, 5, 7.5 or 10 μM) with or without 0.1 μM CpG 2216 or 1 ng/ml LPS or left untreated at 37 °C for 24 h. Untreated cells and cells treated with 0.1 μM CpG 2216 or 1 ng/ml LPS were used as controls. After the incubation time, isolated $CD4^+$ cells were added to the GM-CSF-cultured cells, pulsed with 300 nM $OVA_{323-339}$ peptide and the supernatant was collected after 5 days.

3. Results and discussion

Due to the lack of appropriate guidelines a new pipeline for screening of natural products for immunotherapeutic potential was developed. We discuss which aspects should be considered to decide if a compound might serve in the development of novel anti-cancer drugs. Moreover, the reasons behind the decision for the techniques applied are presented and further methods suggested.

3.1. Criteria for "appropriate" compounds

Natural products that can be categorized to be potential candidates for immunotherapeutic drug development should fulfill certain criteria in first preclinical screenings. First, determination of cytotoxicity early on in drug development is essential as compounds should be non-toxic for target immune cells. In this study, primary immune cells were used because these are non-transformed and thus biologically close to physiological conditions *in vivo*. Secondly, screenings for favorable biological activities e.g. toxicity for cancer cells or modulation of autophagy have to be considered. Lastly, natural products chosen on the basis of the first two aspects should induce or enhance immune stimulation to prove promising for immunotherapeutic application. Compounds that fulfill all three criteria and are non-toxic to primary immune cells, show advantageous biological capacities for cancer treatment and are able to potentially stimulate the immune system can then be selected for more in-depth biochemical analysis and optimization.

3.2. Cytotoxicity assays

Determination of potential cytotoxicity is fundamental when starting the investigation of natural products without previous knowledge about their biological properties. As the primary aim of this screening pipeline is to find compounds that stimulate immune cells, toxicity against this cell type has to be analyzed. Here, the effects on primary cells derived from GM-CSF, Flt3L and M−CSF cultures were tested. These cultures generate cDCs, pDCs and macrophages in different amounts and thus provide cell types crucial to mount effective innate and adaptive immune responses against cancer.[22,10,23]

One type of cytotoxicity assay is the MTT assay which is simple and efficient. It's a widely used and accepted assay which generates highly reproducible data. Alternatives are provided by e.g. one-step solutions such as MTS assays. Living cells convert MTT into formazan which precipitates as violet crystal-like structures. These structures can be dissolved by acidified isopropanol and optical densities (OD) are determined at 570 nm using a spectrophotometer. These ODs are proportional to the amount of metabolically active cells.[24] Before running actual experiments with natural products, optimal cell numbers for an OD of 0.75–1.25 have to be defined (Figure 3). Cell counts for GM-CSF- and M−CSF−cultured cells were determined for an OD of 1, while Flt3L-cultured cells were adjusted to an OD of 0.75, as the cellular yield of this culture is considerably lower as compared to the GM-CSF and M−CSF culture systems. The optimal cell number can be calculated by the formula of a best fit line. In this case, GM-CSF-cultured cells were seeded at a density of 8×10^4 cells/well, Flt3L-cultured cells at 4×10^5 cells/well and M−CSF−cultured cells at 6×10^4 cells/well.

After establishment of optimal cell densities, cells are incubated with natural products at 0.1, 1 and 10 μM for 24 h to provide a range of conceivably effective concentrations (Figure 4). An incubation period of 24 h was chosen due to the fact that time periods of more than 12 h often are necessary for induction of effective immune stimulation and incubation times should be kept similar along different assays.

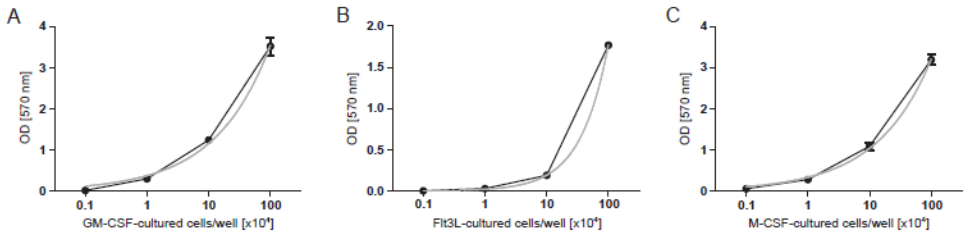

Figure 3. Examination of optimal cell numbers per well for MTT assays. GM-CSF- (A), Flt3L- (B) and M−CSF−cultured cells (C) were titrated to determine appropriate cell counts for an OD of 0.75–1.25 at 570 nm (one biological replicate measured as technical duplicates; error bars indicate standard deviations).

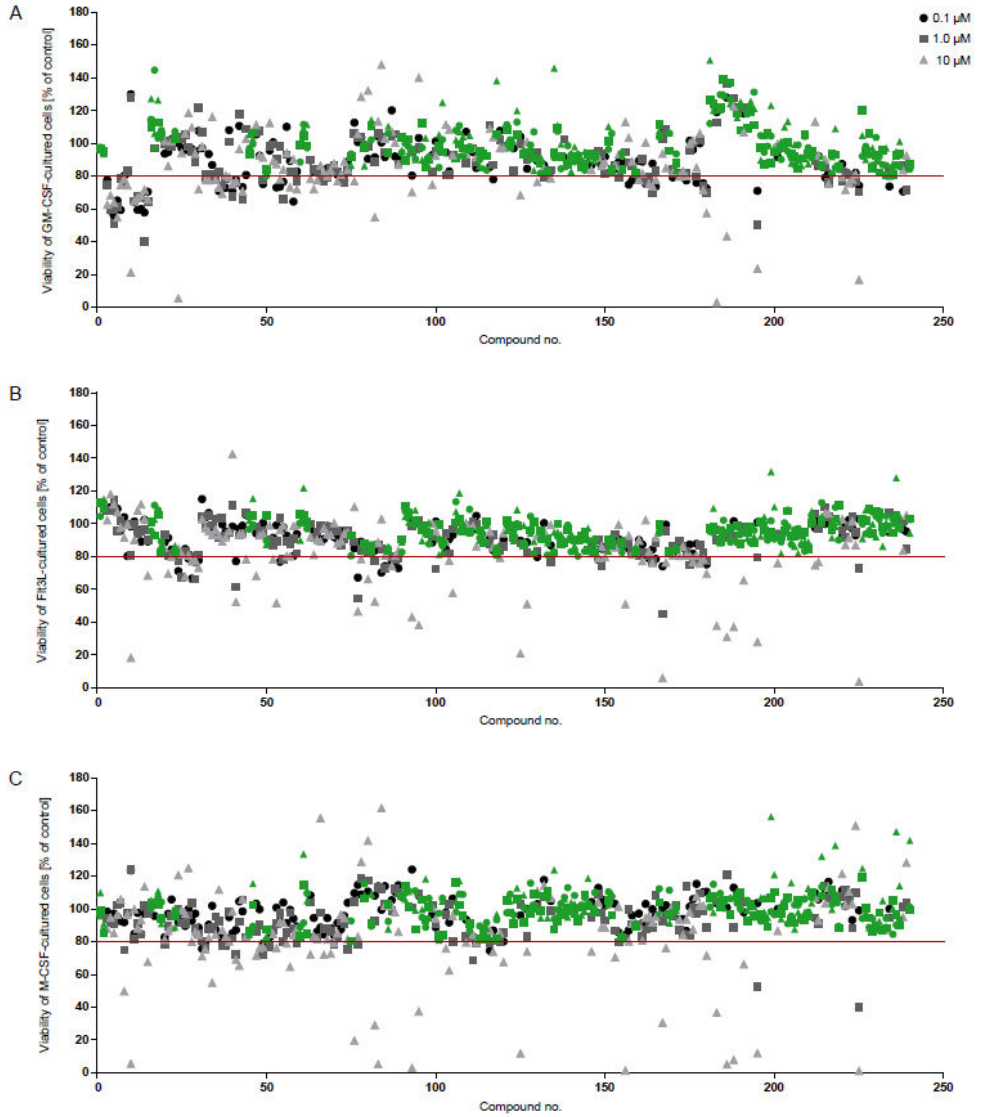

Figure 4. Effects of 240 natural products on the viability of GM-CSF- (A), Flt3L- (B) or M−CSF−cultured cells (C). Natural products were tested in 3 different concentrations for an incubation period of 24 h and viability has been normalized to the DMSO negative control (one biological replicate; one sample per condition). The red line indicates the threshold of 80% viability. Compounds that showed a viability of ≥ 80% for all 3 cultured cell types at all 3 concentrations are highlighted in green. (For interpretation of the references to colour in this figure legend, the reader is referred to the web version of this article.)

Incubation of the cells with the protein kinase inhibitor staurosporine, a potent apoptosis inductor, served as a positive control (data not shown). As negative control, cells were treated with the same amount of solvent as in the 10 µM samples to determine possible toxic effects of the solvent alone. Normalization of the ODs of the samples to the negative control sample and plotting gave the percentage increases or decreases in metabolic activity. Here, cytotoxic as well as proliferative effects become visible of which proliferative effects can indicate positive, desirable effects which involve an increase in APC numbers for potent induction of adaptive immune responses. Among the 240 natural products tested in this work 41 compounds were found to induce a metabolic activity of 120% and above for at least one cell type and concentration. These compounds could also be interesting for further research with a focus on the induction of proliferation of specific cell subsets. However, natural products which are toxic for DCs and macrophages should be excluded according to the guidelines defined in section 3.1.

Natural products are defined here as non-toxic if they show a viability rate of more than 80% in all concentrations and for all cell types. In this work, 240 natural products were tested. From these a minority of

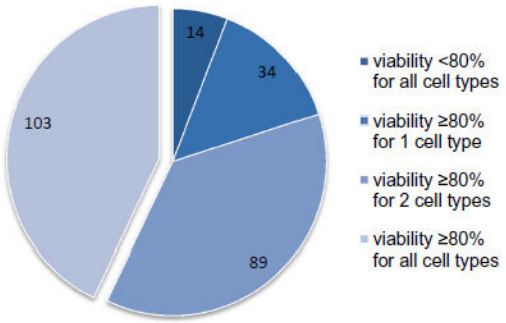

Figure 5. Overview of the cytotoxicity of the analyzed natural products for the immune target cells.

14 exhibited viability rates below 80% for all three cell types, and 34 and 89 showed viability rates below 80% for only one or two cell types. 103 non-toxic compounds were selected for analyses in further immune stimulation assays on the basis of a viability rate of more than 80% in all concentrations and for all cell types (Figure 5).

Besides the impact on viability, conclusions regarding structural similarities of the compounds can be made especially in the case where derivatives exhibit significant differences in cytotoxicity. Such effects might be due to small structural changes and help in drawing conclusions on responsible functional groups. On the other hand, effects of derivatives which show similar properties are probably based on a common basic structure and might be suitable for biochemical modification and optimization.

3.3. Including comparative screening for additional desirable functionalities of compounds

Comparative analyses and the examination of other biological activities are useful as the tested natural products could potentially show similar resistance mechanisms and thus comparisons can help identifying underlying modes of actions. Lambert *et al.* hypothesized that resistances evolve from interacting cells in cell communities as they appear in cancerous tissue as well as in bacterial populations.[25] Thus, studies of bacterial resistance mechanisms might allow conclusions on those of cancers. Additionally, compounds can be identified which are interesting not only for immunotherapeutic anti-cancer treatment but also for other approaches in this field such as the induction of autophagy.[26]

This work was conducted as a cooperative effort together with other teams that investigated different types of activities of the compounds against e.g. tumor cells, pathogenic gram-negative bacteria and intracellular parasites. In more detail, toxicity against Jurkat and Ramos lymphoma cell lines, effects on damage response mechanisms, toxicity for *Mycobacterium tuberculosis* and various gram-negative bacteria strains such as *Escherichia coli*, toxicity for *Toxoplasma gondii* and effects on the induction of autophagy have been assessed. Out of 103 non-toxic natural products 41 compounds showed at least one additional favorable biological capacity. These compounds were chosen as ideal candidates for further screening and an examination in IL-12p40 assays detecting immune activation.

3.4. Immune activation: IL-12p40 production

IL-12 is a cytokine which has been extensively studied over the last years especially with regard to its implications in cancer immunotherapy. It consists of the two subunits p40 and p35 which get upregulated upon Toll-like receptor (TLR) stimulation.[27] TLRs are pattern recognition receptors (PRRs) that detect pathogen-associated molecular patterns (PAMPs). The IL-12 receptor is found on T and NK cells and gets upregulated upon antigen contact. On the cellular level, IL-12 signaling induces interferon γ (IFNγ) production by these cell types and thus promotes innate and adaptive immune responses as well as T and NK cell proliferation.[28] Recently it has been shown that an intratumoral crosstalk of DCs and T cells involving IL-12 and IFNγ is necessary for successful anti-cancer treatment with the immune checkpoint inhibitor anti-PD-1.[29]

Thus, IL-12p40 produced upon stimulation can be used as a reliable readout of immune stimulation. Usage of get40 knockin reporter mice which express IL-12p40 linked to GFP facilitates the detection of IL-12p40 production by tracking GFP via flow cytometry.[17] GM-CSF-cultured cells are potent in IL-12p40 expression upon stimulation and were therefore used for immune activation assays.[22] After staining and flow cytometric measurement events are gated on single, living cells and analyzed for the frequency of IL-12p40/GFP$^+$ cells to detect culture-wide stimulatory effects. In Figure 6 an exemplary gating strategy of a CpG 2216-stimulated sample is shown.

Besides stimulation with natural products in the same concentrations as in the MTT assays (section 2.3) supplementary TLR stimuli were used. Addition of these TLR ligands ensures a weak immune activation and reflects the physiological situation in the presence of a tumor or during an infection.[30] As TLR stimuli, either CpG 2216 or LPS are added to the cells simultaneously to the natural products. CpG 2216 is a synthetic class A oligonucleotide, that mimics e.g. bacterial DNA in which unmethylated CpG motifs are enriched and signals via TLR9.[31] LPS on the other hand is a component of the outer cell membrane of gram-negative bacteria and is detected via TLR4.[32] Both substances are strong stimuli of IL-12p40 secretion by DCs. To avoid a saturated response and allow for the detection of an additive or even synergistic effect of the natural compound to be tested, CpG 2216 and LPS have to be titrated on the target immune cells in advance. A range of 5 concentrations is advisable. Here, CpG 2216 was tested at 0–1 µM while LPS was used at 0–10 ng/ml, both in decadic steps as shown in Figure 7. While it cannot be excluded, IL-12p40 frequencies above 20% could be achieved with higher concentrations of either CpG 2216 or LPS, a final dose should be chosen where a slight but detectable increase in IL-12p40/GFP expression can be seen that is significantly lower as

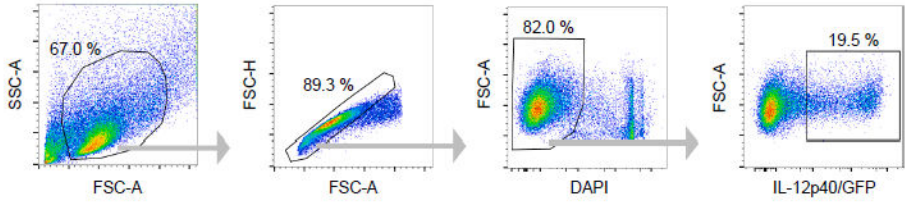

Figure 6. Gating strategy for the flow cytometric analysis of IL-12p40 production by GM-CSF-cultured cells. Cells were stimulated with 0.1 µM CpG 2216 for 16 h and stained for flow cytometry. Measured events were sequentially gated for cells, single cells, live cells and for production of IL-12p40/GFP. Percentages indicate the frequency of the parental population.

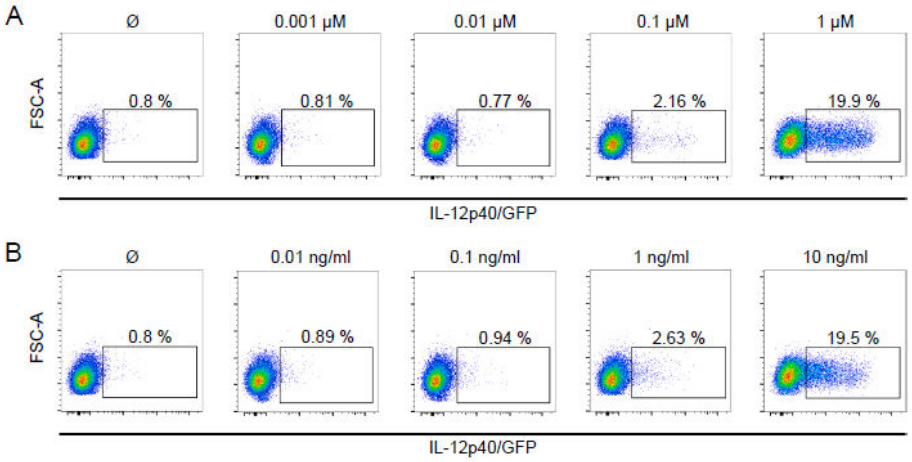

Figure 7. Titration of CpG 2216 (A) and LPS (B) on GM-CSF-cultured cells. CpG 2216 and LPS concentrations were titrated and incubated for 16 h to determine suboptimal stimulation conditions for IL-12p40/GFP production (one biological replicate; one sample per condition).

compared to the highest concentrations of the stimulus used. In this study, for both stimuli the second highest concentration appeared to be most suitable. The suboptimal concentrations of CpG 2216 and LPS, respectively, are also applied for positive controls in the following assays, while untreated cells are used as negative control.

Samples stimulated with natural products and TLR ligands are incubated overnight (16 h) to meet the time requirements of an effective immune stimulation and to minimize slight cytotoxic reactions which could be seen in the MTT assays after 24 h (section 2.3). Natural products have been defined here to be non-toxic if they show a viability of at least 80% for all cell types. Thus, only compounds that met this criterion are included in immune activation assays. Nevertheless, slight inhibiting effects of the natural products indicated by a viability rate in the range of 80–99% in the MTT assays might be compensated by shorter incubation times.

Considering mean fluorescence intensities (MFIs) can be beneficial in addition to examination of the frequency of IL-12p40/GFP$^+$ cells. MFI values are calculated by the sum of all intensity values divided by the number of events. They display the mean expression strength of a marker of a measured sample.[33] Thereby direct conclusions can be drawn on the levels of IL-12p40 production. In Figure 8 the MFI of TLR-stimulated samples as positive controls are presented in comparison to the unstimulated negative control.

IL-12p40 assays were performed as three independent experiments on material from two mice per experiment treated separately to validate the reproducibility of data and stability of the compounds taking variations due to the application of primary cells into account. From the IL-12p40 activation assays natural products are selected which show at least a 2-fold increase in IL-12p40$^+$ cell frequency or MFI compared to cells treated with CpG 2216 or LPS alone to ensure an assortment of sufficiently immunostimulatory compounds, only. Analysis of further markers which – depending on the cell type – change under activating conditions such as MHC class II, CD11c and the surface activation marker CD86 can contribute additional valuable information. Different cell types could be more or less sensitive to natural products and thus need other effective concentrations for stimulation.

In this work, 3 out of the 41 biologically active compounds showed immune activating potency with regard to IL-12p40 production. Of these compounds, one, manzamine J *N*-oxide, was immunostimulatory without an additional TLR stimulus, while the two cytochalasins cytochalasin D and 18-dehydroxycytochalasin H needed additional TLR

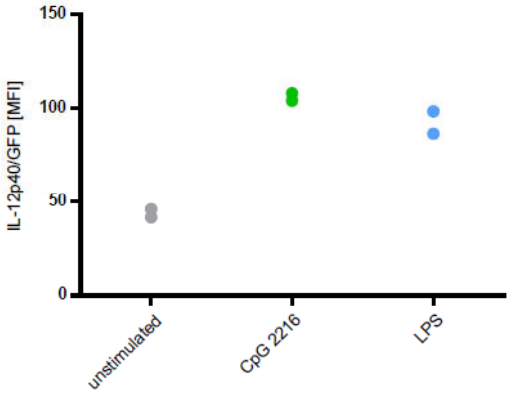

Figure 8. MFIs of unstimulated and TLR-stimulated GM-CSF-cultured cells. Samples were gated for single, live cells and analyzed for MFIs of IL-12p40/GFP by FlowJo 10.5.3 (two biological replicates; one sample per condition. Error bars indicate standard deviations.). Shown is one example out of 11 experiments.

stimulation by CpG 2216. These 3 were chosen for further examination in T cell activation assays.

3.5. *T cell activation*

IL-12p40-producing DCs are capable of inducing T cell activation and thus provide a linkage of innate and adaptive immunity.[17] To test whether IL-12p40-inducing natural products are also competent in activating DCs for T cell priming, Ovalbumin (OVA)-specific CD4$^+$ cells from OT-II transgenic mice are used.

OT-II mice are genetically modified in a way that they harbor CD4$^+$ T cells expressing a transgenic TCR specific for an OVA-derived peptide ($OVA_{323-339}$) when presented by APCs in the context of MHC class II.[18] These mice consequently provide an advantageous source for antigen-specific T cells for T cell activation assays. For establishment of an assay protocol according to Reinhardt *et al.*, optimal DC numbers have to be defined in the first step[17] (Figure 9). As a readout for efficient OTII

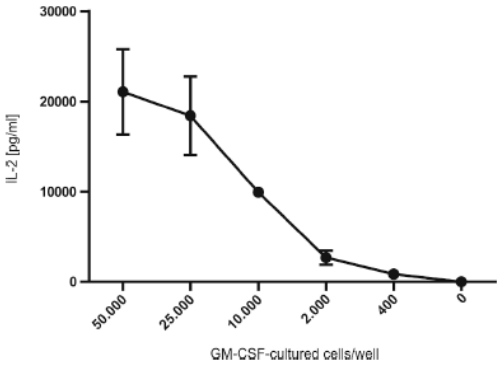

Figure 9. Establishment of experimental conditions for T cell activation assays. OVA-specific OT-II $CD4^+$ T cells were incubated with the indicated amounts of CpG 2216-stimulated GM-CSF-cultured cells for 5 days. IL-2 production has been verified by ELISA (one biological replicate measured as technical triplicates; error bars indicate standard deviations).

$CD4^+$ T cell activation IL-2 production was chosen and analyzed by ELISA. IL-2 is a cytokine which gets secreted by activated $CD4^+$ T cells.[34] Its application in cancer therapy has already been tested in clinical settings and due to side effects combination treatment of IL-2 with other immunostimulatory drugs is in discussion.[35]

For analysis of the T cell activating potential of natural products, a suboptimal amount of GM-CSF-cultured cells has to be chosen to allow detection of an increase in IL-2 secretion after stimulation with natural products. Similar to the IL-12p40 assays, natural products with or without additional TLR stimulation (section 2.4) are added to the cells overnight before cocultivation with OTII $CD4^+$ T cells. The suboptimal concentrations of CpG 2216 and LPS, respectively, are here applied again for positive controls, while untreated cells are used as negative control. An induction of IL-2 production after stimulation indicates a successful DC:T cell crosstalk and an initiation of an adaptive immune response which is fundamental for cancer immunotherapy. There might also be compounds which act agonistically with IL-2 and could help eliminating current side effects of treatment of patients with IL-2 alone. As for the IL-12p40 assays, T cell activation assays should also be performed at least three times with a minimum of two separately treated mice each.

An overview over the structural and biological properties of the 3 most promising natural products according to the presented screening guidelines is provided in Figure 10. All 3 compounds are non-toxic to the tested target immune cells, possess beneficial bioactivities and show an at least 2-fold increase in IL-12p40 production with or without an additional TLR stimulus. Both cytochalasins, namely cytochalasin D and 18-dehydroxycytochalasin H, induce an elevation in IL-12p40 at 1 µM compound plus CpG 2216 and also exhibited successful T cell activation capacities. Manzamine J *N*-oxide displayed the highest number of additional bioactivities in the comparative analyses and a relatively strong increase in IL-12p40 production at 10 µM alone but was not able to induce a sufficient DC:T cell crosstalk.

Natural products which have been identified to support immune activation of T cells by DCs can be further optimized and analyzed for modes of action as discussed below.

3.6. Discussion

In this work a new pipeline for first-line screening of natural products for immunotherapeutic drug development approaches was established with the aim to define guidelines that help in the straightforward identification of promising compounds. The screening pipeline was prototypically performed on 240 natural compounds derived from marine sponges and endophytic fungi using bone marrow-derived murine DCs and macrophages. We found 3 out of 240 natural products as potential candidates for further drug development. Following the guidelines, compounds should be non-toxic to target cells, possess beneficial anti-cancer activities and be immunostimulatory.

For determination of immune activating capabilities of compounds, assays for IL-12p40 production and T cell activation were established. IL-12p40 can be seen as a marker of activation of innate immune cells such as DCs and macrophages. IL-12p40 expression was analyzed via flow cytometry using cells from cytokine fluorescence reporter mice.[17] These mice but also other genetically modified mouse strains like the OTII TCR-transgenic mice used in the T cell activation assays can later be applied for *in vivo* testing of promising natural products. The direct step into the *in vivo* model is hereby optimized, as primary murine cells from the very same mouse model are used in all assays instead of cell lines or primary human cells. This is also where the advantage of phenotypic screenings over target-based approaches comes into effect: Instead of an early focus on a specific target as in target-based drug discovery which later on might be difficult to retrieve in physiological conditions, phenotypic screenings are more open with regard to the complexity of possible modes of action and consequently closer to *in vivo* settings.[36,37,38] Phenotypic screening approaches have already been successfully applied to target deconvolution of natural products and are apparently more efficient in drug discovery processes in general.[39]

Investigation of specific IL-12p40-producing cell subsets from the above mentioned reporter mice by flow cytometry allows deeper insights into biological modes of action. For that, staining of cultures with specific cell markers e.g. CD11b, CD115 and CD135 for the discrimination of cDCs vs. macrophages and analysis via flow cytometry can be implemented.[22]

The presented experimental setup can moreover be complemented with enzyme-linked immunosorbent assays (ELISAs) for IL-12p40. ELISAs provide the opportunity to corroborate the obtained results by an independent method from the same experimental sample and provide a direct definition of the amount of secreted IL-12p40. Additionally, ELISAs specific for the heterodimer IL-12p70 consisting of the two subforms p35 and p40 further deliver information about the amount of the bioactive form of the cytokine necessary for T cell activation.

IL-12 as a key factor for the induction of adaptive immune responses has already been applied in murine and human cancer studies.[40,29] Despite the observation of severe side effects in clinical trials IL-12 is still a focus of research and might be a candidate for combination therapies together with natural product-derived drugs.[41,29] Assays using cocultivation of DCs and T cells can be deployed as an *in vitro* surrogate to determine the effectiveness of immune activation by natural products. IL-2 is a marker for activated T cells after antigen presentation by DCs.[34] The TCR-transgenic mouse model used here provides a simple, advantageous tool for elaboration of an effective DC:T cell crosstalk upon antigen contact.[18] Successful T cell activation should be confirmed by evaluation of T cell proliferation and measurement of the incorporation of [^{3}H]thymidine or a proliferation dye.[17]

The same immune activation assays as shown in this work with GM-CSF cultures can be carried out additionally with other primary cell types such as Flt3L- and M−CSF−cultures to interrogate immunostimulatory effects of natural compounds on additional types of APCs.

The 3 most promising natural products identified by this screening platform are the two cytochalasins cytochalasin D and 18-dehydroxycytochalasin H as well as the alkaloid manzamine J *N*-oxide. The latter one has shown the most encouraging results of all tested 103 compounds in the comparative analyses as it is active against tumor cell lines as well as bacteria. Despite its capacity to induce IL-12p40 it did not exert any T cell activation potential which led to the decision to

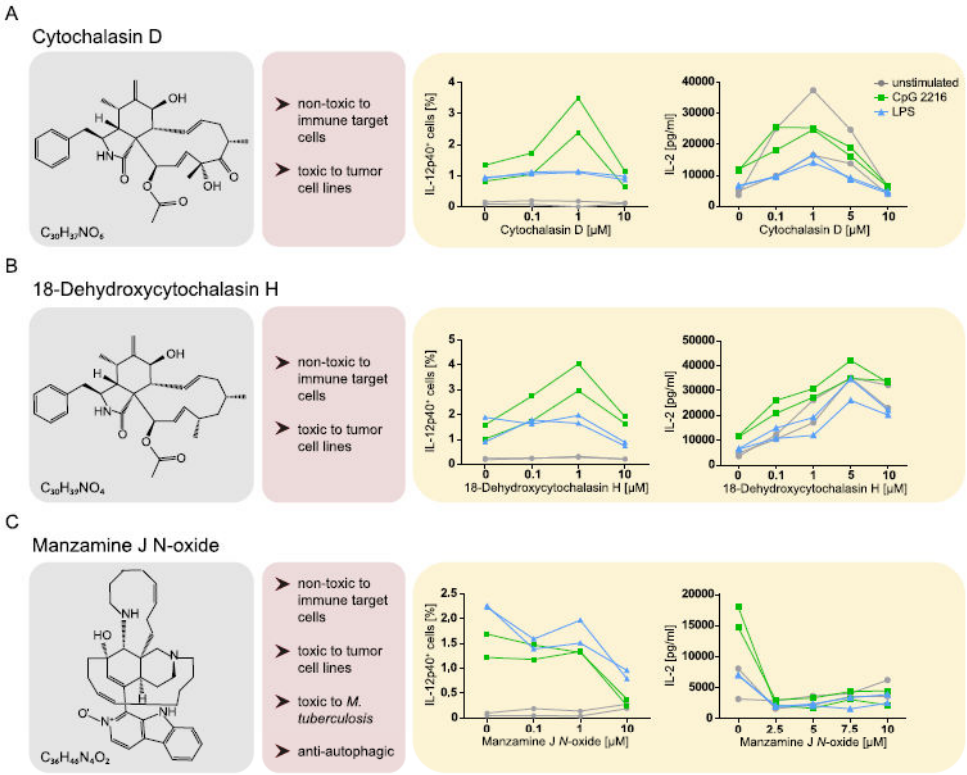

Figure 10. Overview of the results of the most promising natural products. Shown are the structures, additional beneficial bioactivities and immunoactivating capacities regarding IL-12p40 production and T cell activation of cytochalasin D (A), 18-dehydroxycytochalasin H (B) and manzamine J *N*-oxide (C) (two biological replicates are shown measured as technical duplicates). For cytochalasin D and 18-dehydroxycytochalasin H, one example each out of three experiments is shown.

exclude manzamine J *N*-oxide from further screenings. The compound was slightly toxic at 10 µM and IL-12p40 production could be explained by recognition of damage-associated patterns (DAMPs) as a reaction to these toxic effects.[42,43] One manzamine derivative from the screened library, manzamine F, exhibited no immunostimulatory effects while other manzamines have already been shown to possess antibacterial, antiviral and antiparasitic activities.[44] Especially manzamine A and analogs are discussed as anti-cancer therapeutics.[45,46] Biochemically optimized derivatives of manzamine J *N*-oxide might thus provide more favorable characteristics.

Cytochalasins are fungal toxins, well established inhibitors of actin polymerization and have been extensively used in studies of the cytoskeleton.[47] Different cytochalasins including cytochalasin D have been described to have antitumor capacities which probably can be explained by the rapid proliferation cycle of malignant cells.[48–51] Actin plays essential roles in endocytic processes and it has been shown that cytochalasin D forms specific actin aggregates that associate with endosomal proteins.[52,53] As in our experiments the strongest increase in IL-12p40 as well as in IL-2 was observed in combination with CpG 2216 it can be hypothesized that the two cytochalasins that were the only potentially actin-targeting agents present in the compound library induce a concentration-dependent retention of CpG 2216 in endocytic aggregates and consequently a longer exposition time of the stimulus in this TLR containing compartment.[31] Thus, a next step would be to test this hypothesis by e.g. staining of the actin skeleton with phalloidin and to further investigate the immune activating potential of cytochalasins. Here, additional inhibitors of actin polymerization with different chemical scaffolds can be used to functionally verify the molecular mechanism. Beside their immunostimulatory characteristics cytochalasins might also prove promising chemotherapeutic agents especially in combination with other microfilament-directed drugs and have additionally already been shown to have a positive impact on anti-infectious immune responses.[54,55]

3.7. Future outlook

After evaluation of immunostimulatory properties, application of target finding approaches is the next step to generate insights into modes of action of attractive compounds. For target identification, indirect or direct approaches can be used. In indirect target analyses, effects on for example gene expression profiles of primary cells or of *ex vivo* isolated cells treated with natural products are compared to those of a known substance e.g. by DNA microarray analyses or next generation sequencing.[56,57,58] Indirect target deconvolution consequently requires substances with similar phenotypes and gives the first hints on involved pathways but is not as straightforward as direct approaches.[38] In direct approaches protein targets directly interacting with a compound can be identified. For instance, possible target proteins get overexpressed, purified and assigned to protein microarrays to examine compound-binding affinities. Still one challenge here is that many small molecules are hydrophobic and thus also bind unspecifically to non-target proteins.[59,38] Computational approaches can additionally

promote target identification processes by e.g. molecular modelling and machine learning approaches.[60,61] There is a large number of possible methods and the appropriate one has to be chosen according to the structure and chemical characteristics of the natural product. Finally, if the target structure has been identified specific assays for validation can be designed which use for example existing target inhibitors.

After determination of mechanistic properties underlying immune activation chemical optimization of compounds should be carried out. Such optimization approaches aim to improve natural products in regard of their physiological *in vivo* effects, their efficacy and accessibility via e.g. modification of functional groups.[62] Of course, these derivatives would then have to be tested in the listed assays again with special focus on immune activating characteristics.

Natural products which potentially have been chemically modified and which finally have been shown to be non-toxic to the mentioned immune cells, which exert beneficial anti-tumor activities and possess immunostimulatory capacities could then be tested in *in vivo* tumor mouse models e.g. xenograft models. Here, *in vivo* toxicity and dosing of a compound have to be assessed initially. Following this, effects on the tumor burden and size are analyzed to determine direct anti-cancer reactions besides examination of immunostimulatory responses such as infiltration of IL-12p40-producing DC and T cells into tumor microenvironments.[63,29] The exact design of an *in vivo* experiment depends on the biological accessibility of the compound and the type of mouse model used and affects for example the route of drug administration. Natural products potent in tumor mouse models could subsequently be introduced to clinical trials and inspire immunotherapeutic drug development.

The presented pipeline enables screening of natural products especially for academic institutions without access to industrial high throughput facilities. It allows the determination of promising compounds at relatively low financial burden and high success probability according to the presented results. Establishment of a collective compound library with natural products from various sources and with diverse chemical structures affords an unbiased analysis. Particularly when working in consortia which integrate groups working on the same natural products but with different foci, a database centralizing all gained information is highly recommended.[64] Gathering researchers from various fields such as biology, chemistry, pharmacy and computer science promotes a fruitful environment for the investigation of distinct natural products from different points of view and is a promising approach for the detection of resistances early on in drug discovery..

The allocation of the Nobel Prize 2018 for Medicine or Physiology for novel tumor immunotherapeutics and the increasing interest in this field of research highlight the importance of immune activation for anti-cancer treatments. The current knowledge supports the concept of the broad implication of immune activation assays in screening approaches. Immune activation is essential for fighting cancer in new impressive ways and the screening pipeline presented in this work aims to provide a tool for the detection of immunostimulatory natural products and other compounds early on in drug discovery.

Declaration of interest:

None

Acknowledgement

This work was funded by the Deutsche Forschungsgemeinschaft, Germany (DFG, German Research Foundation) – 270650915/GRK2158.

Graphics were created using Servier Medical Art according to Creative Commons Attribution 3.0 Unported License (https://creativecommons.org/licenses/by/3.0/). Changes were made to the original cartoons.

References

1. World Health Organization. World health statistics 2018: Monitoring health for the SDGs, sustainable development goals. https://www.who.int/gho/publications/world_health_statistics/2018/en/. Accessed 26 March 2019.
2. American Association for Cancer Research. Cancer Progress Report 2018. https://www.cancerprogressreport.org/PAGES/CPR18-CONTENTS.ASPX. Accessed 26 March 2019.
3. The Nobel Prize in Physiology or Medicine 2018. https://www.nobelprize.org/prizes/medicine/2018/press-release/. Accessed 26 March 2019.
4. Wei SC, Duffy CR, Allison JP. Fundamental Mechanisms of Immune Checkpoint Blockade Therapy. *Cancer Discov.* 2018;8:1069–1086.
5. Reizis B. Plasmacytoid Dendritic Cells: Development, Regulation, and Function. *Immunity.* 2019;50:37–50.
6. Sisirak V, Faget J, Gobert M, et al. Impaired IFN-alpha production by plasmacytoid dendritic cells favors regulatory T-cell expansion that may contribute to breast cancer progression. *Cancer Res.* 2012;72:5188–5197.
7. Labidi-Galy SI, Treilleux I, Goddard-Leon S, et al. Plasmacytoid dendritic cells infiltrating ovarian cancer are associated with poor prognosis. *Oncoimmunology.* 2012;1:380–382.
8. Drobits B, Holcmann M, Amberg N, et al. Imiquimod clears tumors in mice independent of adaptive immunity by converting pDCs into tumor-killing effector cells. *J Clin Invest.* 2012;122:575–585.
9. Tel J, Aarntzen EH, Baba T, et al. Natural human plasmacytoid dendritic cells induce antigen-specific T-cell responses in melanoma patients. *Cancer Res.* 2013;73:1063–1075.
10. Swiecki M, Colonna M. The multifaceted biology of plasmacytoid dendritic cells. *Nat Rev Immunol.* 2015;15:471–485.
11. van Gulijk M, Dammeijer F, Aerts J, Vroman H. Combination Strategies to Optimize Efficacy of Dendritic Cell-Based Immunotherapy. *Front Immunol.* 2018;9:2759.
12. Sharma P, Hu-Lieskovan S, Wargo JA, Ribas A. Primary, Adaptive, and Acquired Resistance to Cancer Immunotherapy. *Cell.* 2017;168:707–723.
13. Haefner B. Drugs from the deep: marine natural products as drug candidates. *Drug Discov Today.* 2003;8:536–544.
14. Ramakrishna A, Ravishankar GA. Influence of abiotic stress signals on secondary metabolites in plants. *Plant Signal Behav.* 2011;6:1720–1731.
15. Yang L, Wen KS, Ruan X, Zhao YX, Wei F, Wang Q. Response of Plant Secondary Metabolites to Environmental Factors. *Molecules.* 2018;23.
16. Butler MS. The role of natural product chemistry in drug discovery. *J Nat Prod.* 2004;67:2141–2153.
17. Reinhardt RL, Hong S, Kang SJ, Wang ZE, Locksley RM. Visualization of IL-12/23p40 in vivo reveals immunostimulatory dendritic cell migrants that promote Th1 differentiation. *J Immunol.* 2006;177:1618–1627.
18. Barnden MJ, Allison J, Heath WR, Carbone FR. Defective TCR expression in transgenic mice constructed using cDNA-based alpha- and beta-chain genes under the control of heterologous regulatory elements. *Immunol Cell Biol.* 1998;76:34–40.
19. Scheu S, Dresing P, Locksley RM. Visualization of IFNbeta production by plasmacytoid versus conventional dendritic cells under specific stimulation conditions in vivo. *P Natl Acad Sci USA.* 2008;105:20416–20421.
20. Bauer J, Dress RJ, Schulze A, et al. Cutting Edge: IFN-beta Expression in the Spleen Is Restricted to a Subpopulation of Plasmacytoid Dendritic Cells Exhibiting a Specific Immune Modulatory Transcriptome Signature. *J Immunol.* 2016;196:4447–4451.
21. Ali S, Hoven A, Dress RJ, Schaal H, Alferink J, Scheu S. Identification of a novel Dlg2 isoform differentially expressed in IFNbeta-producing plasmacytoid dendritic cells. *BMC Genomics.* 2018;19:194.
22. Helft J, Bottcher J, Chakravarty P, et al. GM-CSF Mouse Bone Marrow Cultures Comprise a Heterogeneous Population of CD11c(+)MHCII(+) Macrophages and Dendritic Cells. *Immunity.* 2015;42:1197–1211.
23. Gordon S, Pluddemann A, Martinez Estrada F. Macrophage heterogeneity in tissues: phenotypic diversity and functions. *Immunol Rev.* 2014;262:36–55.
24. Riss TL, Moravec RA, Niles AL, Benink HA, Worzella TJ, Minor L. Cell Viability Assays. In: Sittampalam GS, Coussens NP, Nelson H, et al., eds. Assay Guidance Manual. Bethesda (MD)2004.
25. Lambert G, Estevez-Salmeron L, Oh S, et al. An analogy between the evolution of drug resistance in bacterial communities and malignant tissues. *Nat Rev Cancer.* 2011;11:375–382.
26. Fulda S. Autophagy in Cancer Therapy. *Front. Oncol.* 2017;7:128.
27. Krummen M, Balkow S, Shen L, et al. Release of IL-12 by dendritic cells activated by TLR ligation is dependent on MyD88 signaling, whereas TRIF signaling is indispensable for TLR synergy. *J Leukoc Biol.* 2010;88:189–199.
28. Zundler S, Neurath MF. Interleukin-12: Functional activities and implications for disease. *Cytokine Growth Factor Rev.* 2015;26:559–568.
29. Garris CS, Arlauckas SP, Kohler RH, et al. Successful Anti-PD-1 Cancer Immunotherapy Requires T Cell-Dendritic Cell Crosstalk Involving the Cytokines IFN-gamma and IL-12. *Immunity.* 2018;49(1148–1161):e1147.
30. Yu L, Wang L, Chen S. Endogenous toll-like receptor ligands and their biological significance. *J Cell Mol Med.* 2010;14:2592–2603.
31. Krieg AM. CpG motifs in bacterial DNA and their immune effects. *Annu Rev Immunol.* 2002;20:709–760.
32. Chow JC, Young DW, Golenbock DT, Christ WJ, Gusovsky F. Toll-like receptor-4 mediates lipopolysaccharide-induced signal transduction. *J Biol Chem.* 1999;274:10689–10692.
33. Cossarizza A, Chang HD, Radbruch A, et al. Guidelines for the use of flow cytometry and cell sorting in immunological studies. *Eur J Immunol.* 2017;47:1584–1797.
34. Boyman O, Sprent J. The role of interleukin-2 during homeostasis and activation of the immune system. *Nat Rev Immunol.* 2012;12:180–190.
35. Lissoni P. Therapy implications of the role of interleukin-2 in cancer. *Expert Rev Clin Immunol.* 2017;13:491–498.
36. Terstappen GC, Schlupen C, Raggiaschi R, Gaviraghi G. Target deconvolution

strategies in drug discovery. *Nat Rev Drug Discov.* 2007;6:891–903.
37. Zheng W, Thorne N, McKew JC. Phenotypic screens as a renewed approach for drug discovery. *Drug Discov Today.* 2013;18:1067–1073.
38. Kubota K, Funabashi M, Ogura Y. Target deconvolution from phenotype-based drug discovery by using chemical proteomics approaches. *BBA-Proteins and Proteomics.* 2019;1867:22–27.
39. Chang J, Kwon HJ. Discovery of novel drug targets and their functions using phenotypic screening of natural products. *J Ind Microbiol Biotechnol.* 2016;43:221–231.
40. Nastala CL, Edington HD, McKinney TG, et al. Recombinant IL-12 administration induces tumor regression in association with IFN-gamma production. *J Immunol.* 1994;153:1697–1706.
41. Lasek W, Zagozdzon R, Jakobisiak M. Interleukin 12: still a promising candidate for tumor immunotherapy? *Cancer Immunol Immunother.* 2014;63:419–435.
42. Piccinini AM, Midwood KS. DAMPening inflammation by modulating TLR signalling. *Mediat Inflamm.* 2010;2010..
43. Abdi K, Singh NJ. Making many from few: IL-12p40 as a model for the combinatorial assembly of heterodimeric cytokines. *Cytokine.* 2015;76:53–57.
44. Rao KV, Kasanah N, Wahyuono S, Tekwani BL, Schinazi RF, Hamann MT. Three new manzamine alkaloids from a common Indonesian sponge and their activity against infectious and tropical parasitic diseases. *J Nat Prod.* 2004;67:1314–1318.
45. Guzman EA, Johnson JD, Linley PA, Gunasekera SE, Wright AE. A novel activity from an old compound: Manzamine A reduces the metastatic potential of AsPC-1 pancreatic cancer cells and sensitizes them to TRAIL-induced apoptosis. *Invest New Drugs.* 2011;29:777–785.
46. Song X, Xiong Y, Qi X, et al. Molecular Targets of Active Anticancer Compounds Derived from Marine Sources. *Mar Drugs.* 2018;16.
47. Sampath P, Pollard TD. Effects of cytochalasin, phalloidin, and pH on the elongation of actin filaments. *Biochemistry.* 1991;30:1973–1980.
48. Bousquet PF, Paulsen LA, Fondy C, Lipski KM, Loucy KJ, Fondy TP. Effects of cytochalasin B in culture and in vivo on murine Madison 109 lung carcinoma and on B16 melanoma. *Cancer Res.* 1990;50:1431–1439.
49. Udagawa T, Yuan J, Panigrahy D, Chang YH, Shah J, D'Amato RJ. Cytochalasin E, an epoxide containing Aspergillus-derived fungal metabolite, inhibits angiogenesis and tumor growth. *J Pharmacol Exp Ther.* 2000;294:421–427.
50. Huang FY, Mei WL, Li YN, et al. The antitumour activities induced by pegylated liposomal cytochalasin D in murine models. *Eur J Cancer.* 2012;48:2260–2269.
51. Trendowski M, Mitchell JM, Corsette CM, Acquafondata C, Fondy TP. Chemotherapy with cytochalasin congeners in vitro and in vivo against murine models. *Invest New Drugs.* 2015;33:290–299.
52. Mooren OL, Galletta BJ, Cooper JA. Roles for actin assembly in endocytosis. *Annu Rev Biochem.* 2012;81:661–686.
53. Mortensen K, Larsson LI. Effects of cytochalasin D on the actin cytoskeleton: association of neoformed actin aggregates with proteins involved in signaling and endocytosis. *Cell Mol Life Sci.* 2003;60:1007–1012.
54. Trendowski M. Using cytochalasins to improve current chemotherapeutic approaches. *Anti-Cancer Agent Me.* 2015;15:327–335.
55. Dey S, Majhi A, Mahanti S, Dey I, Bishayi B. In Vitro Anti-inflammatory and Immunomodulatory Effects of Ciprofloxacin or Azithromycin in Staphylococcus aureus-Stimulated Murine Macrophages are Beneficial in the Presence of Cytochalasin D. *Inflammation.* 2015;38:1050–1069.
56. Lamb J, Crawford ED, Peck D, et al. The Connectivity Map: using gene-expression signatures to connect small molecules, genes, and disease. *Science.* 2006;313:1929–1935.
57. Chengalvala MV, Chennathukuzhi VM, Johnston DS, Stevis PE, Kopf GS. Gene expression profiling and its practice in drug development. *Curr Genomics.* 2007;8:262–270.
58. Woollard PM, Mehta NA, Vamathevan JJ, Van Horn S, Bonde BK, Dow DJ. The application of next-generation sequencing technologies to drug discovery and development. *Drug Discov Today.* 2011;16:512–519.
59. Schirle M, Jenkins JL. Identifying compound efficacy targets in phenotypic drug discovery. *Drug Discov Today.* 2016;21:82–89.
60. Li YY, An J, Jones SJ. A computational approach to finding novel targets for existing drugs. *PLoS Comput Biol.* 2011;7:e1002139.
61. Chen X, Yan CC, Zhang X, et al. Drug-target interaction prediction: databases, web servers and computational models. *Brief Bioinform.* 2016;17:696–712.
62. Xiao Z, Morris-Natschke SL, Lee KH. Strategies for the Optimization of Natural Leads to Anticancer Drugs or Drug Candidates. *Med Res Rev.* 2016;36:32–91.
63. Hu-Lieskovan S, Mok S, Homet Moreno B, et al. Improved antitumor activity of immunotherapy with BRAF and MEK inhibitors in BRAF(V600E) melanoma. *Sci Transl Med.* 2015;7:279ra241.
64. Xie T, Song S, Li S, Ouyang L, Xia L, Huang J. Review of natural product databases. *Cell Prolif.* 2015;48:398–404.

Eidesstattliche Erklärung

Ich versichere an Eides Statt, dass die Dissertation von mir selbständig und ohne unzulässige fremde Hilfe unter Beachtung der „Grundsätze zur Sicherung guter wissenschaftlicher Praxis an der Heinrich-Heine-Universität Düsseldorf“ erstellt worden ist.

Lisa Richter

Düsseldorf, 25.11.2019

Danksagung

Ein so großes Projekt wie eine Doktorarbeit ist nur möglich mit der Unterstützung von Kollegen, Freunden und Familie.

An erster Stelle gilt mein Dank meiner Erstbetreuerin Stefanie Scheu. Danke für deine unermüdliche Unterstützung, immer konstruktives Lob und Kritik und dass du jederzeit ein offenes Ohr hattest. Ich weiß das sehr zu schätzen.

Gleichermaßen gilt mein Dank Rainer Kalscheuer, der sich bereit erklärt hat, meine Arbeit als Zweitbetreuer zu begleiten und in Vorträgen stets Fragen hatte, die zum Weiterdenken angeregt haben.

Danke an die Deutsche Forschungsgemeinschaft für die Förderung des GRK2158 und die Finanzierung meines Projekts sowie an alle Kollegen innerhalb des Graduiertenkollegs. Ein besonderer Dank geht hierbei an die AGs Kalscheuer, Pfeffer, Fritz, Stork und Wesselborg für den Austausch und die Bereitstellung ihrer Daten, um vielversprechende Naturstoffe für weitere Experimente zu identifizieren.

Vielen Dank an die ganze AG Scheu und alle weiteren Kollegen des Instituts. Danke für alle spannenden, inspirierenden Gespräche über unsere Forschung aber auch Privates. Danke vor allem Sonja, dass du mir bei jedem noch so großen Experiment geholfen hast. Ohne dich wäre vieles nicht so einfach gewesen.

Dass aus Kollegen auch ganz schnell Freunde werden können – sogar innerhalb eines Tages – hat Anne mir gezeigt. Danke für diese großartige Zeit und das gegenseitige Fördern und Fordern. Erst durch dich stehe ich heute da, wo ich stehe.

Danke Jonas, dass du bedingungslos für mich da bist und mich durch alle Höhen und Tiefen begleitest. Du gibst mir Mut, jeden neuen Schritt zu gehen, und bist dabei immer an meiner Seite.

Mein Dank gilt zudem meiner Familie, die während des Studiums und der Promotion immer hinter mir stand und stolz auf jedes Ziel war, das ich erreicht habe. Durch eure Freude habt ihr mir immer wieder gezeigt, dass das alles nicht selbstverständlich ist.

Nicht zuletzt vielen Dank an alle fleißigen Korrekturleser meiner Arbeit. Danke! Ihr habt mir viele neue Ideen gebracht und mir dabei geholfen, dass ich diese Arbeit zufrieden abgeben kann.

Vielen, vielen Dank euch allen.